SKB

TECHNICAL REPORT 89-28

Earthquake mechanisms in Northern Sweden Oct 1987—Apr 1988

Ragnar Slunga

National Defence Research Institute
Stockholm

October 1989

SVENSK KÄRNBRÄNSLEHANTERING AB
SWEDISH NUCLEAR FUEL AND WASTE MANAGEMENT CO

BOX 5864 S-102 48 STOCKHOLM
TEL 08-665 28 00 TELEX 13108 SKB

EARTHQUAKE MECHANISMS IN NORTHERN SWEDEN OCT 1987 - APR 1988

Ragnar Slunga
National Defence Research Institute
Stockholm

October 1989

EARTHQUAKE MECHANISMS IN NORTHERN SWEDEN
OCT 1987 - APR 1988

Ragnar Slunga

Oct 1989

ABSTRACT

A network of six vertical short-period seismometers distributed over an area 200*100 square km in northern Sweden has been in operation since Oct 1987. During the first six months 38 earthquakes within or close to the network have been located and analysed. The focal depths are in the range 4-30km, the most frequent depths are 7-9 km which is 5km shallower than in southern Sweden. The boundary between the upper and middle crust seismicity thus seems to be at about 13km in comparison to about 18 km in southern Sweden. The stresses released by the earthquakes have the horizontal principal compression in or close to the NW-SE quadrant. The most likely regional stress component has the principal compression in the direction N60W (N120E). If one interprete all Baltic Shield earthquake data one gets the same most likely orientation for the regional stress component. The relation between the surface faults and the earthquake fault plane intersections with the surface is preliminary investigated. There seems to be a good agreement between the fault plane strikes of the upper crustal earthquakes and the surface fault strikes. The dominating type of fault movements is strike-slip at subvertical planes. This is in agreement with the fault plane solutions for other areas in the Baltic Shield. There is also a reverse faulting component indicating the possibility that there exists a plate tectonic uplift component in Sweden. Finally an alternative view on the Baltic Shield seismicity is given. It is based on the Baltic Shield earthquake studies and on the results of geodetic levellings in Finland and Norway. It assumes the earthquakes to be preceeded by aseismic sliding (normally called stable sliding or creep) episodes over large parts of the faults, the earthquakes are unstable sliding events at small locked parts (asperities) of the faults. This view means for instance that for the geodynamical interpretation of the earthquakes the peak slip is a more relevant parameter than the seismic moment. It also leads to estimates of the crustal deformations over southern Sweden of the order of 1mm/year.

TABLE OF CONTENTS

SUMMARY

The results of the first six months of the operation of a six station seismological network in northern Sweden are presented. Totally 38 earthquakes have been located and analysed for source mechanisms. The results are:

- the focal depths are in the range 4-30km, the main peak is around 8km which is 5km more shallow than the southern Sweden seismicity
- the stresses released by the earthquake faulting show that the regional stress in the Baltic shield have a principal horizontal compression in the direction N60W
- the estimated dynamic source parameters; the seismic moments, the static stress drops, and the peak slips are similar to the results from the other parts of the Baltic Shield area
- the peak slips are typically in the range 0.1-10mm
- the fault plane solutions are for upper crustal events in agreement with the strikes of the fault lineaments observed at the surface
- strike-slip motion at subvertical faults is the dominating type of faulting (transpression)
- there is also a reverse faulting component (compressive component) indicating the possibility that part of the land uplift has a plate tectonic origin.

Based on the earthquake studied and on results of interpretations of the geodetic observations in Finland, Norway, and Estonia an alternative view on the Baltic shield earthquakes is presented and discussed. It assumes the earthquakes to be preceeded by aseismic sliding over a fairly large fault surface. The earthquakes occur at fault asperities that have locked a small part of the fault. From a statistical analysis of the interevent distances the aseismicly sliding fault surface per earthquake is estimated to have lengths of 20-25km. This gives the total crustal lateral deformation over southwestern Sweden to be about 1 mm per year. The rate of seismic activity in northern Sweden is rather similar to southwestern Sweden which means that the total deformation also may be similar. This view on the crustal deformations and seismic activity in the Baltic Shield area should be kept in mind as a possibility when planning future research on the bedrock deformation processes.

1 INTRODUCTION

SKB AB (Swedish Nuclear Fuel and Waste Management Co) finances a seismic network in northern Sweden. The network has been established and is operated by Foa (National defence research institute) in Stockholm. Figure 1 shows the locations of the six stations. During the summermonths in addition mobile seismic stations are operated in the area by the Uppsala University.

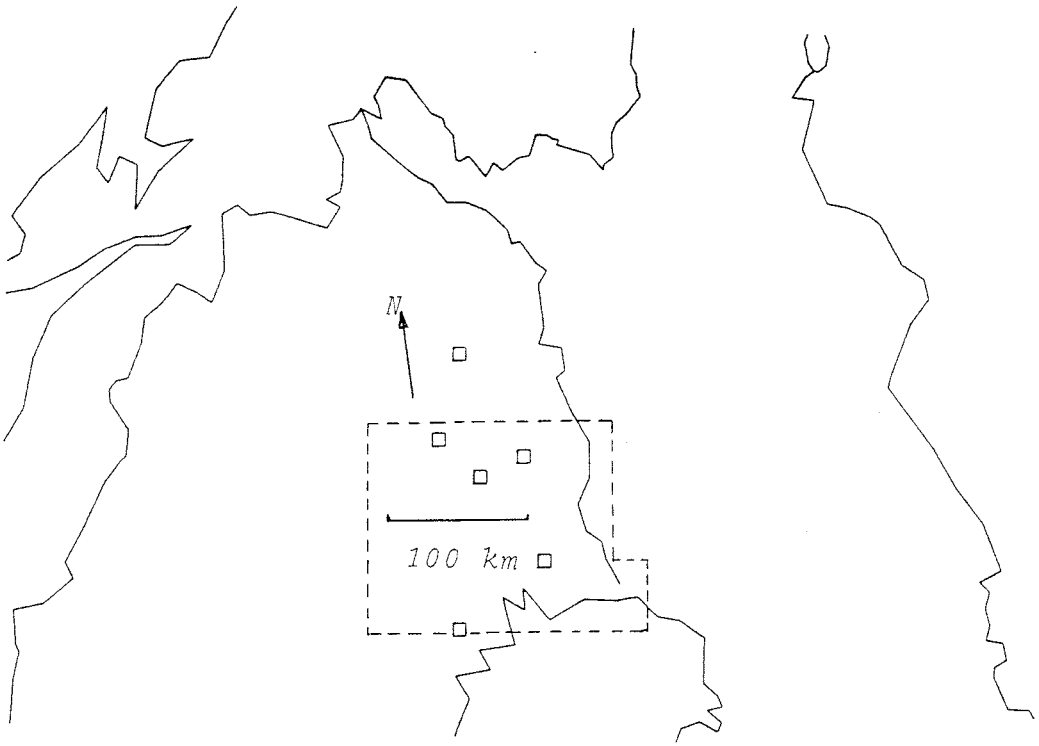

Figure 1. The six stations of the network operated by Foa within this project.

Table 1-1 The station coordinates

		Latitude north	Longitude east
Masugnsbyn	MUG	67.462	22.045
Lansjärv	LJV	66.655	22.182
Hakkas	HAK	66.925	21.560
Kalix	KLX	66.067	23.031
Korpilombolo	KPM	66.755	22.905
Västmark	VMK	65.680	21.587

This report covers the period 871001-880416.

2 THE DATA ACQUISITION AND EVENT DETECTION METHODS

All stations transmit continuosly frequency modulated signals to the central computer at Foa in Stockholm. Permanent telephone lines are used. Gain ranging amplifiers prohibit overloading. The signals and gain information are sampled at a rate of 60 Hz. At Stockholm the analogue signals are bandpass filtered (5-15Hz) and fed into a S/N-detector. When three or four close stations give detections within a time window corresponding to the seismic travel time between the stations an event detection is declared and the unfiltered data is saved on digital tape. At least one minute of data before the detections are included. In this way about 20 detected "events" per day are stored on tape. This means that the continous data flow has been reduced by a factor 0.05. The detection threshold is adjusted continously in order not to run out of magnetic tape. It is mainly the wind that determines the actual detection level. During favourable conditions events below ML 1 are detected within the network.

The magnetic tapes are then copied into the disc-memory, demultiplexed and submitted to an automatic analysis. The output of this analysis is a list of located seismic events which are given together with plots of the signals. The list and plot are then checked by the seismologist. Most of the regular mining explosions are in this way automaticly located and identified (waveform similarity with previous explosions) and there is normally no need for further interactive analysis of most of the events. As almost all local events are explosions this means a great reduction of the time consuming interactive analysis.

In the interactive analysis the seismologist decides what to save for further source mechanism studies. This means that automatic algorithms for fault plane solution, size determination and if needed relative location are run.

The methods for fault plane solution, for estimation of the dynamic source parameters, and for relative location are described by Slunga (1981, 1982). The fault plane solution algorithm is also presented and validated in paragraph 3.5.1 below.

The data for the period (871001-880416) is contained on 300 magnetic standard tapes at 800 BPI.

3 THE EARTHQUAKES

The earthquakes analysed in this report are listed in table 3-1 together with the origin times, locations, depths, and magnitudes.

Table 3-1 The earthquakes analysed in this report, values within parenthesis are less reliable.

Date	Origin time GMT	Epicenter lat N	Epicenter long E	Focal depth (km)	Seismic moment (Nm)	ML
871011	060123.8	66.336	19.892	(26.0)	0.15E+12	1.2
871017	040638.8	66.742	22.878	8.2	0.35E+12	1.5
871017	072913.7	64.316	20.895	(18.9)	0.55E+13	2.7
871220	195226.7	65.675	22.500	9.9	0.19E+12	1.3
871226	0829 8.1	67.759	19.552	4.8	0.49E+14	3.6
871229	165643.5	67.754	19.562	4.8	0.92E+12	2.0
871230	032452.3	65.391	22.947	11.6	0.14E+12	1.2
880104	144335.8	65.280	22.528	4.5	0.10E+12	1.0
880108	081423.1	67.537	21.575	26.5	0.11E+13	2.0
880110	104938.1	67.454	22.341	4.0	0.40E+12	1.6
880118	063436.0	67.247	23.723	15.8	0.11E+12	1.0
880131	050212.2	66.756	19.195	24.8	0.12E+13	2.1
880202	111321.0	67.491	21.889	6.8	0.17E+12	1.2
880206	145134.2	67.560	22.210	12.0	0.79E+11	0.9
880206	201544.0	67.651	19.363	4.9	0.20E+12	1.3
880207	192256.2	66.071	23.517	6.7	0.37E+11	0.6
880208	074844.3	67.703	23.358	(6.7)	0.24E+12	1.4
880219	2303 4.8	66.631	22.782	6.9	0.53E+11	0.7
880225	1249 9.3	66.701	21.993	24.6	0.12E+11	0.1
880227	0637 1.8	64.885	21.032	21.6	0.17E+13	2.2
880229	140826.5	64.690	22.730	4.9	0.14E+13	2.1
880304	215050.5	65.480	21.538	11.7	0.44E+11	0.6
880307	160227.2	66.312	22.133	8.4	0.48E+12	1.7
880318	110014.8	65.767	22.820	7.3	0.15E+12	1.2
880322	040537.3	67.486	22.261	10.5	0.80E+11	0.9
880322	202832.8	67.463	24.287	5.4	0.95E+12	2.0
880322	235836.0	65.426	22.609	9.1	0.93E+11	1.0
880329	060737.5	67.952	19.390	(12.8)	0.79E+12	1.9
880330	022112.1	65.220	20.032	8.0	0.12E+13	2.1
880330	120635.0	67.518	22.413	8.9	0.27E+12	1.4
880401	013610.5	67.493	22.194	9.0	0.11E+12	1.0
880404	022522.9	67.779	19.621	8.2	0.49E+12	1.7
880404	023316.2	67.662	22.114	8.6	0.10E+13	2.0
880404	174834.8	66.387	22.601	18.5	0.38E+11	0.6
880407	212431.6	67.974	20.781	29.1	0.15E+12	1.2
880408	185110.0	67.539	22.665	4.3	0.91E+11	1.0
880410	194810.6	66.175	21.904	(9.6)	0.47E+11	0.7
880416	175634.4	66.312	23.738	6.2	0.85E+11	0.9

Figure 2 shows their geographical distribution.

Figure 2. The earthquakes that are included in this report are given by the solid circles. The area where geophysical lineaments are mapped by Henkel (1988) is also marked.

Observational details and results for each earthquake are given in Appendix 1.

3.1 RELATION TO PREVIOUS SEISMICITY

The time period covered by the present study is about 6 months, all six stations in operation for 5 months. It is however striking how well the small events of this short time interval fits the previous seismicity, see figure 3.

Figure 3. The solid circles mark the earthquakes of this study. The dotted circles mark previous seismicity from the period 1650-1983 as given by the catalogue from the Helsinki University, FENCAT (1987).

Notice that the both the activity west of Kiruna, A, and the activity around Masugnsbyn, B, are in previously active sites. In the central part, C, the events fill up a previously empty spot.

3.2 FOCAL DEPTHS

The distribution of the focal depths of the earthquakes is of great geophysical interest. The depths are determined by locating the earthquakes with latitude, longitude, focal depth, and origin time as free parameters. This is a nonlinear inversion problem which is solved iteratively by minimizing the weighted square sum of the time differences between the observed and the theoretical arrival times of the first P- and S-waves. The uncertainty of the estimated location is normally estimated by statistical considerations. The time differences (the residuals) are typically assumed to be uncorrelated and to have a normal distribution with zero mean value. The size of the uncertainties depends on the station configuration around the event and on the standard deviation assumed for the time residuals. In the application within this project the first P-wave arrival times have been assumed to have a distance dependent standard deviation going from 0.1s at zero distance to 0.25s at 160km and to 0.63s at 200km. In figure 4a the typical confidence intervals are shown for events at different crustal depths. As the depth estimate problem is nonlinear the confidence limits will be asymmetric in length if both sides (upper and lower) have the same probability.

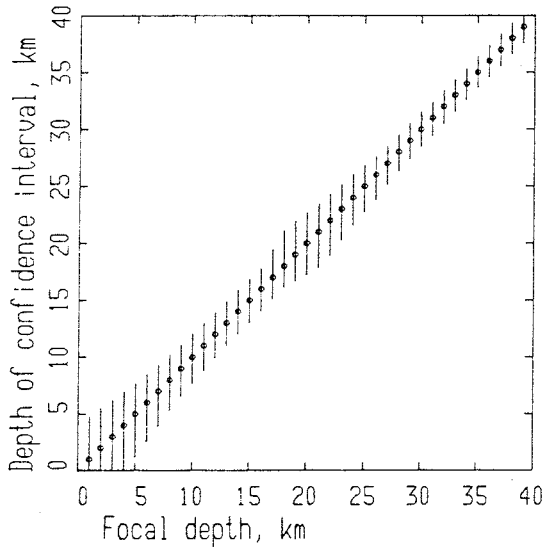

Figure 4a. The typical 68% confidence intervals for the events within the network. The circle marks the depth around which the confidence interval has been computed. The upper and lower part of the confidence intervals have the same probability. As the depth estimate procedure is nonlinear this causes the confidence intervals to be assymmetric.

The accuracy of the location procedure and the validity of the error estimates are most easily checked by locating events with known true positions. To check the focal depth determinations and the uncertainty estimates I therefore located 190 surface events (events with clear short period surface waves, Rg) within or close to the network. Some of these events were located to nonzero depths while some had no optimum deeper than zero depth. If the location algorithm is unbiased one would expect 50% of these events to be located to depths below the true depth and 50% to be located to depths above. Figure 4b shows the results of this test. It can there be seen that this test gave hardly any bias at all. Furthermore the distribution of the distance to the surface in units of estimated standard deviations for the events given nonzero depths is smaller than expected for a normal distribution. This shows that the estimated uncertainty is larger than the true uncertainty. In conclusion the statistical assumptions about the standard deviations of the time residuals are not too optimistic. Note that the fact that there is no bias for these surface events not necessarily means that there is no bias for deeper events but it means that there are no indications of such a bias.

In the following the depth distribution of the earthquakes will be estimated. In estimating the relative frequency both the nonlinearity and the uncertainty of the focal determination procedure have been included. To illustrate the effects of the procedure figure 4c shows both the frequency of the estimated focal depths for the surface events and the estimated focal depth distribution when the uncertainties have been included. The vertical uncertainties of the free depth location procedure are rather large for very shallow events. Full consideration of this means that it only can be stated that the events are distributed in the depth range 0-5km.

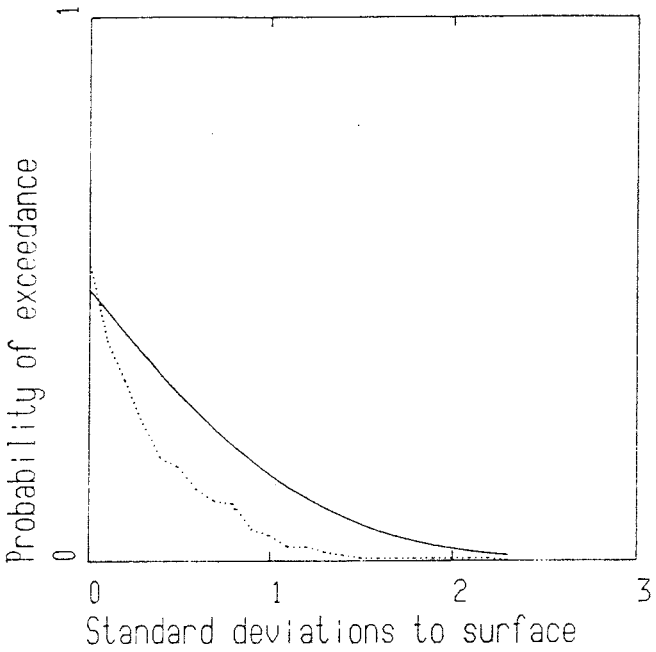

Figure 4b. The results of locating 190 surface events (mostly explosions, all with clear Rg-waves) with the focal depth as a free parameter. The x-axis gives the resulting focal depth expressed in terms of the number of standard deviations to the surface (the true depth). In estimating this distance the nonlinearity of the depth determination has been included. The y-axis gives the probability of exceeding the values of the x-axis. The solid curve is the normal distribution implicitly assumed in the estimate of depth errors. It has the 50% value at zero depth. The dotted curve gives the resulting probabilities for the 190 events. We see a small bias, the 50% value (0.5 value) is at 0.04 standard deviations from the surface, this means a depth of 0.6km as the standard deviation at the surface is about 15km. If the same bias (0.04 s.d.) existed at say 10km depth it would correspond to 0.2km. It is however possible that there exist bias for deeper events. What is more important in the figure is that the dotted curve shows that the estimated errors (solid curve) are larger than the true errors (dotted curve). The difference is about a factor 2. The error estimates are thus not too optimistic but rather on the conservative side.

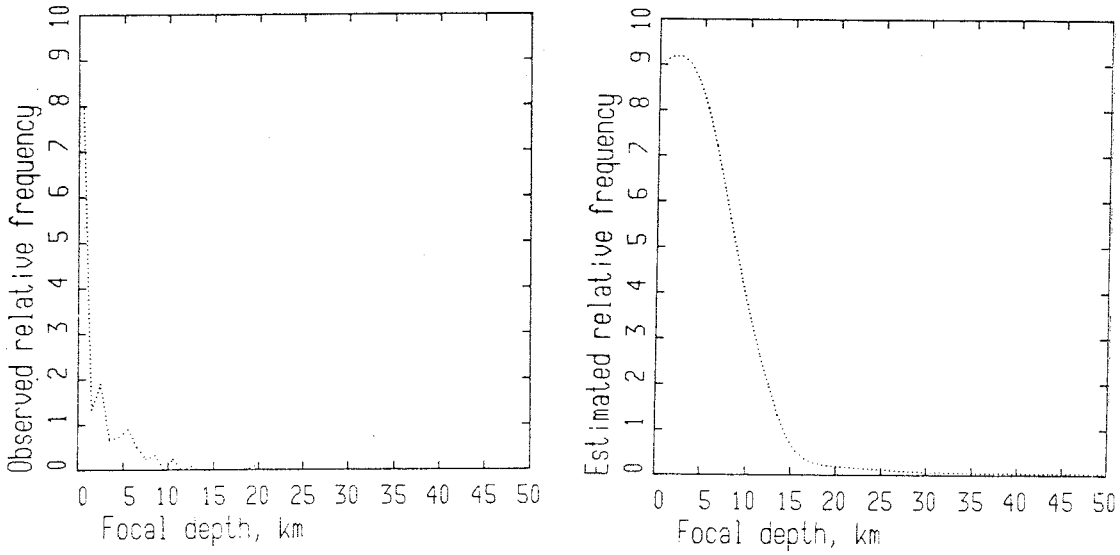

Figure 4c. To the left is shown the frequencies of the estimated focal depths (free depth location) of 190 surface events. To the right the estimated focal depth distribution is given when the uncertainties of the depth estimates have been included. As the estimated uncertainties are rather conservative it can only be stated that the "surface" events are distributed in the depth range 0-5km.

The figure above shows that by including the uncertainty of the depth determination in the estimate of the focal depth distribution we avoid going further in the conclusions than the data allow.

In figure 4d the estimated focal depth distribution of the Norrbotten earthquakes is shown.

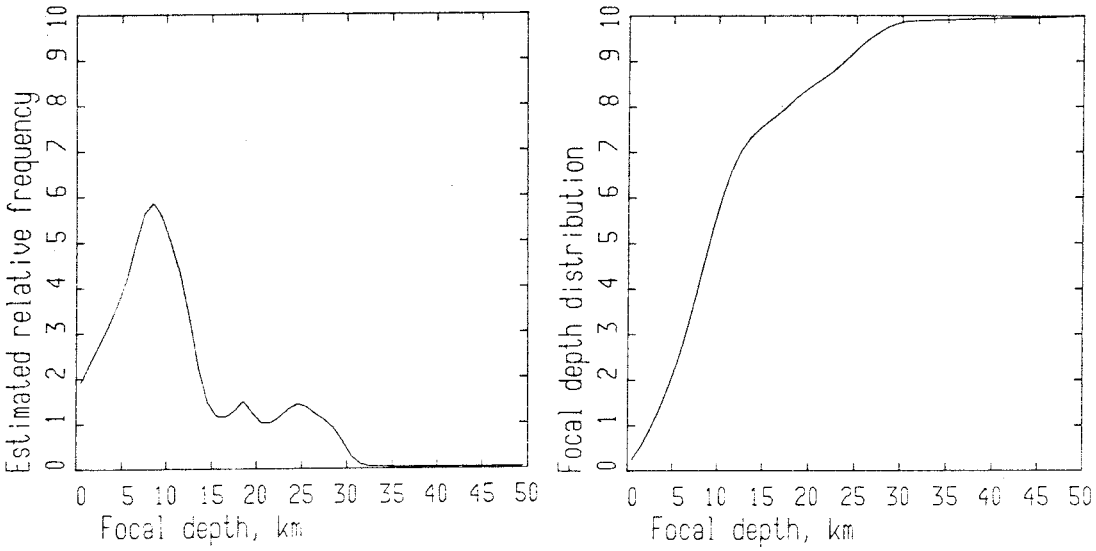

Figure 4d. The focal depths of the earthquakes. This estimated relative frequency has been achieved by considering the nonlinearity and uncertainty of the focal depths estimates.

It is obvious from figure 4d that the we have at least two different populations, the events at less than some 13 km depth, and the events at 13-30 km depth. No events are deeper than 30-35km. A rather similar type of depth distribution was found by Slunga (1985) for the southern Sweden events. The limits of the two depth intervals are however different, see figure 5.

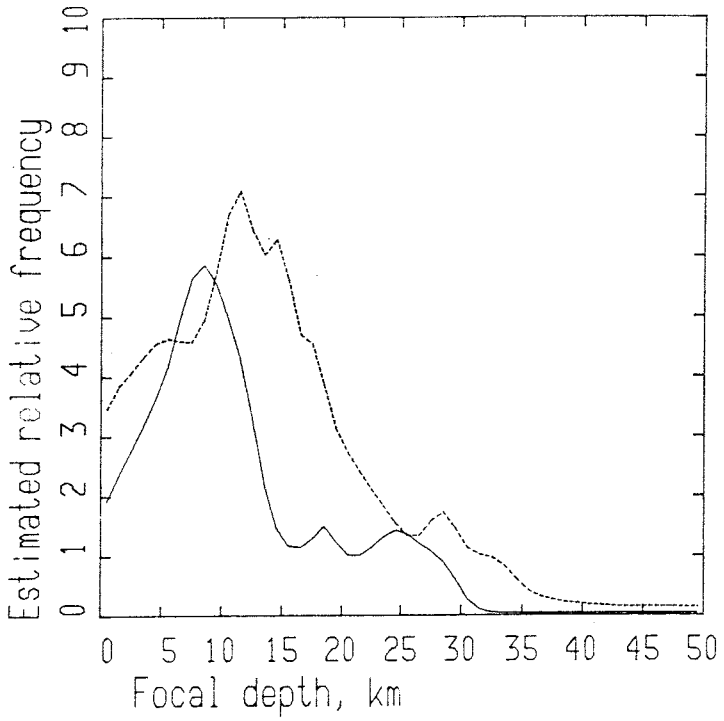

Figure 5. The estimated relative frequencies of the northern Sweden earthquakes, solid line, compared to the southern Sweden events, dotted line, estimated by Slunga (1985). The northern first (main) peak drops about 5 km shallower than the southern first peak.

Slunga (1985) interpreted the two drops in relative frequencies for the southern Sweden earthquakes as due to temperature effects on quartz (18 km drop) and feldspar (35 km). At higher temperatures they become ductile. With this interpretation applied to figure 5 one should conclude that the temperature gradient is 30-40% higher in the upper crust (0-13km) in Norrbotten than in southwestern Sweden. This is probably not true. Other possibilities include differencies in the composition of the upper crustal rock and/or differencies in their depth distribution (a more shallow Conrad discontinuity in Norrbotten). The crust in northern Sweden is severel hundred million years older than in southwestern Sweden and has been eroded several kilometers more, this may favour the interpretation of the drop in seismicity at 13 or 18 km depths as due to a lithological boundary (the Conrad discontinuity). The lack of seismic activity below 30-35km is probably mostly a temperature effect.

The conclusion is that the earthquakes in Norrbotten during this time period had a more shallow main peak in their relative frequency of focal depths than the earthquakes of southwestern Sweden studied by Slunga (1985). The midcrustal activity in both areas go down to

30-35km depth.

3.3 HORIZONTAL STRESSES

One of the early important results of the Foa research on the Nordic seismic activity was the estimate of the orientation of the regional horizontal stresses, Slunga (1981).

I use in the following presentation the concepts introduced by Slunga (1981): the azimuth of principal compression of the horizontal deviatoric stress relaxed by the earthquake slip and the relative size of this deviatoric horizontal stress.

A few facts about the results normally given by the seismic fault plane solutions:

- the deviatoric stress released by the earthquake slip is in principle uniquely determined

- there are normally two possible fault planes given by the fault plane solution, one is the true fault plane, the other has no physical meaning

- the rock stresses cannot be directly estimated from the fault plane solution, not even by additional use of rock failure criteria as most earthquakes occurs on pre-existing planes of weakness, see McKenzie (1969)

- strike-slip events on vertical fault planes are much more valuable than normal or reverse faulting events in the determination of the crustal horizontal stresses as for vertical strike-slip events the horizontal rock stress and the horizontal relaxed stress are in general closer to each other, see Slunga (1981). This motivates the use of the relative size of the horizontal deviatoric stress relaxed by the earthquake slip in discussing the regional horizontal stresses.

The fault plane solution consists of the orientation of the principal stress axes: the compressive P-axis, the tensional T-axis, and the intermediate principle axis B often called the null axis. Let P be the unit vector of the P-axis and T be the unit vector of the T-axis, and let N denote a unit vector in the normal direction of an arbitrary vertical plane. Let also pairs of vectors within brackets denote scalar products. Then the relative normal stress, S, on the plane is

$$S = (NT)(NT) - (NP)(NP)$$

with the possible size range -1 to 1. The orientation

of N, for which the largest compression is achieved, is the direction of the principal horizontal compression, the largest compression is always in the range 0 to -1. The orientation of the largest horizontal tension is always normal to the compression and in the range 0 to 1. The relative size, RS, of the horizontal deviatoric stress is defined as

$$RS = (S(max)-S(min))/2$$

and will be in the range zero to one. These are the concepts introduced by Slunga (1981) in establishing the regional stress fields from earthquake fault plane plane solutions, see also Slunga, Norrman, and Glans (1984).

As stated above one cannot accurately estimate the crustal deviatoric stresses directly from single fault plane solutions as the deviations between the stresses relaxed by the earthquake slip may deviate quite a lot from the orientation of the rock deviatoric stress. However, in the long run the accumulated earthquake stress release must equal the stress generated by the tectonic forces. This can also be expected to have the same orientation as the regional deviatoric stress. Thus if the stresses relaxed by the earthquakes tend to cluster around any direction, especially for strike-slip events, this direction is close to the corresponding direction of the crustal deviatoric stress. See further Slunga (1981).

Now, after establishing the concepts needed, figure 6 shows the direction of the horizontal principle compression and the relative sizes of the horizontal deviatoric stress for earthquakes in southern Sweden and Denmark, Slunga (1981, 1982, 1985), Slunga, Norrman, and Glans (1984), Slunga and Nordgren (1988), in Finland, Slunga (1979), Slunga and Ahjos (1986), and finally in northern Sweden, this study.

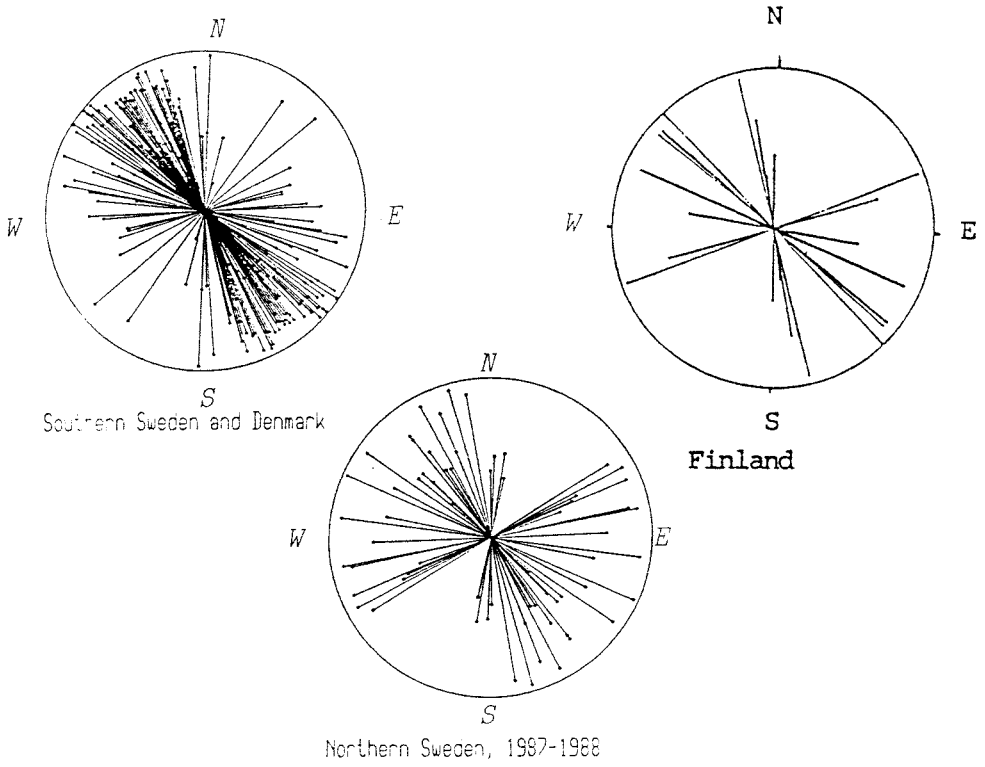

Figure 6. The direction of the horizontal compression, that means the direction of the principal compression of the horizontal deviatoric stress relaxed by the earthquakes, are given by the directions of the lines. The length of the lines are proportional to the relative size, RS, of the horizontal deviatoric stress. Each line is the very best fitting fault plane solution of one earthquake. Totally 130 earthquakes are included. If RS equals unity the length of the line will equal the diameter of the circle, that means a pure strike-slip event on a vertical fault.

The scatter of the distributions of the compressive directions for southern Sweden and northern Sweden are quite different. There is a clear clustering of large RS-events in the direction N20W-N60W for southern Sweden. Only two events have directions of compressions with large RS-values inconsistent with rock stresses having principal horizontal compression within this range. Thus the southern Sweden data indicates that the horizontal regional stress of that area has a NW-SE principal compression.

In northern Sweden the scatter is very uniform within about half of the circle. If one interpretes these fault plane solutions in terms of a regional stress field its principal compression must be N60W in order to

avoid contradictions. However the lack of clustering indicates that the stress is truely inhomogeneous. We see the picture of a complex pattern of fault movements.

If one interpretes all events of the Baltic Shield area together looking for the orientation of one regional stress field giving the lowest number of contradictions one again comes to N60W as the best fitting direction of the principal compression.

Slunga (1981) pointed out that this direction, WNW-NW, of the horizontal principal compression is in agreement with a number of stress estimates in Europe north of the Alps based on a number of different geological and geophysical methods.

3.4 FAULT PLANE SOLUTIONS

3.4.1 THE FAULT PLANE SOLUTION ALGORITHM - METHOD AND SIGNIFICANCE

Classical fault plane solution algorithms make use of the observed first motion direction of the seismic waves radiated from the source. As for regional recordings of weak events typcally less than 3-5 clear first motions are observed this method is of restricted value in such cases. This was the reason to include the amplitudes in the fault plane solution algorithm that was developed at FOA during 1980-1982. The method have earlier been described and published, Slunga (1981), Slunga (1982). I will however give the main principles here.

- The observed signals (for this network the vertical component of the P- and SV-waves) are deconvolved with the instrumental response and corrected for the Q-damping. The corner frequency and the low frequency spectral level are estimated from the spectra of the deconvolved and corrected signal. The Q-model used is

  Q = 320 * SQRT(frequency) for P-waves, and

  Q = 480 * SQRT(frequency) for S-waves.

- Based on the location of the event the waves entering the time window used in the analysis above are determined. Body wave geometrical spreading is assumed (1/R, R=total distance) and the response of the free ground surface is determined for each ray. At short distances, up to 70km, only the direct waves are considered, at larger distances waves reflected from the Moho-discontinuity will be important. For events at less than 25km depth an crustal reflector at 25km depth is also included. The ray amplitudes of the wave reflected from the internal crustal reflector is assumed to be the same as the direct wave while the amplitude of the ray reflected from the Moho-discontinuity is assumed to have a different distance dependency. At distances less than the critical reflection they are smaller than the direct wave, around critical reflection up to 1.5 times the direct wave and for larger distances falling off to the size of the direct wave.

- The earthquakes have, in the fault plane solutions of this report, been treated as pure shear slip events, that means the double couple radiation pattern for P- and S-waves have been used. For each ray direction the radiation factor is determined and multiplied with the ray amplitude above (geometrical spreading, free surface response, etc.) which gives the expected observed spectral amplitude for the ray at the station. This

amplitude corresponds to the fault plane solution used in computing the radiation factor. All rays entering the time window used for the spectral estimate are treated in this way and the total amplitude is assumed to be given by the third root of the sum of the cubes of the individual ray amplitudes. The choice of the cube instead of square is due to comparison with full wave theory computations (synthetic seismograms).

- The differencies between the observed and the theoretical spectral amplitudes are then computed. Only fault plane solutions fitting the amplitude observations as well as the first motion observations are accepted. Normally a range of acceptable mechanisms are found. All fault plane solutions are investigated (typically 20 000 are tested for each event).

Of special importance in the validation of the use of the amplitudes is the statistical treatment of the amplitude residuals. I assume that the amplitude residuals (errors) have lognormal distribution, that means the logarithmic errors follow a normal distribution. I also assume "a priory" that the amplitude residuals at different stations are statistically independent (uncorrelated) while the P- and S-amplitude residuals at the same stations are highly correlated. The reason for this is that there are several possible causes to such a correlation: the ray paths are almost the same, the same instrument is used, the same local receiver conditions etc. The following covariance matrix for the P and SV observation at the same station was used (e denotes the natural logarithm of the ratio of observed and theoretical amplitudes):

$$\begin{array}{c} \\ e(P) \\ e(SV) \end{array} \begin{bmatrix} 1/2 & 2/3 \\ 2/3 & 3/2 \end{bmatrix}$$

which means a standard deviation factor of 2 for the P-wave amplitude errors and a factor 3.4 for the SV-wave. The correlation coefficient above is slightly less than 0.8.

Statistically independent varibles are wanted in the statistical evaluation of the fit between theoretical and observed amplitudes. The covariance matrix above gives the following independent residuals at each station: e(P), and e(P)-0.75 e(SV). The variance of the latter is 0.34. The fit to the observations is then expressed by the size of the weighted sum of the squares:

$$e(P)*e(P)/0.5 + (e(P)-0.75e(SV))*(e(P)-0.75e(SV))/0.34.$$

These squares are summed over the N observing stations. The sum S has a chi-square distribution with (2N) degrees of freedom. The four free parameters are the seismic moment and the three angles defining the fault plane solution. The resulting minimum of S, Smin, has then (2N-4) degrees of

freedom.

To get a measure of the statistical significance of the resulting source mechanisms, the following procedure was adopted. First the sum S was minimized by only varying the seismic moment, while the spatial radiation factors for the P- and S-waves were both kept constant, each equal to its spatial mean value. This minimum Sref is chi-square distributed with (2N-1) degrees of freedom. After establishing this reference sum, we can use an F test where the ratio of the two sums, Sref/(2N-1) and Smin/(2N-4), is computed. This gives the significance of the resulting source orientation. Note that the concept in computing Sref, the use of the mean values of the radiation factors, is generally accepted by seismologists in analysing earthquakes recorded by local/regional networks, most such seismic moments determinations are done in this way. The F-test gives the significance of the further step to include the fault plane solution in the analysis.

The significance value of the F-test gives the probability that similar or better reduction of the sum S would be achieved by pure chance. The distribution of the F-values as computed for 274 earthquakes recorded by the Swedish networks operated by FOA 1979-1988 is given in figure 7a. The expected cumulative distribution if the double-couple radiation factor had no physical reality is also shown. One can see that 50% of the events have a significance that is better (less) than 15%. This result is highly significant. Note that if the rays to the stations are well away from the nodal lines the resulting fault plane solution will be nonsignificant although it may give a perfect fit to the data. The results also show that one should take the radiation pattern into consideration when estimating the seismic moments as more than 25% of the events show significant improvements (significance better than 5%).

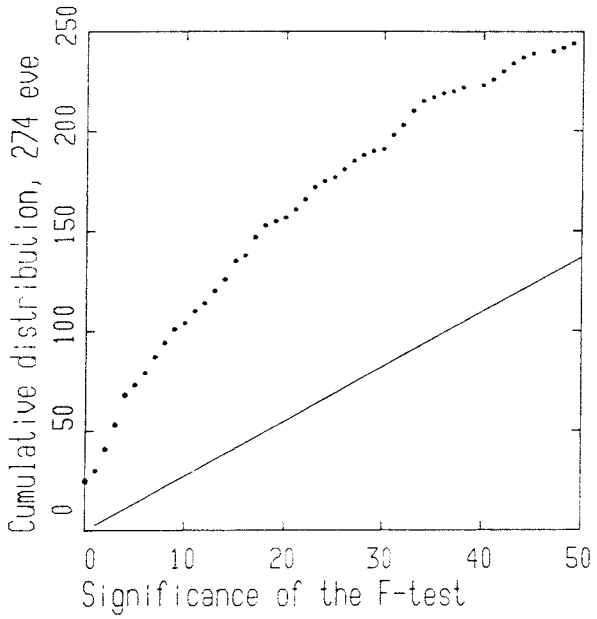

Figure 7a. The significance of the F-test when the fault plane solution algorithm has been applied to 274 earthquakes. The x-axis gives the significance level of the resulting radiation pattern (source orientation). The y-axis gives the distribution functions, the straight line for a random distribution, the dots mark the results for the earthquakes. The deviation from the line is highly significant.

The fit between the theoretical and the observed spectral amplitudes can be expressed in terms of the estimated standard deviations for the amplitude residuals. As log-normal distributions are assumed the standard deviation for the residuals can be expressed by the error factor for instance for the P-waves, the corresponding error factor for the S-waves is above assumed to be 1.7 times larger. Figure 7b shows the estimated standard deviation factor for the P-wave amplitudes as given by the fault plane solutions for the 274 earthquakes.

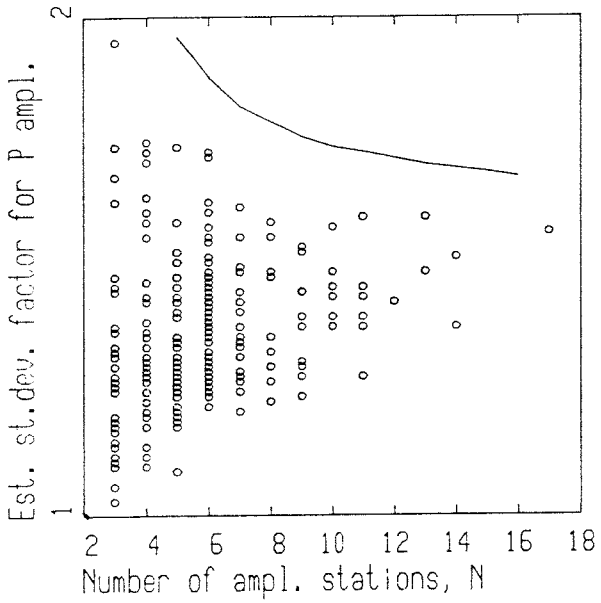

Figure 7b. The x-axis shows the number, N, of stations at which the P- and S-wave spectral amplitudes have been observed. The y-axis shows the estimated standard deviation factor for P-wave amplitudes. For each of the 274 earthquakes the circles mark the estimated st. dev. factor based on the value of Smin. The solid line shows the amplitude criterion used for accepting the mechanisms, it is based on the assumption that the standard deviation factor is 1.6 (or less) for the P-waves. It can be seen that all events have fault plane solutions satisfying this amplitude criterion.

The value of including the amplitude criterion (as illustrated by the solid curve in figure 7b) into the fault plane solution algorithm is evident from figure 7c. The value of a fault plane solution depends very much on its uniqueness. This can be expressed as the percentage of all source orientations that fullfills the fault plane solution criteria. In this case we have two criteria, the observed clear first motion directions must be in agreement with the theoretical ones, and the amplitude residuals must be in agreement with the assumption of an error factor 1.6 for the P-amplitudes. The value of adding the amplitude criterion to the conventional first motion requirement is illustrated by figure 7c. Very few events can be given welldefined fault plane solutions by use of only first motions. This is typical in the study of small earthquakes by local or regional networks. Only few clear first motions are normally observed. It can be seen in figure 7c that the number of events having well defined

fault plane solutions increases drasticly when the amplitude requirement is included.

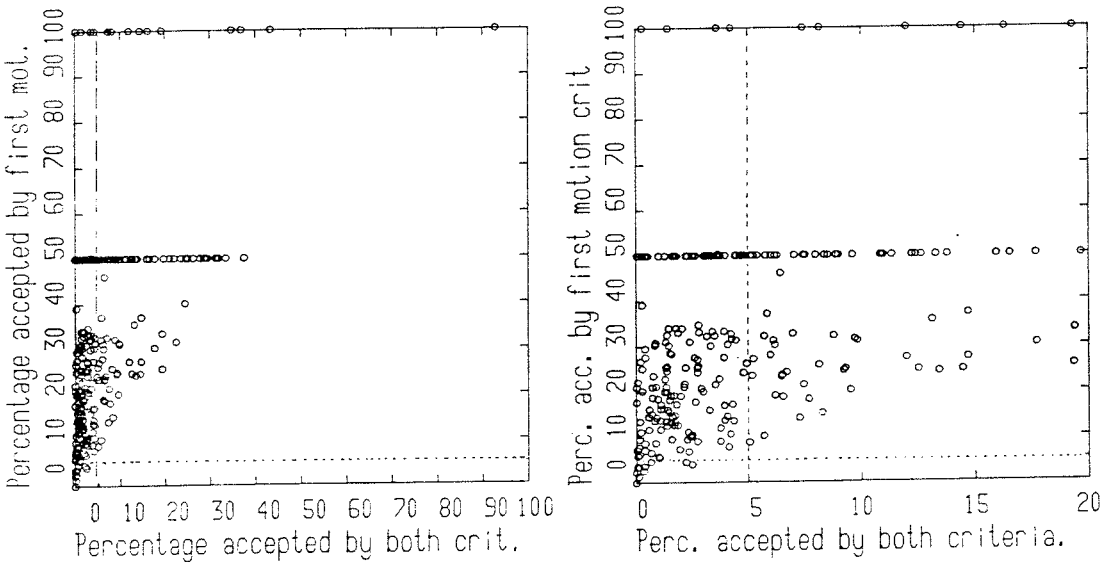

Figure 7c. The two figures show the results of applying the fault plane solution algorithm to 274 regionally recorded Swedish earthquakes. To the left an overview, to the right a blow-up. The uniqueness of the fault plane solutions is expressed by the percentage of all source orientations that fit the criteria. If only first motion directions are used only the events below the horizontal dotted line give a reasonable degree of uniqueness (5%). When the amplitude criterion is added all events to the left of the vertical dashed lines have a uniqueness of 5% or better. This improvement is drastic and without the use of amplitudes in the fault plane solutions our knowledge about the Swedish seismicity had been at a lower level.

So far I have shown that the inclusion of the amplitude radiation pattern (or equivalently the fault plane solution) into the seismic moment estimation algorithm gives significant improvements. It now only remains to show that the amplitude criterion and the first motion requirement give the same fault plane solutions. This is best illustrated by the Lake Vänern earthquake Febr 13 1981, ML=3.3. For this event 12 clear first motions were observed, which gave a highly unique fault plane solution already from the first motion directions. Figure 7d shows that the use of only the amplitudes, without any use the first motions, gives the same fault plane solution.

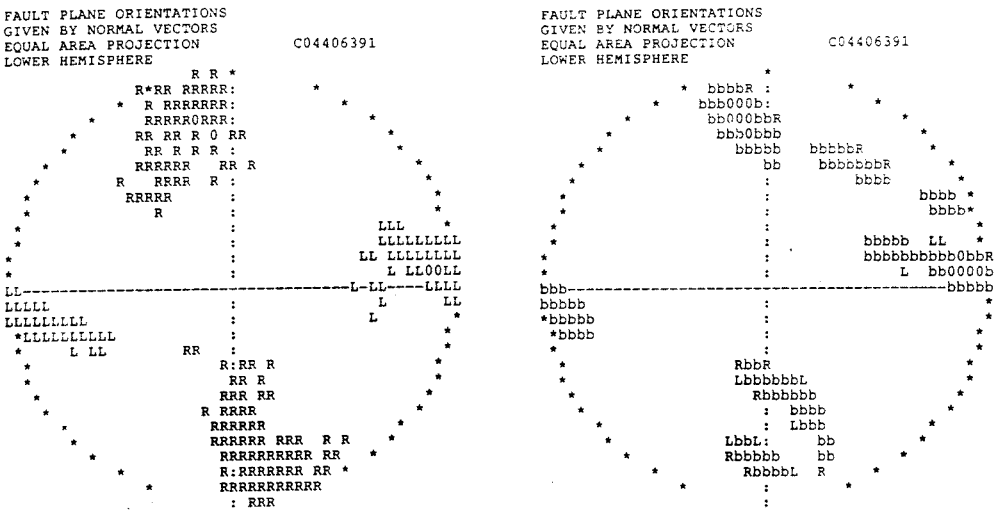

Figure 7d. The similarity of the fault plane solutions for the Febr 13 1981 earthquake in the Lake Vänern area. The circles are lower hemisphere equal are projections. The fault plane orientations are given by the position of the normals within the circles. To the left all fault plane orientations fitting the 12 clearly observed first motion directions are given (no use of amplitudes). To the right all fault planes fullfilling the amplitude criterion is shown (no use of first motion observations). The best fitting fault plane solution of the amplitude criterion is within the 1.4% fault plane solutions fitting the 12 observed first motion directions.

The fault plane solution algorithm presented and validated here has been applied to the northern Sweden earthquakes. The results are given in the following paragraph.

3.4.2 THE RESULTING FAULT PLANE SOLUTIONS

The fault plane solutions can be illustrated and classified according to the relative sizes of the horizontal principal stresses computed from the fault plane solution, that means from the deviatoric stress released by the earthquake slip. This is illustrated in figure 8.

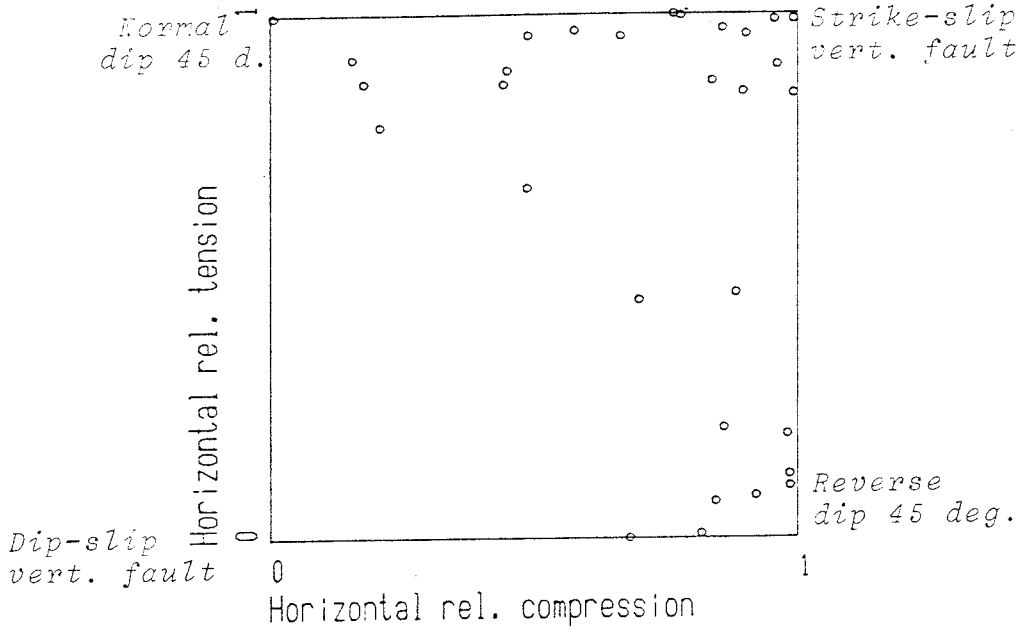

Figure 8. Each circle marks one earthquake and illustrates its very best fitting fault plane solution. For a strike-slip earthquake at a vertical fault both the relative size of the principal horizontal compression and the relative size of the horizontal principal tension will equal unity. The mechanisms pertaining to the other corners of the square are also given. Note that strike-slip mechanisms are dominating but that there are many clear reverse faulting earthquakes too. In this figure only earthquakes having at least one first motion direction for P-waves, having at least three stations giving spectral amplitudes, and having only 10% of the fault plane solutions as acceptable, are included.

In the earlier earthquake studies for southern Sweden and for Finland Slunga (1981, 1982, 1985), Slunga and Ahjos (1986), and Slunga, Norrman, and Glans (1984), found strike slip faulting on subvertical planes to dominate. Even if strike-slip faulting is dominating also in northern Sweden the many clear reverse faulting events in figure 8 are of great interest. Slunga (1985b) pointed out that in an area of tectonic stress build-up of reverse faulting type large instabilities will be induced in the entire brittle crust during deglaciation. Thus reverse faulting movements are expected at the time of deglaciation as has been reported by Lagerbäck (1979) in northern Sweden. The number of reverse faulting earthquakes may be taken as an indication that an excess of horizontal stresses may have been accumulated by the tectonic processes in the area.

Each fault plane solution gives two possible fault planes. Figure 9a shows the dips of these planes for the northern Sweden earthquakes. Only earthquakes having less than 10% acceptable fault plane solutions have been included.

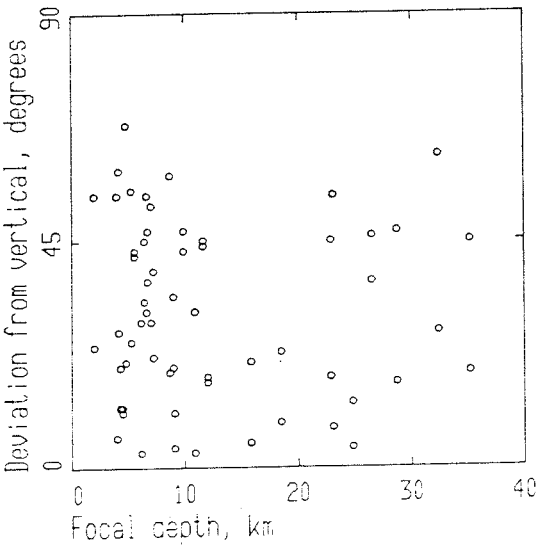

Figure 9a. The dips of planes of the optimum mechanisms for northern Sweden earthquakes. The horizontal axis gives the depth of the earthquake and the vertical axis gives the deviation from the vertical. For each earthquake two circles are given, one for each of the two possible fault planes. Due to the ambiguity one cannot draw very far reaching conclusions from such a diagram but it seems the dips of the fault planes may be similar at all depths.

In figure 9b I give the same type of plot as figure 9a but now for all earthquakes studied by Foa since 1979 and having less than 10% acceptable fault plane solutions. The 162 earthquakes of figure 9b are from southern and northern Sweden, Denmark, and Finland. See the references given in the discussion of the regional stress.

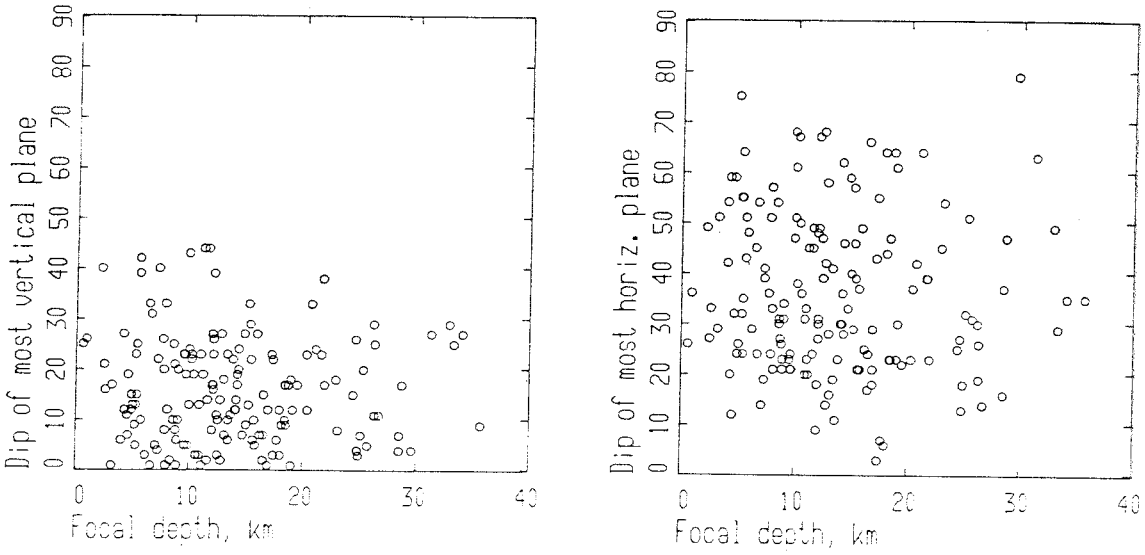

Figure 9b. The two diagrams show dip versus depth for the rather well defined fault plane solutions of 162 earthquakes in Sweden, Finland, and Denmark. The left diagram shows the more vertical fault plane for each earthquake, and to the right the more horizontal ones are shown.

One must remember that figures like figure 9 contain many different possibilities, there may be systematic differencies at different depths between the distribution of the real fault plane on the vertical or horizontal one. It is however obvious that subhorizontal fault planes are very rare but there are some examples within this data set. The most clear is the event at slightly less than 30km depth which is almost purely dip-slip (one fault plane horizontal). This event is from southwestern Sweden.

One can further illustrate the variation of the faulting mechanisms with depth by plotting functions of the relative horizontal principal stresses given by the fault plane solutions and computed as discussed in a previous paragraph. If we define tension as positive and compression as negative the relative horizontal principal stresses, Sh1 (principal compression) and Sh2 (principal tension), will have the following ranges: Sh1 will be -1 to 0, Sh2 will be 0 to 1. Then as previously the size of the relative horizontal deviatoric stress, RS, is defined:

RS = (Sh2 - Sh1) / 2 and be in the range 0 to 1.

Another valuable parameter is the sum, Sh1+Sh2, which will be in the range -1 to 1.

For a strike-slip event on a vertical fault RS=1 and the sum will equal 0. Negative sum values show reverse faulting, crustal compression, and positive values show normal faulting, crustal extension.

In figure 10 these fault mechanism measures are shown for the 162 earthquakes.

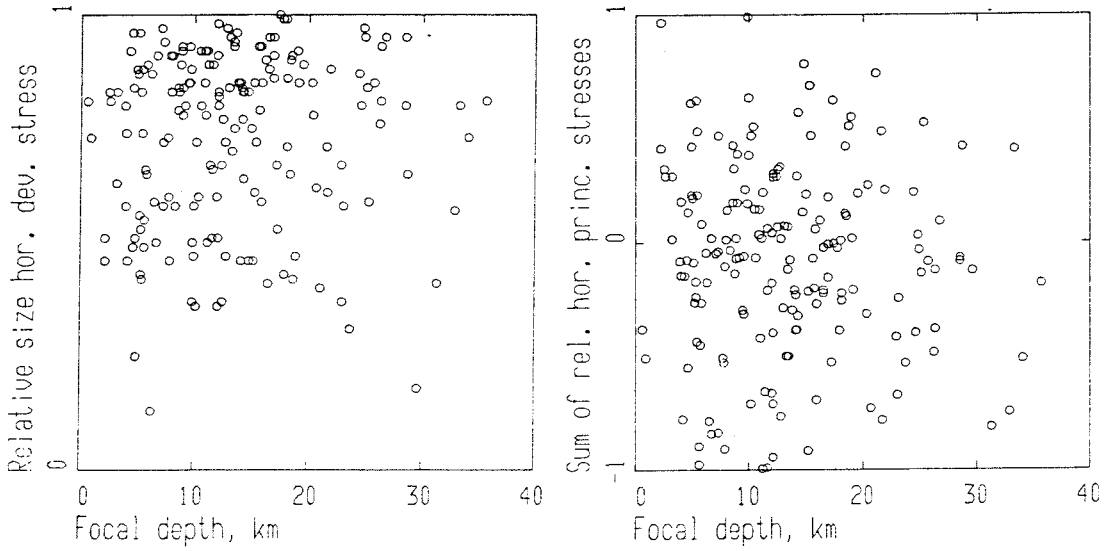

Figure 10. The relative size of the horizontal deviatoric stress, RS, is given to the left, and the arithmetic sum of the relative horizontal principal stresses is given to the right. Each circle denotes the best fitting mechanism of one earthquake. Totally 162 earthquakes are included.

The mean value of the arithmetic sum in figure 10 is -0.06 +/-0.03. Thus there is a weak excess of horizontal compressive stresses in the earthquake stress release in the Baltic shield area. In principle this means that there may be a tectonic land uplift component.

As pointed out by Slunga, Norrman, and Glans (1984) the earthquakes close to the Tornquist line has normal faulting components. If we divide the Baltic shield area we get the following mean values of the arithmetic sum

of the horizontal relative principal stresses:

latitude range	number of earthquakes	mean of the sum		
54-57 N	22	0.080	+/- 0.076	this is the Tornquist area
57-61 N	90	-0.094	+/- 0.045	SW Sweden
65-69 N	34	-0.097	+/- 0.074	N Sweden.

We see that the Tornquist area has an excess of extension (normal faulting) while both SW Sweden and northern Sweden have excesses of compression. The dominating faulting in all regions (but not for all earthquakes) is strike-slip, that means transpression.

3.5 FAULT PLANE SOLUTIONS AND GEOPHYSICAL LINEAMENTS

In the studies of southern Sweden earthquakes it was found many cases where surface bedrock faults fitted very well the fault plane solutions. The best example was a ML=3.2 event at 9 km depth for which the fault plane could be uniquely estimated from the analysis of aftershocks, Slunga, Norrman, and Glans (1984). When this fault plane was extended up to the surface it coincided with a dominating some 30 km long surface fault.

It was also found that the strikes of the fault plane solutions normally were the same as the strikes of the dominating surface faults. A good example of this is the change from N-S-, E-W-faults to NW-SE faults when crossing the Törnquist line from the north, Slunga, Norrman, and Glans (1984).

As shown in figure 2 nine earthquakes are within the map of geophysical lineaments produced by Henkel (1988). I will in the following compare the fault plane solutions of these event to the geophysical lineaments on the map by Henkel. As more events accumulate within the area of main interest (the area close to the Lansjärv fault) more certain conclusions can be drawn.

The earthquakes are in all pictures marked by circles with radii showing the location uncertainty. I will show the intersections of the extended possible fault planes with the surface. These intersections are defined by the location of the earthquake (epicenter and depth) together with the fault plane solution. I will sometimes show all possible fault plane intersections and sometimes only the very best fitting possibilities. The lineaments marked by dots in the following maps just happens to have the right surface position and the right strike. In order to be possible actual fault planes to the earthquake under consideration the dip must also be in agreement. Each fault outside the epicenter circle of the earthquake must have a dip towards the circle and in agreement with the focal depth range and distance from the circle. Only then the surface lineament may really mark the true fault plane of the earthquake. Thus if complete dip information also was available the uniqueness would be better.

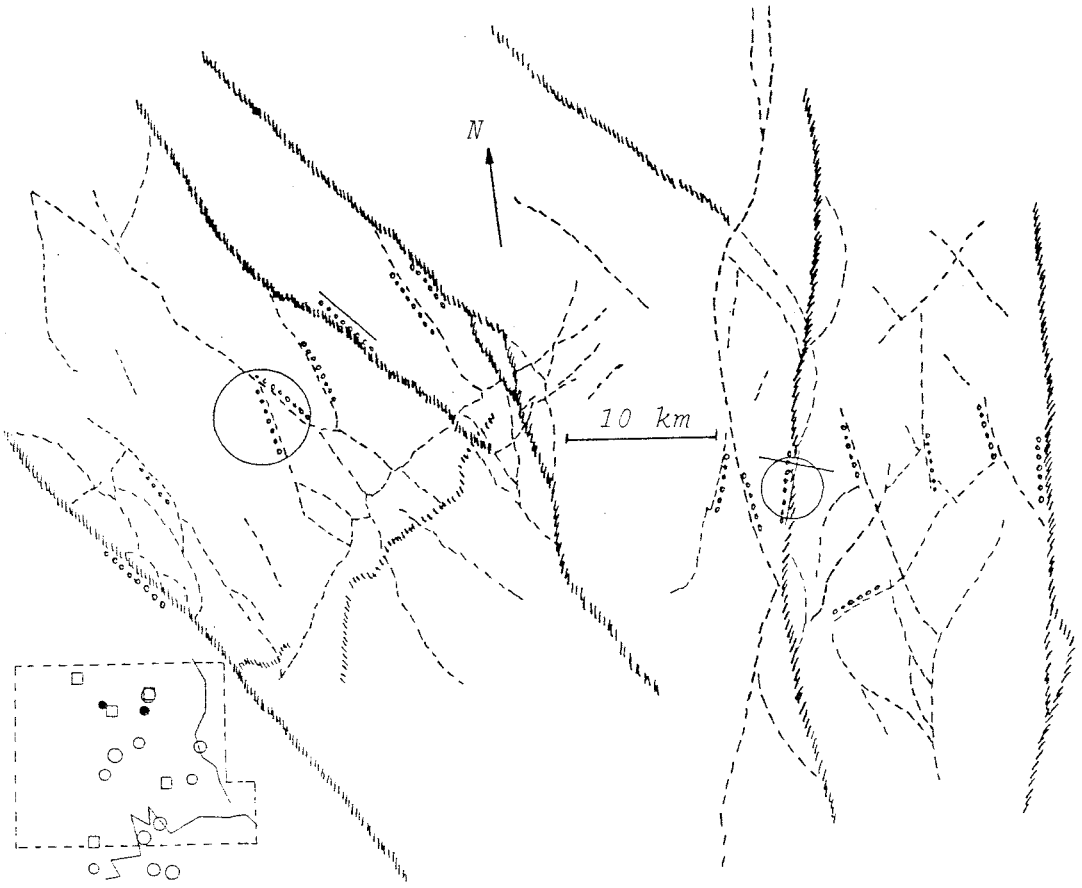

Figure 11. The map shows the results for two earthquakes marked by circles at the epicenters. The radii shows the location uncertainty. The dashed lines are the lineaments on the map by Henkel (1988). The solid straight lines shows the surface intersections of the most likely fault planes for each earthquake, that means the fault plane solution best fitting the observed amplitudes. These events are further discussed in the text. The dotted parts of the lineaments fit the acceptable fault plane solutions of the event. In order to be a possible fault plane intersection for the earthquake the lineament must have the right dip in the direction of the center of the circle.

* The earthquake 880225 1249GMT ML=0.1 (!), deep crust, to the left in figure 11, (map 27L):

  We see that "all" the NW-SE faults are among the possible fault plane intersections as marked by the dotted segments. As the event has a focal depth of 22-27 km it is quite possible that none of the surface lineaments is relevant. However, one should note that one of the three wide zones, the first NE of the epicenter, in the map by Henkel has a dip 60 deg SW at a point 15km north of the epicenter. The dip required by the location and fault plane solution is about 70 deg SW, which is the dip of the very best fitting fault plane solution marked the solid line NE of the epicenter. This indicates a possibly quite good agreement. The major lineament SW of the epicenter, also marked by dots, is dipping 73 deg SW according to Henkel, and thus cannot be the fault plane. The second major lineament to the NE has no dip in the map by Henkel, to fit the earthquake the dip must be 60 deg SW. The smaller fault lineaments are less likely as the event is below the upper seismic layer, 0-13km. In conclusion this deep earthquake seems to give a good fit to one of the major NW lineaments dipping SW.

* The earthquake 880219 2303GMT ML=0.4, upper crust, to the right in figure 11, (map 27L):

  The epicenter of this event is close to one of the major lineaments. This lineament is very similar to one of the fault planes of the best fitting mechanism as marked by the solid lines in the map. The dip from the fault plane solution is very close to vertical. Ten kilometer to the north Henkel give the dip 81 deg E for this fault but he also gives the dip 75 deg W at a point about 8 km south of the epicenter. There may thus be a very good fit between the earthquake analysis and one of the wide zones. Another quite likely candidate marked by dots in the map is the lineament east of the epicenter striking NNW. The dip required, about 60 deg W, is rather common in the map by Henkel. The fault also has a length, 15 km, well in excess of the focal depth, probably 4-12km.

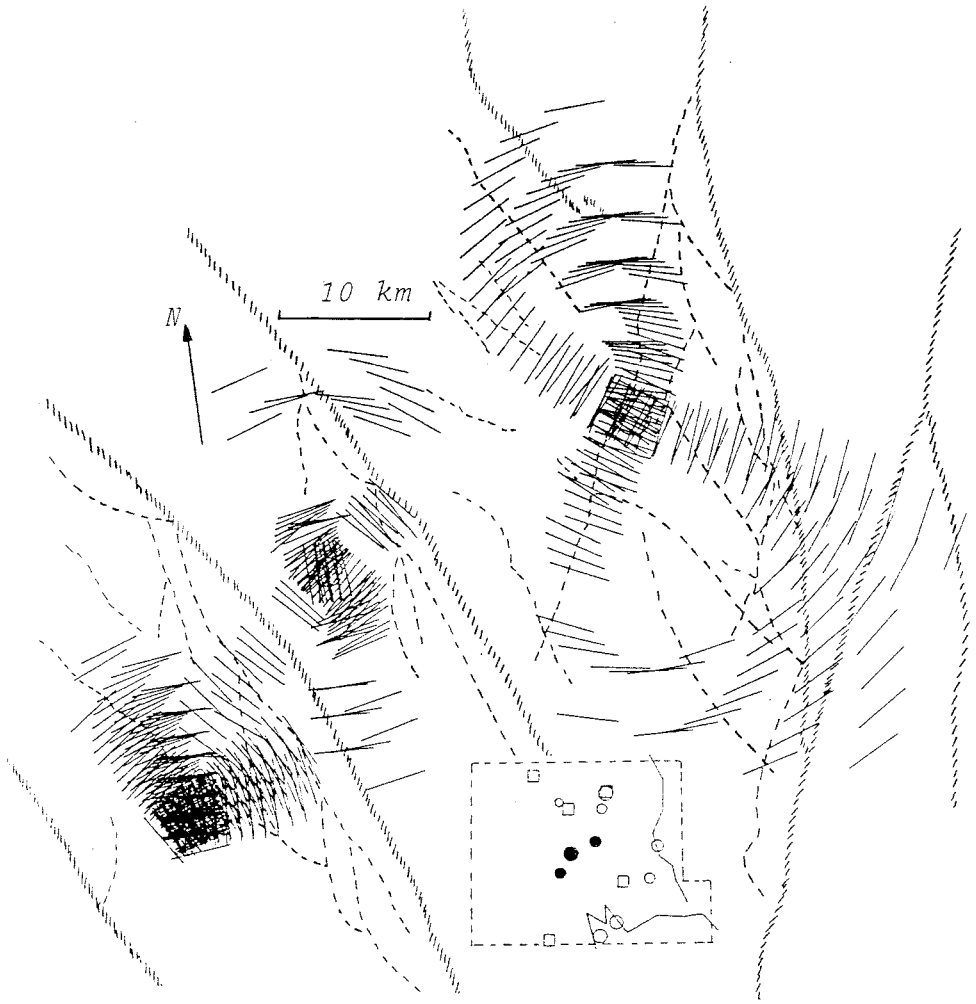

Figure 12a. This figure is similar to figure 11 but for three other events, two in the upper crust and one in middle crust. The circles mark the epicenters of the earthquakes, the radii show the location uncertainty. The solid lines mark in this case all acceptable fault plane intersections with the surface. For reference some lineaments from the map by Henkel (1988) are marked. See further figure 12b where the circles are better visible.

Figure 12b. The lineaments given by Henkel (1988) for the area of the three events of figure 12a. The dotted lines mark the lineaments having positions and strikes that fit the fault plane solutions.

* The earthquake 880404 1748GMT, ML=0.6, middle crust, to the right in figure 12a, b, map 26M:

  The lineament going through the epicenter circle seems to be a likely candidate. However, the dip for a point 10km south of the epicenter is 59 deg W according to Henkel (1988). This makes this lineament less likely. The closest major lineament does not fit. In conclusion there remains no definite candidate although both the NW-SE and NNE-SSW directions of the fault plane solutions are well represented by surface lineaments in the area. There is for instance a lineament NW of the epicenter which, if extended SE, would fit the event.

* The earthquake 880307 1602GMT, ML=1.7, upper crust, the central event in figure 12a,b, map 26L:

  There are no lineaments at all in the close vicinity of the epicenter. A check on the topographic map, 26L SO, shows that the surface topography is dominated by NNW-NW striking lineaments. The wide zone NE of the epicenter is among the possible faults. Its dip direction given by Henkel is also in agreement with the fault plane solution. Also this event may thus be a strike-slip event at a major fault zone. The very best fitting mechanism is however normal faulting at E-W or NE-SW faults which are not seen on the map by Henkel.

* The earthquake 880410 1948GMT, ML=0.7, upper crust, to the left in figure 12a,b, map 26L:

  This earthquake has essentially two possible fault strikes, NNW and ENE. Only the NNW fits the lineaments on the map by Henkel. Two of the three dotted fits are rather curved and at least one of them has totally different dip. Thus the short segment close to the epicenter seems to be a likely candidate. If it is dipping steeply to the west it may be the fault plane of this event. Note however again that the wide zone NE of the epicenter is close to fit the fault plane solution.

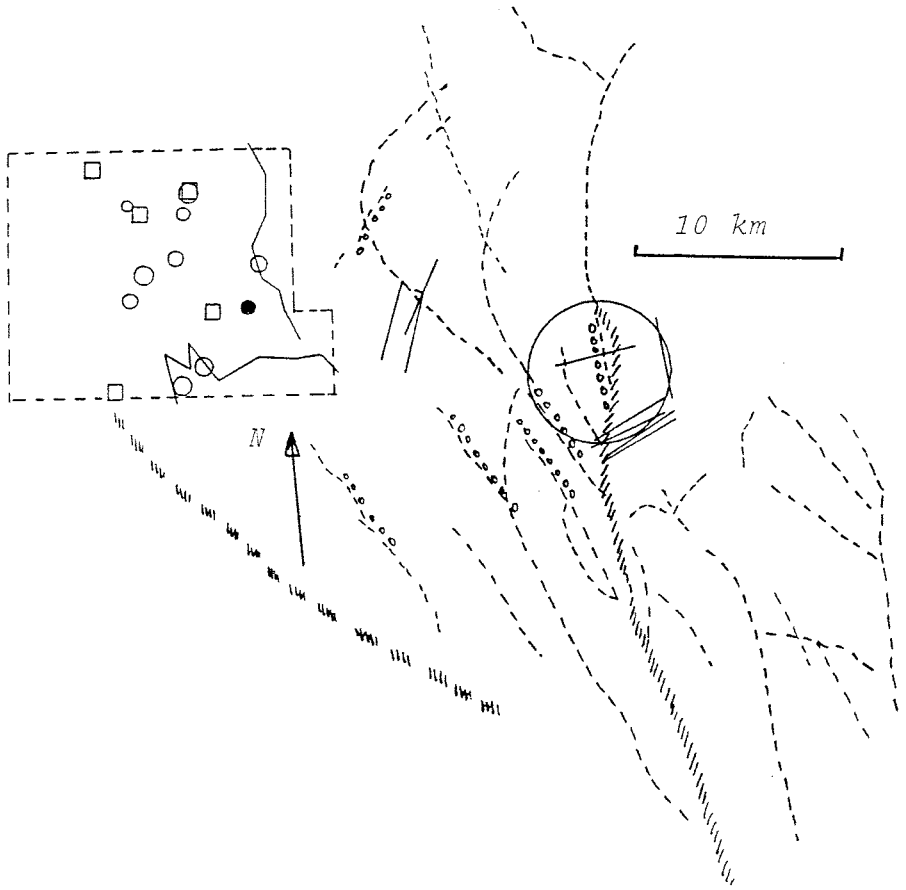

Figure 13. The same as figure 11, and 13. The size of the circle shows the location uncertainty and the solid lines shows the intersections of the extensions of the best fitting fault planes with the surface. The dotted parts of the lineaments indicate that they do fit acceptable fault planes.

* The earthquake 880207 1923GMT, ML=0.6, upper crust, the event of figure 13, map 26M:

  There are four lineaments striking NW-NNW fitting the fault plane solutions. The dips of these lineaments are not known but in order to fit to this earthquake they must be dipping NE with dips 40-90 deg depending on the distance from the epicenter. Note however again that the wide N-S fracture zone passing through the epicenter fits the data of this earthquake provided that the zone is dipping steeply which seems to be the case for these zones.

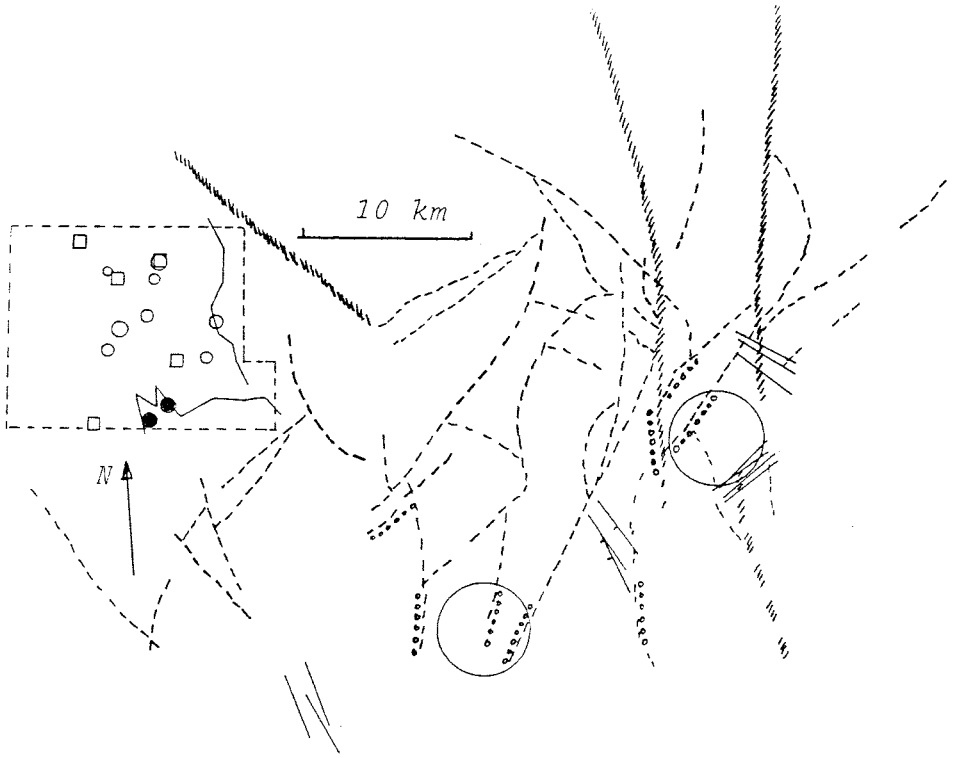

Figure 14. Similar to the previous figure. These two events are just at the southern boundary of the lineament map by Henkel (1988). The solid lines show the best fitting source mechanisms for the events. The dots mark lineaments that fit acceptable source mechanisms.

* The earthquake 880318 1100GMT, ML=1.2, upper crust, the right event in figure 14, map 25M:

  Two main directions are dominating among the acceptable fault planes, NE-SW and NW-SE. Both directions occur in the area. Even if on of the wider zones, W of the epicenter, has been marked by dots it does not give a very good fit. The NNW-SSE zone just south of the epicenter seems more likely if it continues further north. The dip should be almost vertical for a fit.

* The earthquake 871220 1952GMT, ML=1.3, upper crust, the left event in figure 14, map 25M:

  The surface intersections of the extensions of the fault planes proposed by the fault plane solution fit five of the lineaments given by Henkel. We have no dip estimates for these lineaments. The best fitting fault plane intersections give no fit with lineaments. The planes NE of the epicentre may be fitting the extension of the wide NW-SE zone seen NNW of the epicenter. If this zone continues to SE it would very likely be the fault plane.

  One should note that if more earthquake mechanisms are available in the interpretation more unique conclusions can hopefully be made for the individual events. This is at least expected if the earthquakes are part of a consistent deformation of the crust as is indicated by the both this and previous earthquake studies. One can thus expect much more conclusions in the later reports within this project.

  The conclusions of this very preliminary investigation are:

  - the major zones (the wide zones) are in most cases within the sets of possible fault planes

  - the possibility that the earthquakes primarily occur on the major, wide zones cannot be excluded

  - there are events that are likely to have fault planes outside the set of wide zones in the map by Henkel.

3.6 SEISMIC MOMENTS, STATIC STRESS DROPS, FAULT RADII, AND FAULT SLIPS

The seismic moments focal depths and ranges of static stress drops and fault slips are given in appendix 1. The values of these parameters are computed from the estimated corner frequencies. This is discussed by Slunga et al (1984).

In figure 16 the static stress drops, peak slips, and seismic moments are related to the previous seismicity as given by Slunga et al (1984), Slunga and Ahjos (1986), and Slunga and Nordgren (1987).

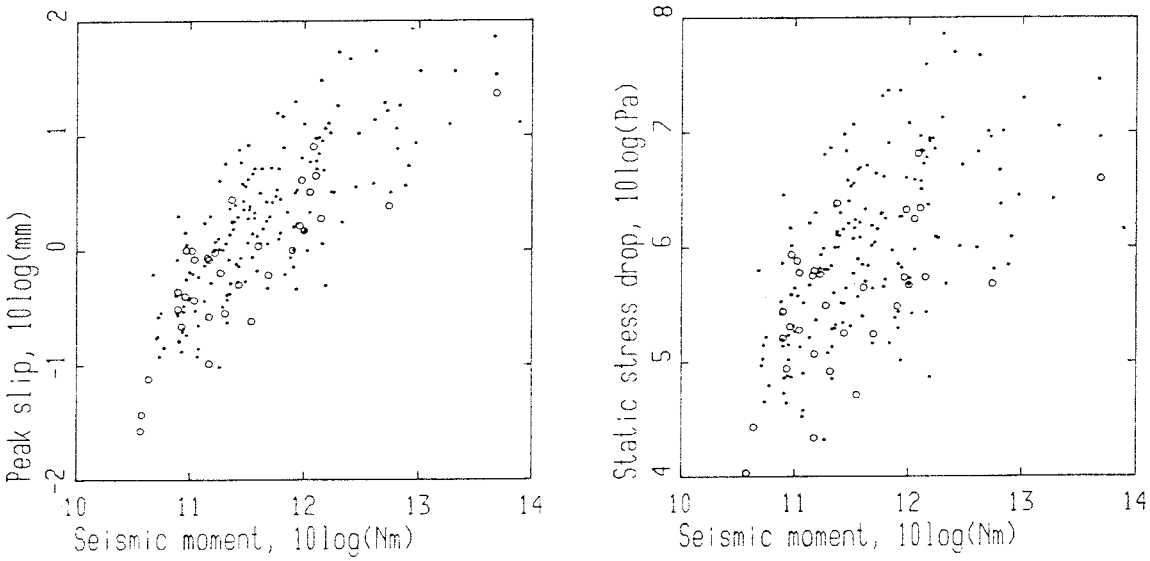

Figure 16. The static stress drops and the peak slips plotted against the seismic moments. The larger circles denote the northern Sweden earthquakes while the smaller circles denote the previous seismicity in southern Sweden, Denmark, and Finland.

The size of the slip at the fault is typically in the range 0.1-3 mm for these small earthquakes. The ML=3.5 event has a slip of 8-30 mm.

Figure 17 shows the depths and seismic moments of the northern Sweden events. It is clear from figure 17 that the detection threshold for the whole Norrbotten area for the present 6-station network is about ML=1, for the central parts (the area of main interest in this project) it is around ML=0.7 during low-noise periods.

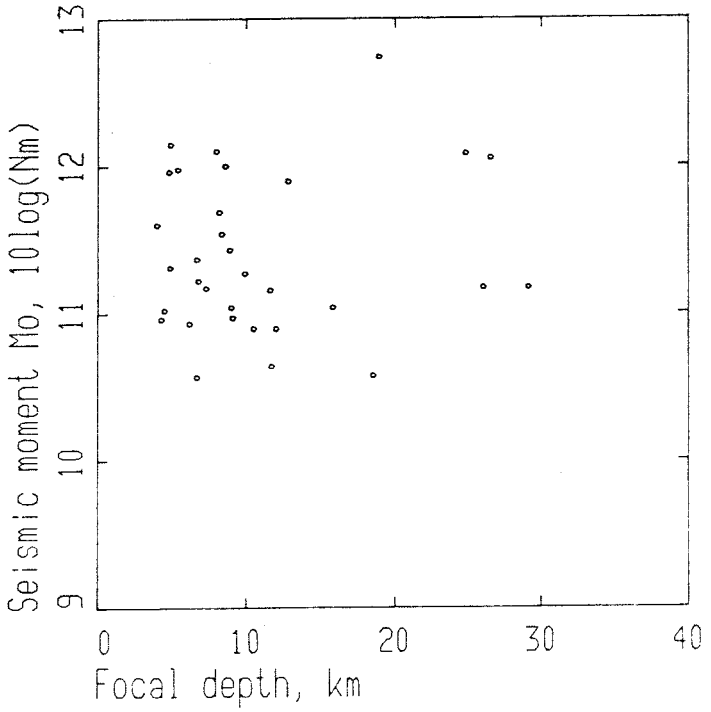

Figure 17. The seismic moments and focal depths of the northern Sweden earthquakes analysed in this report.

4 FAULT MOVEMENTS AND THE BALTIC SHIELD EARTHQUAKES - AN ALTERNATIVE VIEW

In this paragraph I will present some ideas that are quite hypothetical. However, the present knowledge of the seismicity and of the irregularities in land uplift discussed below may be interpreted as leading to the hypothetical view below.

First I summarize some statements representing the present knowledge of relevance for the interpretation of the small Baltic Shield earthquakes:

- mostly strike-slip faulting on subvertical faults, that means mostly horizontal slip
- typically 0.3-10mm peak slip
- the size of the stress drop (static stress drop) does not depend on the depth (for the same size events)
- the earthquake mechanisms indicate a very consistent regional stress field component in agreement with aspects of the plate tectonics
- the estimated fault surfaces are small, diameters less than 300 m for most events
- even earthquakes of magnitudes below ML=1 seems to be part of the same systematic crustal deformations as the larger earthquakes (up to ML=5 so far studied).

The last point may be quite significant. If one looks at the Baltic shield seismicity as a relict from previous more significant crustal deformations one could expect to find a more scattered deformation picture for the very small events. This because they then would be late adjustments around previous larger movements. The remarkable consistency is much more easily understandable if the small events are directly linked to the present large scale tectonic deformations of the crust.

In Finland repeated geodetic levellings have indicated vertical fault movements up to 30 mm at rates of up to the order of 1 mm/year, Talvitie (1977), Veriö (1979, 1982a,b), and Kiviniemi (1980). Veriö gives the following statements:

- vertical relative movements occur correlating with the crustal faults
- movements take place both in seismicly active and nonactive areas.

One example given by Veriö (1982b) is connected to two of the earthquakes studied by Slunga and Ahjos (1986). The Lappajärvi area was levelled 1972 and seven years later 1979, the earthquakes occurred a couple of months before the relevelling. The earthquakes, strike-slip on subvertical faults, both with the same mechanism, had

peak slips of 10-30mm (ML=3.8 and 2.7). The vertical differential displacements were 10mm, which is magnitudes larger than this Mo=1E+14 Nm earthquake will give. It seems likely that considerable aseismic faulting (creep) has taken place between the levellings. This aseismic faulting seems to have been of the same mechanism and on the same fault as the earthquakes at the end of the period. In order to get the geodeticly observed vertical displacements the whole fault at a length of about 20 km must have slipped about 100 mm. This is of the same order of size as the estimated seismic peak slip of 30 mm. It thus seems possible to interprete the earthquakes as asperities locked during the aseismic sliding and then suddenly slipping seismicly. This is the simplest way to interprete the remarkable geodetic observations.

In a recent study of geodetic levelling data in Estonia Vallner et al (1988) stated that the area can be divided in crustal blocks exhibiting different vertical movements and tilting. If these differential block movements are interpreted as fault movements and compared to the seismic activity, (the largest earthquake for 350 years was the 1976 earthquake with the seismic moment 3.5E+15 Nm, Slunga (1979)), one finds that the geodetic (aseismic) fault movement is at least 20000 times more extensive than the seismic fault movements.

In southern Norway both Bakkelid (1986) and Anundsen (1988) found by geodetic measurements aseismic fault movements of about 1 mm/year vertically. Anundsen (1988) found also 1 mm/year horizontal fault movements.

In conclusion there are several indications from Fennoscandia and the neighbouring countries of extensive aseismic fault movements of the order of 10000 times more extensive than the seismicly observed fault movements.

That a fault sliding movement is aseismic means just that it cannot be detected by seismic measurements. This means that it does not produce earthquakes large enough to be detected. It is well known that significant aseismic fault sliding occurs in the form of stable sliding in many parts of the world even if it probably is best studied in California.

The results summarized above suggest the following view on the Baltic shield faulting:

- most of the fault movements is episodic aseismic sliding (creep, stable slip) along the crustal faults
- the earthquakes are small areas (asperities) that happen to be locked during the aseismic fault movements and suddenly break
- the fault area sliding aseismicly before an earthquake occurs (if parts of the fault is locked by an asperity)

may be up to more than 10000 times larger than the estimated earthquake fault area
- the most interesting geophysical parameter for these small Baltic shield earthquakes is then not the seismic moment but the peak slip as it gives information about the size of the aseismic fault movement.

In conclusion the earthquakes possibly occur when the aseismic slip is locked by asperities which then fail. The estimated peak slip will then be a lower bound for the size of the aseismic fault slip preceeding the earthquake.

This view on the Baltic shield earthquakes points out the possibilty of a dominating role played by the aseismic sliding. The seismic event only shows that sliding has occurred and gives the fault plane orientation, the direction of the slip, and a lower bound of the aseismic slip during the sliding event.

The concept of aseismic sliding preceeding the later asperity failures giving rise to earthquakes is simple and makes the earthquakes easily understandable. The problems are pushed to the understanding of the aseismic sliding, its mechanisms and general behaviour. This understanding is in fact quite good and numerical models for fault behaviour based on laboratory results of rock sliding have been quite successful (Tse and Rice (1986), Stuart (1988)). These models give both seismic and aseismic fault movements.

In a study of the Californian seismicity Wesson and Nicholson (1988) gave the following statements:

- larger earthquakes along faults exhibiting fault creep tend to occur at the ends of creeping sections

- large earthquakes tend to occur adjacent to previous large earthquakes

- the occurrence of any significant earthquake increases the intermediate-term probability of future earthquakes on adjacent fault segments.

All these three statements will be included if one accepts the following statement:

- slip (seismic or aseismic) on a fault segment (block) will increase the probability to have slip (earthquake or creep) on adjacent fault segments (blocks).

This is the basic idea behind the efforts to estimate the extension of the aseismic fault slip from the spatial distribution of the Swedish earthquakes as done by Slunga (1988). In this kind of investigation one requires a sufficient number of accurately located

earthquakes. The idea behind this investigation is as follows:

- it is likely that after an earthquake there will be an increased probability to have a following earthquake on the very same fault close to the border of the previously sliding area (seismic or aseismic) as the stress will be increased there (the domino theory discussed above).

In the case that all fault sliding is seismic there must be expected to exist an increased probability to have the following earthquake very close to the preceeding one, the distance should be of the order twice the radius of the fault area of the earthquakes. One thus expects a distance dependance with increased earthquake probability at very small distances for the earthquakes following any given earthquake. In the case that the earthquakes are asperities on mostly creeping faults one would expect no such increased probability at close distances.

One assumption that must be made (due to the short time period for which we have good data) is that the seismic preparation time (the time between stress concentration and earthquake) is less than about one year. This seems quite reasonable as the earthquakes are quite small, in most cases less than ML=2.

For each earthquake I computed the distance to the closest later earthquake. This was done for southwestern Sweden, 100 earthquakes. In one case no restriction was put on the closest later event, in the other case I required that the later event had to have an acceptable fault plane solution fitting a plane through the hypocenters of the events and that also the first event should have a similar fault plane solution among its range of acceptable fault plane solutions. This later case means that complete consistancy with the basic idea, that the two events are on the same fault plane and due to a similar fault slip, was required. See figure 18.

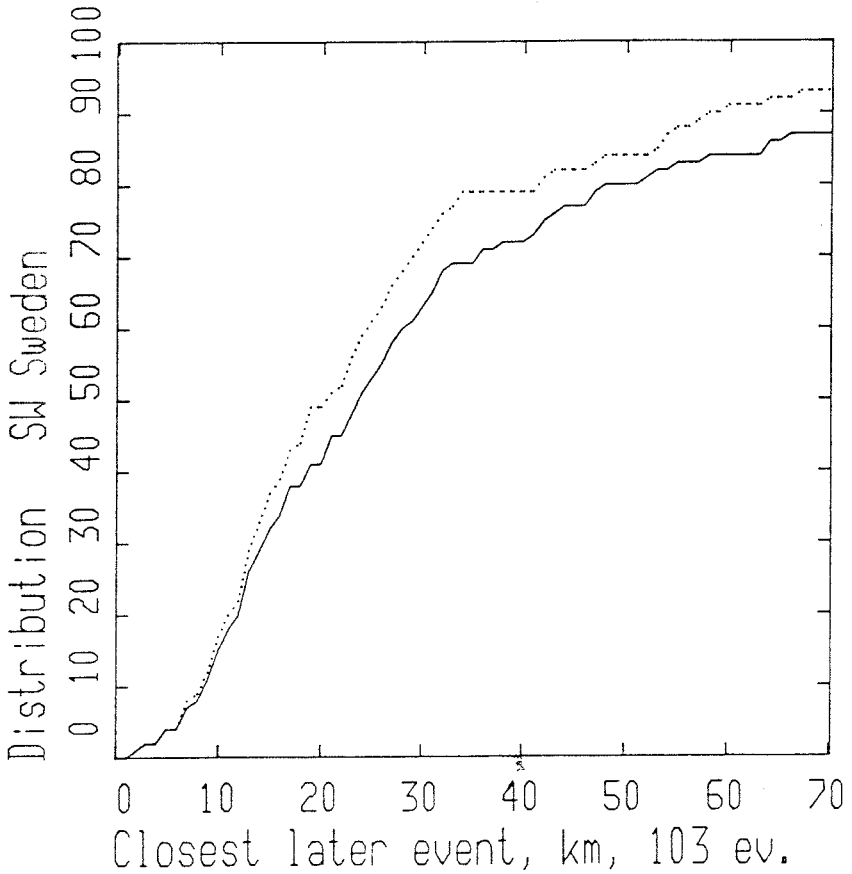

Figure 18. The figure is based on the main earthquakes in southwestern Sweden, 54-61 deg north, 10-14.5 deg east, totally 100 events during 1980-1984. The x-axis gives the 3D-distance to the closest later event, the y-axis gives the accumulated distribution. The diagram shows the two observed distributions, the dotted line with no fault plane restriction, the solid line requiring consistancy with the main idea that the two events have similar source mechanisms and are on the same fault plane.

In figure 19 the two observed distributions of figure 18 is compared to two theoretical laterally uniform distributions. The depth distribution is assumed to be the one defined by the actual depth distribution of the 100 events involved and is also given in figure 19. One of the theoretical distributions assumes laterally uniform three-dimensional (3D) distribution of the events, the other assumes laterally uniform distribution over a plane through the event, that means a laterally

uniform two-dimensional (2D) distribution. The 2D-distribution is what we would expect for the proposed asperity model if the asperities have a laterally uniform distribution on the fault planes.

We see from figure 19 that at larger distances the upper observed distribution (no fault plane restrictions) gives a good fit to a three-dimensional distribution up to about 35 km. For larger closest event distances there is a clear deviation from also the uniform three-dimensional distribution (the events are not uniformly distributed over the whole SW Sweden area). For closer distances there is an excess of events. From the comparison with the 2D-distribution we can conclude:

- there is no indication of an increased earthquake probability in the close vicinity (less than 7km) of an earthquake (this is the most important conclusion and a very strong support for my proposed model for the earthquake generation)

- there is an increased earthquake probability in the distance range 9-15km (this may be taken as an indication of a crustal block structure of 9-15km typical dimension if the seismic events are close to block corners (fault intersections)).

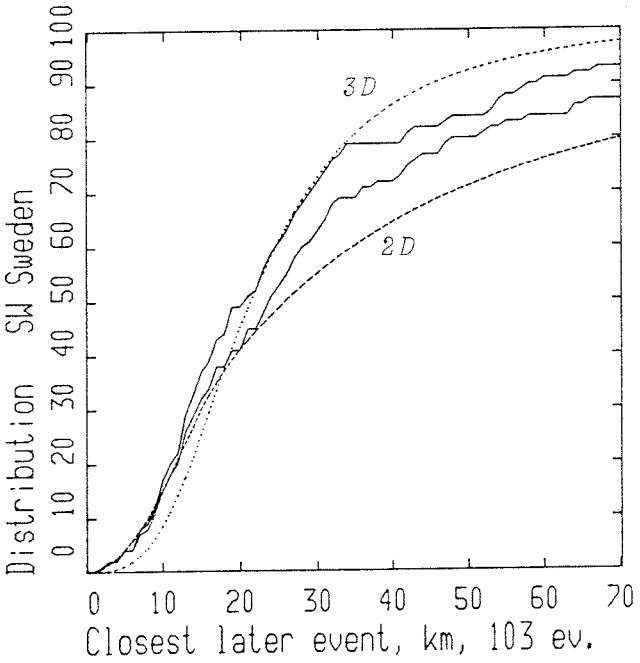

Figure 19. The two solid lines are the two observed distributions of figure 18. The dashed line is the theoretically expected distribution for events having a laterally uniform 3D distribution. The dotted line is

the expected distribution for events having a laterally uniform 2D (plane) distribution. The depth distribution of these 100 events is given by the diagram to the right.

From fitting the 2D-distribution to the observed distribution in figure 19 one can estimate the fault length of aseismic slip per earthquake. If the basic assumptions are reasonable (as they seem to be) the estimated length of the sliding fault segment per earthquake is 23-25km depending upon if the upper or lower observed curve is used. The discrepancy between this value and the typical spacing of the earthquakes (9-15km) can be taken as an indication that for this data set (ML down to 1.3) not all of the "block segments" sliding caused a detected earthquake.

One consequence implicit in my proposed model is that the earthquakes occur on faults having lengths of at least 9-15km. This is in agreement with the observations that the earthquake fault planes in SW Sweden has the same orientation (mostly N-S and E-W) as the major faults in the area.

The consequences on the estimated crustal deformations by the view presented here can easily be roughly estimated. During the five years of measurements in the southwestern Sweden about 20 main (aftershocks and swarms represented by the main event) earthquakes per year occur with a mean peak slip of 1.3mm. Based on the hypothetical view on the earthquake generation presented here each of these earthquakes can be taken as an indication of an event of aseismic fault sliding at least an amount of 1.3mm. If this sliding is assumed to have affected the whole fault at a length of 23 km it will mean that a total fault length of 460 km moves 1.3 mm per year. Distributed over a fault length of 600 km (sothern Sweden) it means that the extreme points of southern Sweden move 1 mm relative to each other per year. In achieving this result one must also rely on the observed consistency of the fault plane solutions of the SW Sweden events.

The real rate of deformation can be quite different from this speculative example as it contains many implicit assumptions:

- the estimated peak slips may be biased (they are rather uncertain in general) and/or the fault slip may often be larger than the seismic slip
- some faults may be sliding without any seismicity at all (for instance the lack of seismic events on the Protogene zone may possibly be due to the mechanical properties of the zone).

What is interesting to note is that arguments based completely on the analysis of the microseismicity may lead to estimate of the horizontal crustal deformations

in SW Sweden of the orders of 1 mm per year. This is in remarkable agreement with the statement by Kakkuri at the symposium on neotectonics in Lejondal Sept 1988 that the geodetic measurements in Finland indicates a horizontal crustal deformation with a rate of 1 mm/year per 10-100km.

Geodetic monitoring may give answers to the many questions about the role of the aseismic fault movements and clarify the real rate of the Baltic shield crustal deformations. Note however that it will be essential to continue the monitoring of the microseismicity as geodetical measurements seldom can be extensive enough for a unique interpretation, together with seismic monitoring the interpretation will be much stronger.

I also want to mention that the view on the Baltic shield seismicity discussed here explains why the very small and by themselves insignificant ML=1 earthquakes show such a consistent fault mechanism pattern. Within the view given here they are seismic manifestations of much more significant aseismic fault movements.

Finally, the view on the Baltic shield seismicity presented here is not the only possible one at the present stage. It is however in agreement with many aspects of the seismicity and of the geodeticly observed crustal movements. This makes it one of the main hypothetical models to have in mind in planning further research.

5 REFERENCES

Anundsen, K., (1988). Variations in Quaternary (Late Weichselian relative sea-levels in southwest Norway; observations of isostatic/eustatic movements and active faulting. Paper presented at the Neotectonics Symposium at Lejondal Sept 5-6 1988. (Karl Anundsen, Dept. of Geology, Section B, Univ. of Bergen, N-5007 Bergen, Norway).

Bakkelid, S., (1986). The discovery in Norway of a strongly active geological fault and some of its practical consequences. Proceed. of the 100th General Meeting of the Nordic Geodetic Commission, Sept-Oct, Helsinki, pp 237-245.

Båth, M. (1956). An earthquake catalogue for Fennoscandia for the years 1891-1950. Sveriges Geologiska Undersökning, Avhandlingar och uppsatser, C 545, Stockholm.

Båth, M. (1979). Earthquakes in Sweden 1951-1976. Sveriges Geologiska Undersökning, Avhandlingar och uppsatser, C 750, Uppsala.

Ben-Menahem, A., and Singh, S.J. (1972). Computation of models of elastic dislocations in the earth, in Methods in Computational Physics, 12, pp. 299-375, Academic Press, New York.

Boatwright, J. (1980). A spectral theory for circular seismic sources; simple estimates of source dimension, dynamic stress drop and radiated seismic energy. Bull. Seism. Soc. Am., 70, pp. 1-27.

Brune, J.N. (1970). Tectonic stress and the spectra of seismic shear waves from earthquakes. J. Geophys. Res., 75, pp. 4997-5009.

Cook, N.G.W. (1981). Stiff testing machines, stick slip sliding, and the stability of rock deformation. In Mechanical Behaviour of Crustal Rocks, Geophysical Monograph 24, AGU Washington D.C., pp. 93-102.

Eshelby, J.D. (1957). The determination of the elastic field of an ellipsoidal inclusion and related problems. Proc. Roy. Soc. London, 241, pp. 276-296.

FENCAT (1987). Fennoscandian seismic event catalogue. Compiled by Institute of Seismology, University of Helsinki.

Henkel, H., Hult, K., Eriksson, L., and Johansson, L. (1983). Neotectonics in northern Sweden - geophysical investigations. SKBF/KBS Technical report 83-57, Swedish Nuclear Fuel and Waste Management Co, Box 5864 10248 Stockholm.

Henkel, H. (1988). Tectonic studies in the Lansjärv region. SKB Technical Report 88-07, Stockholm.

Hill, D.P. (1982). Contemporary block tectonics: California and Nevada, J. Geophys. Res., 87, pp. 5433-5450.

Lagerbäck, R. (1979). Neotectonic structures in northern Sweden. Geol. Fören. i Stockholm Förh., 100, pp. 263-269.

Lagerbäck, R., Witschard, F. (1983). Neotectonics in northern Sweden - geological investigations. SKBF Teknisk Rapport 83-58.

Madariaga, R. (1976). Dynamics of an expanding circular fault. Bull. Seism. Soc. Am., 66, pp. 639-666.

McKenzie, D.P. (1969). The relation between fault plane

solutions for earthquakes and the directions of the principal stresses, Bull. Seism. Soc. Am., 59, pp 591-601.
Savage, J.C. (1974). Relation between P-wave and S-wave corner frequencies in the seismic spectrum. Bull. Seism. Soc. Am., 64, pp. 1621-1627.
Seismology 1984 (1985). Annual report from the division of applied seismology, Foa 2, 10254 Stockholm.
Silver, P.G. (1983). Retrieval of source-extent parameters and the interpretation of corner frequency, Bull. Seism. Soc. Am., 73, pp. 1499-1511.
Slunga, R.S. (1979). Source mechanism of a Baltic earthquake inferred from surface wave recordings, Bull. Seism. Soc. Am., 69, pp. 1931-1964.
Slunga, R.S. (1981a). Earthquake source mechanism determination by use of body-wave amplitudes - an application to Swedish earthquakes. Bull. Seism. Soc. Am., 71, pp. 25-35.
Slunga, R.S. (1981b). Fault mechanisms of Fennoscandian earthquakes and regional crustal stresses. Geol. För. i Stockholm Förhandlingar, 103, pp. 27-31.
Slunga, R. (1981c). Focal mechanisms of earthquakes in Scandinavia - A review. Earth evolution sciences, 1, pp. 61-65.
Slunga, R.S. (1982). Research on Swedish earthquakes 1980--1981. FOA Report C 20477-T1.
Slunga, R.S., Norrman, P. and Glans A.-C. (1984a). Baltic shield seismicity, the results of a regional network. Geophys. Res. Letters, 11, pp. 1247-1250.
Slunga, R.S., Norrman, P. and Glans A.-C. (1984b). Seismicity of southern Sweden. FOA Report C 20543-T1.
Slunga, R.S. (1985). The seismicity of southern Sweden, 1979-1984, final report. Foa report C 20572-T1, April 1985, ISSN 0347-3694, Stockholm.
Slunga, R.S. (1985b). Research on bedrock stability, (in Swedish), Foa report C 20578-T1, ISSN 0347-3694.
Slunga, R., and Ahjos, T. (1986). Fault mechanisms of Finnish earthquakes, crustal stresses and faults. Geophysica, 22 1-2, pp. 1-13.
Slunga, R., and Nordgren, L. (1987). Earthquake measurements in southern Sweden Oct 1, 1986 - Mar 31, 1987. SKB Technical Report 87-27, Swedish Nuclear Fuel and Waste Management Co, Box 5864 10248 Stockholm.
Stuart, W. D. (1988). Forecast model for great earthquakes at the Nankai Trough Subduction Zone. PAGEOPH vol 126, pp 619-641.
Talvitie, J. (1977). Seismotectonics of northern Finland and the Fennoscandian shield. Univ. of Oulu, Dep. of Geophysics, Contrib. 82.
Tse, S. T., and Rice, J. R. (1986). Crustal earthquake instability in relation to the depth variation of frictional slip properties. J. Geophys. Res. 91, pp 9452-9472.
Vallner, L., Sildvee, H., and Torim, A. (1988). Recent crustal movements in Estonia. Journal of Geodynamics, vol 9, pp 215-233.
Veriö, A. (1979). Problemet med rörelser i jordskorpan vid

grundavvägning i Finland (Problems with crustal movements in connection with levellings in Finlans). Det åttende nordiske geodetmöte, Bind 2, Oslo.

Veriö, A. (1982a). Muhoksen montun muotuilua (Remodelling of the Muhos grave). Geologi 2/82, Vammela.

Veriö, A. (1982b). På jakt efter den obekanta mekanismen i landhöjningen. Nordiskt symposium: Landhöjning och kust-bygdsförändring Luleå 2-4 juni 1982, symposiepublikation volym 1.

Wahlström, R. (1978). Magnitude scaling of earthquakes in Fennoscandia, Seismological Institute, Uppsala University, Report 3-78.

Wesson, R. L., and Nicholson, C. (1988). Intermediate-term, pre-earthquake phenomena in California 1975-1986, and preliminary forecast of seismicity for the next decade, PAGEOPH, vol 126, pp 407-446.

APPENDIX 1

THE EARTHQUAKE SOURCE PARAMETERS AND FAULT PLANE SOLUTIONS

The source parameters of the following earthquakes are given:

Date	Origin time GMT	Epicenter lat N	long E	Focal depth (km)	Seismic moment (Nm)	ML
871011	060123.8	66.336	19.892	(26.0)	0.15E+12	1.2
871017	040638.8	66.742	22.878	8.2	0.35E+12	1.5
871017	072913.7	64.316	20.895	(18.9)	0.55E+13	2.7
871220	195226.7	65.675	22.500	9.9	0.19E+12	1.3
871226	0829 8.1	67.759	19.552	4.8	0.49E+14	3.6
871229	165643.5	67.754	19.562	4.8	0.92E+12	2.0
871230	032452.3	65.391	22.947	11.6	0.14E+12	1.2
880104	144335.8	65.280	22.528	4.5	0.10E+12	1.0
880108	081423.1	67.537	21.575	26.5	0.11E+13	2.0
880110	104938.1	67.454	22.341	4.0	0.40E+12	1.6
880118	063436.0	67.247	23.723	15.8	0.11E+12	1.0
880131	050212.2	66.756	19.195	24.8	0.12E+13	2.1
880202	111321.0	67.491	21.889	6.8	0.17E+12	1.2
880206	145134.2	67.560	22.210	12.0	0.79E+11	0.9
880206	201544.0	67.651	19.363	4.9	0.20E+12	1.3
880207	192256.2	66.071	23.517	6.7	0.37E+11	0.6
880208	074844.3	67.703	23.358	(6.7)	0.24E+12	1.4
880219	2303 4.8	66.631	22.782	6.9	0.53E+11	0.7
880225	1249 9.3	66.701	21.993	24.6	0.12E+11	0.1
880227	0637 1.8	64.885	21.032	21.6	0.17E+13	2.2
880229	140826.5	64.690	22.730	4.9	0.14E+13	2.1
880304	215050.5	65.480	21.538	11.7	0.44E+11	0.6
880307	160227.2	66.312	22.133	8.4	0.48E+12	1.7
880318	110014.8	65.767	22.820	7.3	0.15E+12	1.2
880322	040537.3	67.486	22.261	10.5	0.80E+11	0.9
880322	202832.8	67.463	24.287	5.4	0.95E+12	2.0
880322	235836.0	65.426	22.609	9.1	0.93E+11	1.0
880329	060737.5	67.952	19.390	(12.8)	0.79E+12	1.9
880330	022112.1	65.220	20.032	8.0	0.12E+13	2.1
880330	120635.0	67.518	22.413	8.9	0.27E+12	1.4
880401	013610.5	67.493	22.194	9.0	0.11E+12	1.0
880404	022522.9	67.779	19.621	8.2	0.49E+12	1.7
880404	023316.2	67.662	22.114	8.6	0.10E+13	2.0
880404	174834.8	66.387	22.601	18.5	0.38E+11	0.6
880407	212431.6	67.974	20.781	29.1	0.15E+12	1.2
880408	185110.0	67.539	22.665	4.3	0.91E+11	1.0
880410	194810.6	66.175	21.904	(9.6)	0.47E+11	0.7
880416	175634.4	66.312	23.738	6.2	0.85E+11	0.9

For each event the following are given:

The arrival time observations and the results of the location algorithm.

The input data to the fault plane inversion, first motion directions and spectral amplitudes for vertical P and S.

The output of the fault plane inversion algorithm: the dynamic source parameters, the very best fitting fault mechanism, and statistical information.

Plots showing all acceptable orientations of the P- and T-axes and of the fault plane normals. These are given in equal area projections of the lower hemisphere. A fourth circular diagram gives all acceptable relative horizontal deviatoric stresses. This plot of the horizontal deviatoric stress is symmetric around the center of the circle, each point marked in the circle is an endpoint of a line going through the center to corresponding symmetrical point. The lines marked by the endpoints gives the orientation and relative size of the horizontal deviatoric stresses for acceptable solutions. The relative size is 1 for a diameter (strike slip on a vertical fault). The orientation of the line gives the orientation of the principal horizontal compression, the principal horizontal tension is normal to the line.

The marks in the plots of the P- and T-axes and of the horizontal deviatoric stresses have the following meaning:

O well fitting mechanism
0 optimum mechanisms.

The marks in the plot of the fault plane normals mean:

R well fitting right-lateral plane
L well fitting left-lateral plane
b well fitting plane both right- and left-lateral
0 best fitting planes.

ORIGIN TIME 87 10 11 06H 01M 23.8S +/- 0.65S
LATITUDE 66.336 +/- 0.012 DEG.
LONGITUDE 19.892 +/- 0.094
FOCAL DEPTH 26.0 +/- 24.2 KM

STA		ARR. TIME	RES.	WEIGHT	DIST.	AZIMUTH	
HAK	P	06 01 39.85	-0.03	28.0	98.9	47.6	P UP
HAK	S	06 01 52.11	0.21	1.8	98.9	47.6	
VMK	P	06 01 40.98	0.02	26.1	106.3	132.8	P DOWN
VMK	S	06 01 53.65	-0.17	1.7	106.3	132.8	
KLX	P	06 01 46.71	0.01	18.9	144.7	100.5	
KLX	S	06 02 3.79	-0.11	1.1	144.7	100.5	

INPUT DATA FOR FAULT PLANE SOLUTION

STN	DIST. KM	AZIMUTH DEGREES		OMEGA(PZ) METER-SEC	OMEGA(SZ) METER-SEC
HAK	99.	47.8	+	0.16E-09	0.34E-09
VMK	107.	132.9	-	0.11E-09	0.22E-09
KLX	145.	100.7		0.14E-09	0.85E-09

DYNAMIC SOURCE PARAMETERS

SIZE MEASURES
SEISMIC MOMENT: 0.149E+12 Nm
LOCAL MAGNITUDE: 1.2

SHEAR WAVE CORNER FREQUENCY RANGE AT CLOSE DISTANCES (130km)
10.1Hz -19.5Hz (14.4Hz)

FAULT RADIUS RANGE 35m - 68m (47m)

STRESS DROP RANGE 0.20MPa - 1.47MPa (0.59MPa)

RANGE OF THE PEAK SLIP AT THE FAULT 0.4mm - 1.3mm (0.7mm)

THE ORIENTATION OF THE RELAXED STRESS

	AZIMUTH	DIP	
P-AXIS	167.	28.	degrees
T-AXIS	75.	3.	

THE HORIZONTAL DEVIATORIC STRESS AS GIVEN BY THE P- AND T-AXES
THE AZIMUTH OF COMPRESSION -14 degrees
THE RELATIVE SIZE 0.89

THE TWO POSSIBLE FAULT PLANES

	STRIKE	DIP	SLIP
PLANE A	124.	72.	22. degrees
PLANE B	207.	111.	199.

THE NORMAL DIRECTIONS OF THE FAULT PLANES

	AZIMUTH	DIP	
PLANE A	214.	18.	degrees
PLANE B	117.	21.	

STATISTICAL INFORMATION

OF 2 FIRST MOTION POLARITY OBSERVATIONS
AT LEAST 2 ARE REQUIRED TO FIT

THE OPTIMUM MECHANISM HAS 0 POLARITY MISFITS

AMPLITUDES FOR P AND S AT 3 STATIONS ARE USED
ONLY MECHANISMS GIVING AN ESTIMATED STANDARD
DEVIATION OF THE AMPLITUDE ERROR FACTOR OF LESS
THAN 1.60 FOR SINGLE P-WAVE OBSERVATIONS ARE
TAKEN AS ACCEPTABLE AND INCLUDED IN THE FIGURES

4.26 % OF ALL MECHANISMS ARE ACCEPTABLE
32.8 % ACCEPTABLE DUE TO FIRST MOTION OBSERVATIONS
13.0 % OF THESE FITTED ALSO THE AMPLITUDES
THE PART OF WELL FITTING PLANES IS 39.7%

THE AMPLITUDE FIT OF THE OPTIMAL MECHANISM
GIVES A MEAN ERROR FACTOR OF 1.24
THIS CORRESPONDS TO A STANDARD DEVIATION FACTOR OF 1.45
FOR SINGLE P-WAVE OBSERVATIONS

THE DOUBLE COUPLE SOLUTION IS SIGNIFICANT
AT 44 % LEVEL
(F-VALUE: F(5, 2) = 1.57)

THE MEASURE OF THE MISFIT TO AN EARTHQUAKE SPECTRUM
P-WAVES 0.21
S-WAVES 0.22

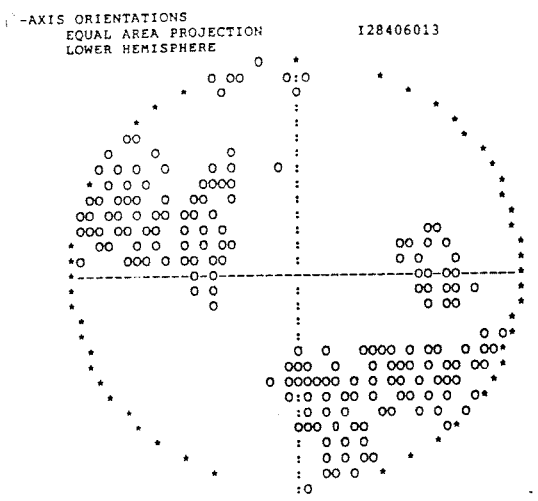
-AXIS ORIENTATIONS
EQUAL AREA PROJECTION
LOWER HEMISPHERE
I28406013

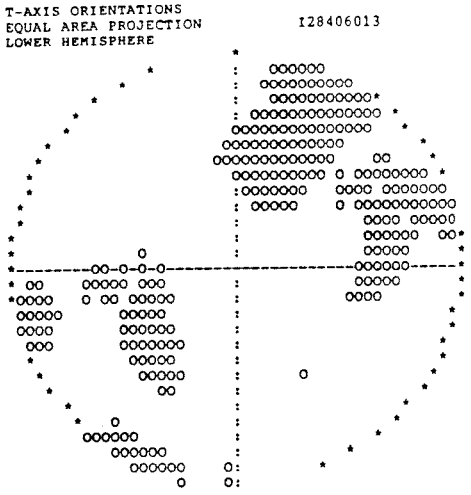
T-AXIS ORIENTATIONS
EQUAL AREA PROJECTION
LOWER HEMISPHERE
I28406013

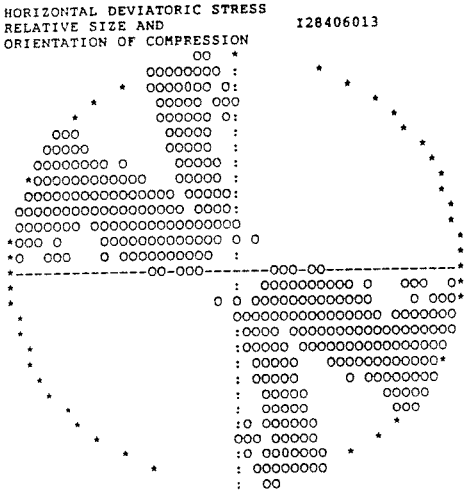
HORIZONTAL DEVIATORIC STRESS
RELATIVE SIZE AND
ORIENTATION OF COMPRESSION
I28406013

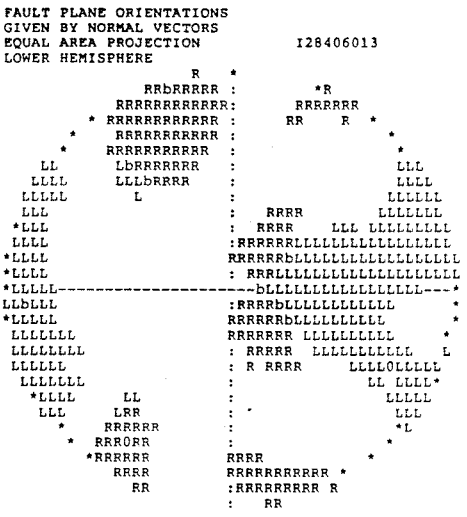
FAULT PLANE ORIENTATIONS
GIVEN BY NORMAL VECTORS
EQUAL AREA PROJECTION
LOWER HEMISPHERE
I28406013

ORIGIN TIME 87 10 17 04H 06M 38.8S +/- 0.67S
LATITUDE 66.742 +/- 0.025 DEG.
LONGITUDE 22.878 +/- 0.113
FOCAL DEPTH 8.2 +/- 4.9 KM
HAK no Rg

STA		ARR. TIME	RES.	WEIGHT	DIST.	AZIMUTH	
HAK	P	04 06 48.89	-0.04	41.5	61.4	289.5	P UP
HAK	S	04 06 56.59	0.17	3.0	61.4	289.5	
KLX	S	04 07 0.49	-0.01	2.4	76.1	174.9	
VMK	P	04 07 0.41	0.18	20.8	132.6	206.7	
VMK	S	04 07 15.81	-0.47	1.2	132.6	206.7	

INPUT DATA FOR FAULT PLANE SOLUTION

STN	DIST. KM	AZIMUTH DEGREES		OMEGA(PZ) METER-SEC	OMEGA(SZ) METER-SEC
HAK	60.	290.6	+	0.30E-09	0.11E-08
VMK	131.	206.3		0.12E-09	0.42E-09

DYNAMIC SOURCE PARAMETERS

SIZE MEASURES
SEISMIC MOMENT: 0.353E+12 Nm
LOCAL MAGNITUDE: 1.5

SHEAR WAVE CORNER FREQUENCY RANGE AT CLOSE DISTANCES (130km)
12.5Hz -30.0Hz (18.5Hz)

FAULT RADIUS RANGE 23m - 55m (37m)

STRESS DROP RANGE 0.92MPa - 12.71MPa (2.98MPa)

RANGE OF THE PEAK SLIP AT THE FAULT 1.6mm - 9.3mm (3.5mm)

THE ORIENTATION OF THE RELAXED STRESS

	AZIMUTH	DIP	
P-AXIS	168.	-12.	degrees
T-AXIS	80.	13.	

THE HORIZONTAL DEVIATORIC STRESS AS GIVEN BY THE P- AND T-AXES
THE AZIMUTH OF COMPRESSION -10 degrees
THE RELATIVE SIZE 0.95

THE TWO POSSIBLE FAULT PLANES

	STRIKE	DIP	SLIP	
PLANE A	124.	108.	1.	degrees
PLANE B	214.	91.	162.	

THE NORMAL DIRECTIONS OF THE FAULT PLANES

	AZIMUTH	DIP	
PLANE A	34.	18.	degrees
PLANE B	124.	1.	

STATISTICAL INFORMATION

OF 1 FIRST MOTION POLARITY OBSERVATIONS
AT LEAST 1 ARE REQUIRED TO FIT

THE OPTIMUM MECHANISM HAS 0 POLARITY MISFITS

AMPLITUDES FOR P AND S AT 2 STATIONS ARE USED
ONLY MECHANISMS GIVING AN ESTIMATED STANDARD
DEVIATION OF THE AMPLITUDE ERROR FACTOR OF LESS
THAN 1.60 FOR SINGLE P-WAVE OBSERVATIONS ARE
TAKEN AS ACCEPTABLE AND INCLUDED IN THE FIGURES

10.85 % OF ALL MECHANISMS ARE ACCEPTABLE
50.0 % ACCEPTABLE DUE TO FIRST MOTION OBSERVATIONS
21.2 % OF THESE FITTED ALSO THE AMPLITUDES
THE PART OF WELL FITTING PLANES IS 71.6%

THE AMPLITUDE FIT OF THE OPTIMAL MECHANISM
GIVES A MEAN ERROR FACTOR OF 1.07

THE MEASURE OF THE MISFIT TO AN EARTHQUAKE SPECTRUM
P-WAVES 0.26
S-WAVES 0.25

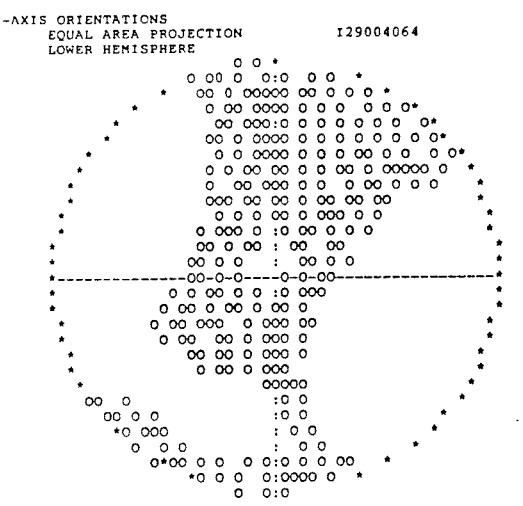
-AXIS ORIENTATIONS
EQUAL AREA PROJECTION
LOWER HEMISPHERE
I29004064

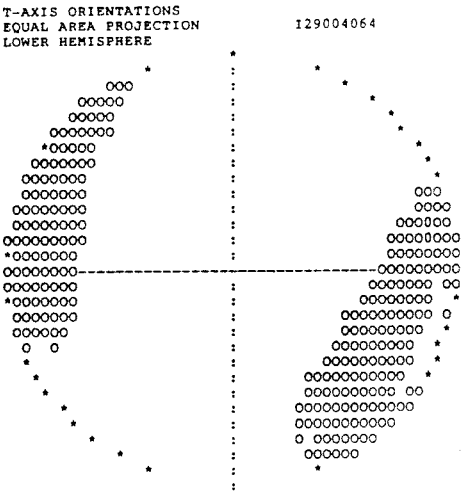
T-AXIS ORIENTATIONS
EQUAL AREA PROJECTION
LOWER HEMISPHERE
I29004064

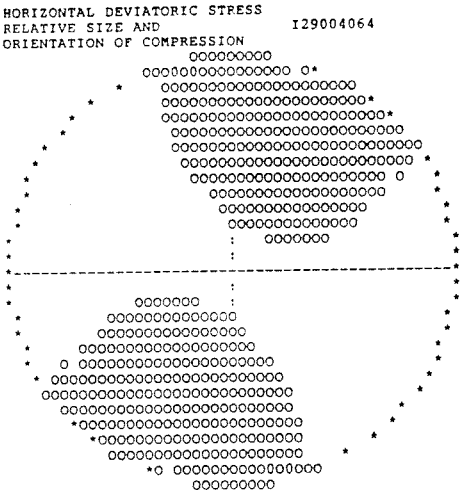
HORIZONTAL DEVIATORIC STRESS
RELATIVE SIZE AND
ORIENTATION OF COMPRESSION
I29004064

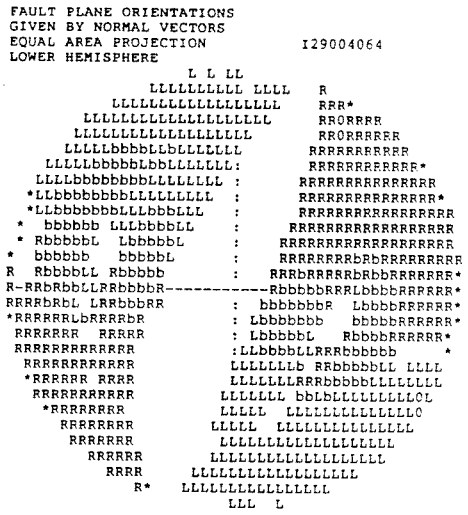
FAULT PLANE ORIENTATIONS
GIVEN BY NORMAL VECTORS
EQUAL AREA PROJECTION
LOWER HEMISPHERE
I29004064

ORIGIN TIME 87 10 17 07H 29M 13.7S +/- 1.39S
LATITUDE 64.316 +/- 0.081 DEG.
LONGITUDE 20.895 +/- 0.484 ***
FOCAL DEPTH 18.9 +/- 11.1 KM

STA	ARR.	TIME	RES.	WEIGHT	DIST.	AZIMUTH	
VMK	P	07 29 38.22	-0.01	17.3	155.9	11.9	P UP
VMK	S	07 29 56.56	-0.16	1.0	155.9	11.9	
KLX	P	07 29 46.82	-0.11	2.2	219.9	26.2	P UP
KLX	S	07 30 13.20	1.08	0.1	219.9	26.2	
HAK	P	07 29 55.94	-0.01	1.5	293.0	5.7	P UP

INPUT DATA FOR FAULT PLANE SOLUTION

STN	DIST. KM	AZIMUTH DEGREES	OMEGA(PZ) METER-SEC	OMEGA(SZ) METER-SEC
VMK	155.	11.8	+ 0.24E-08	0.48E-08
KLX	219.	26.2	+ 0.11E-08	- 0.12E-07
HAK	292.	5.7	+ 0.16E-08	0.65E-08

DYNAMIC SOURCE PARAMETERS

SIZE MEASURES
SEISMIC MOMENT: 0.554E+13 Nm
LOCAL MAGNITUDE: 2.7

SHEAR WAVE CORNER FREQUENCY RANGE AT CLOSE DISTANCES (130km)
 3.3Hz -30.0Hz (4.0Hz)

FAULT RADIUS RANGE 23m - 209m (172m)

STRESS DROP RANGE 0.27MPa -199.28MPa (0.47MPa)

RANGE OF THE PEAK SLIP AT THE FAULT 1.6mm -128.4mm (2.3mm)

THE ORIENTATION OF THE RELAXED STRESS

	AZIMUTH	DIP	
P-AXIS	63.	-29.	degrees
T-AXIS	153.	0.	

THE HORIZONTAL DEVIATORIC STRESS AS GIVEN BY THE P- AND T-AXES
THE AZIMUTH OF COMPRESSION 63 degrees
THE RELATIVE SIZE 0.88

THE TWO POSSIBLE FAULT PLANES

	STRIKE	DIP	SLIP	
PLANE A	-76.	111.	201.	degrees
PLANE B	202.	70.	22.	

THE NORMAL DIRECTIONS OF THE FAULT PLANES

	AZIMUTH	DIP	
PLANE A	194.	21.	degrees
PLANE B	292.	20.	

STATISTICAL INFORMATION

OF 4 FIRST MOTION POLARITY OBSERVATIONS
AT LEAST 4 ARE REQUIRED TO FIT

THE OPTIMUM MECHANISM HAS 0 POLARITY MISFITS

AMPLITUDES FOR P AND S AT 3 STATIONS ARE USED
ONLY MECHANISMS GIVING AN ESTIMATED STANDARD
DEVIATION OF THE AMPLITUDE ERROR FACTOR OF LESS
THAN 1.60 FOR SINGLE P-WAVE OBSERVATIONS ARE
TAKEN AS ACCEPTABLE AND INCLUDED IN THE FIGURES

1.82 % OF ALL MECHANISMS ARE ACCEPTABLE
13.4 % ACCEPTABLE DUE TO FIRST MOTION OBSERVATIONS
13.6 % OF THESE FITTED ALSO THE AMPLITUDES
THE PART OF WELL FITTING PLANES IS 23.6%

THE AMPLITUDE FIT OF THE OPTIMAL MECHANISM
GIVES A MEAN ERROR FACTOR OF 1.19
THIS CORRESPONDS TO A STANDARD DEVIATION FACTOR OF 1.36
FOR SINGLE P-WAVE OBSERVATIONS

THE DOUBLE COUPLE SOLUTION IS SIGNIFICANT
AT 29 % LEVEL
(F-VALUE: F(5, 2) = 2.83)

THE MEASURE OF THE MISFIT TO AN EARTHQUAKE SPECTRUM

P-WAVES	0.22
S-WAVES	0.27

-AXIS ORIENTATIONS
EQUAL AREA PROJECTION
LOWER HEMISPHERE
I29007293

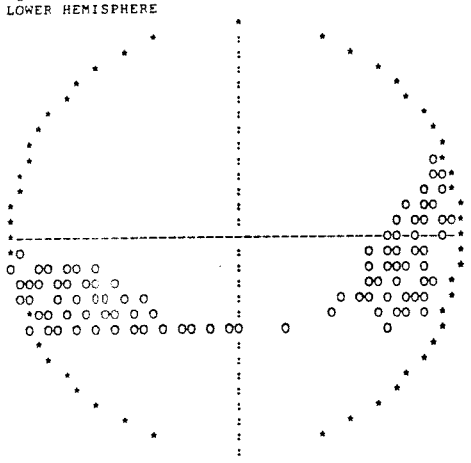

T-AXIS ORIENTATIONS
EQUAL AREA PROJECTION
LOWER HEMISPHERE
I29007293

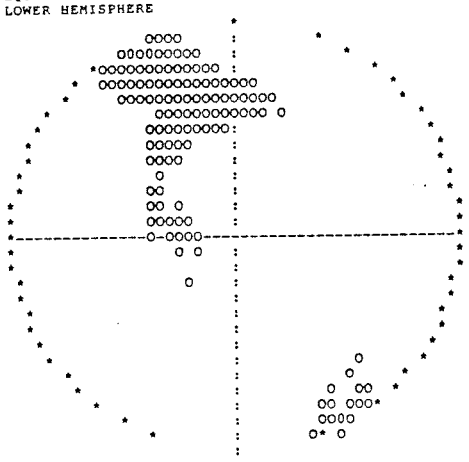

HORIZONTAL DEVIATORIC STRESS
RELATIVE SIZE AND
ORIENTATION OF COMPRESSION
I29007293

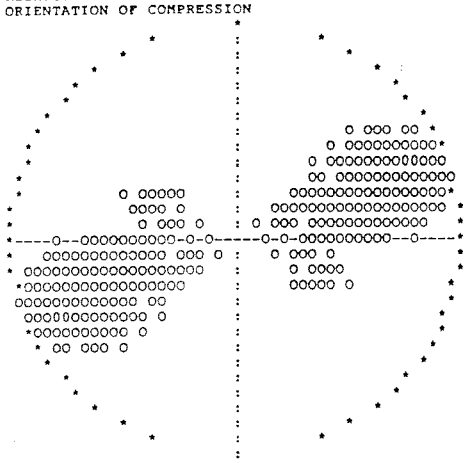

FAULT PLANE ORIENTATIONS
GIVEN BY NORMAL VECTORS
EQUAL AREA PROJECTION
LOWER HEMISPHERE
I29007293

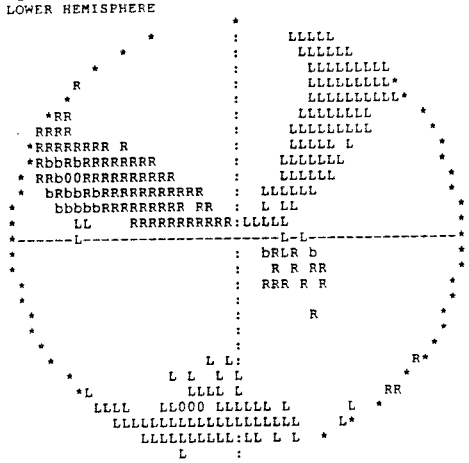

ORIGIN TIME 87 12 20 19H 52M 26.7S +/- 0.33S
LATITUDE 65.675 +/- 0.021 DEG.
LONGITUDE 22.500 +/- 0.033
FOCAL DEPTH 9.9 +/- 3.2 KM

STA	ARR.	TIME	RES.	WEIGHT	DIST.	AZIMUTH	
VMK	P	19 52 33.75	0.00	52.7	42.0	271.2	P UP
VMK	S	19 52 38.76	-0.19	4.2	42.0	271.2	
KLX	P	19 52 35.00	-0.03	47.5	50.1	28.7	P UP
KLX	S	19 52 41.13	-0.05	3.6	50.1	28.7	
LJV	P	19 52 44.96	0.20	25.2	110.4	352.3	
LJV	S	19 52 58.29	0.25	1.6	110.4	352.3	
KPM	P	19 52 46.63	-0.01	22.7	122.0	8.4	
KPM	S	19 53 0.32	-0.98	1.4	122.0	8.4	
HAK	P	19 52 50.21	-0.06	18.7	145.8	343.6	
HAK	S	19 53 7.26	-0.63	1.1	145.8	343.6	
MUG	P	19 52 58.78	0.31	2.5	200.6	354.4	
MUG	S	19 53 22.60	0.26	0.1	200.6	354.4	

INPUT DATA FOR FAULT PLANE SOLUTION

STN	DIST. KM	AZIMUTH DEGREES		OMEGA(PZ) METER-SEC	OMEGA(SZ) METER-SEC
VMK	44.	273.4	+	0.27E-09	0.10E-08
KLX	51.	26.5	+	0.21E-09	0.40E-09
LJV	112.	351.8		0.16E-09	0.11E-08
KPM	123.	7.7		0.16E-09	0.72E-09
HAK	148.	343.3		0.16E-09	0.65E-09
MUG	202.	354.1		0.22E-09	0.12E-08

DYNAMIC SOURCE PARAMETERS

SIZE MEASURES
SEISMIC MOMENT: 0.187E+12 Nm
LOCAL MAGNITUDE: 1.3

SHEAR WAVE CORNER FREQUENCY RANGE AT CLOSE DISTANCES (130km)
8.9Hz -12.6Hz (10.7Hz)

FAULT RADIUS RANGE 54m - 77m (64m)

STRESS DROP RANGE 0.18MPa - 0.50MPa (0.31MPa)

RANGE OF THE PEAK SLIP AT THE FAULT 0.4mm - 0.9mm (0.6mm)

THE ORIENTATION OF THE RELAXED STRESS

	AZIMUTH	DIP
P-AXIS	-2.	85. degrees
T-AXIS	60.	-2.

THE HORIZONTAL DEVIATORIC STRESS AS GIVEN BY THE P- AND T-AXES
THE AZIMUTH OF COMPRESSION -30 degrees
THE RELATIVE SIZE 0.50

THE TWO POSSIBLE FAULT PLANES

	STRIKE	DIP	SLIP
PLANE A	155.	43.	96. degrees
PLANE B	146.	133.	-84.

THE NORMAL DIRECTIONS OF THE FAULT PLANES

	AZIMUTH	DIP
PLANE A	245.	47. degrees
PLANE B	56.	43.

STATISTICAL INFORMATION

OF 2 FIRST MOTION POLARITY OBSERVATIONS
AT LEAST 2 ARE REQUIRED TO FIT

THE OPTIMUM MECHANISM HAS 0 POLARITY MISFITS

AMPLITUDES FOR P AND S AT 6 STATIONS ARE USED
ONLY MECHANISMS GIVING AN ESTIMATED STANDARD
DEVIATION OF THE AMPLITUDE ERROR FACTOR OF LESS
THAN 1.60 FOR SINGLE P-WAVE OBSERVATIONS ARE
TAKEN AS ACCEPTABLE AND INCLUDED IN THE FIGURES

2.97 % OF ALL MECHANISMS ARE ACCEPTABLE
20.1 % ACCEPTABLE DUE TO FIRST MOTION OBSERVATIONS
14.8 % OF THESE FITTED ALSO THE AMPLITUDES
THE PART OF WELL FITTING PLANES IS 32.0%

THE AMPLITUDE FIT OF THE OPTIMAL MECHANISM
GIVES A MEAN ERROR FACTOR OF 1.19
THIS CORRESPONDS TO A STANDARD DEVIATION FACTOR OF 1.24
FOR SINGLE P-WAVE OBSERVATIONS

THE DOUBLE COUPLE SOLUTION IS SIGNIFICANT
AT 7 % LEVEL
(F-VALUE: F(11, 8) = 2.74)

THE MEASURE OF THE MISFIT TO AN EARTHQUAKE SPECTRUM
P-WAVES 0.30
S-WAVES 0.25

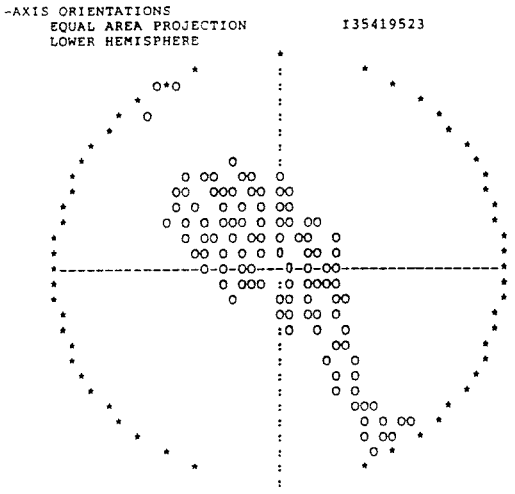
-AXIS ORIENTATIONS
EQUAL AREA PROJECTION
LOWER HEMISPHERE
I35419523

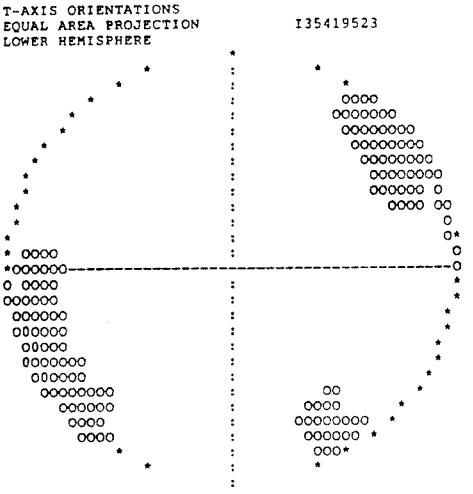
T-AXIS ORIENTATIONS
EQUAL AREA PROJECTION
LOWER HEMISPHERE
I35419523

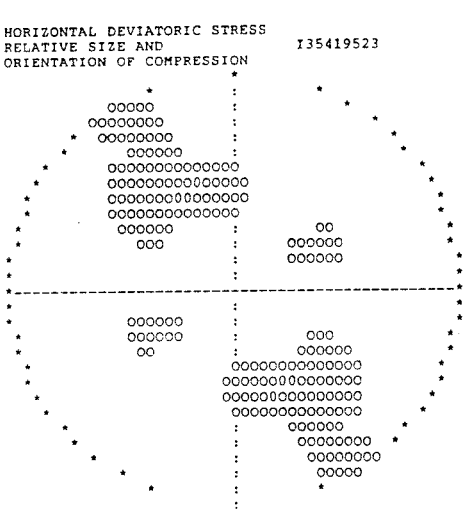
HORIZONTAL DEVIATORIC STRESS
RELATIVE SIZE AND
ORIENTATION OF COMPRESSION
I35419523

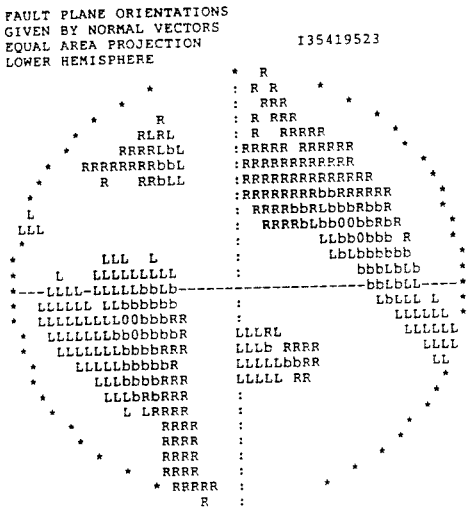
FAULT PLANE ORIENTATIONS
GIVEN BY NORMAL VECTORS
EQUAL AREA PROJECTION
LOWER HEMISPHERE
I35419523

ORIGIN TIME 87 12 29 16H 56M 43.5S +/- 0.70S
LATITUDE 67.754 +/- 0.032 DEG.
LONGITUDE 19.562 +/- 0.092
FOCAL DEPTH 4.8 +/- 4.3 KM

STA	ARR. TIME	RES.	WEIGHT	DIST.	AZIMUTH	
MUG	P 16 57 1.60	0.02	25.1	110.7	106.0	P UP
MUG	S 16 57 14.79	-0.12	1.6	110.7	106.0	
HAK	P 16 57 4.15	0.00	21.9	126.5	136.2	
HAK	S 16 57 19.24	-0.11	1.3	126.5	136.2	
LJV	P 16 57 10.52	0.03	16.0	166.8	136.2	
LJV	S 16 57 30.86	0.19	0.9	166.8	136.2	
KPM	P 16 57 12.74	-0.11	6.4	182.5	126.1	
KPM	S 16 57 35.26	0.42	0.4	182.5	126.1	
KLX	P 16 57 20.93	-0.02	2.0	242.1	139.5	
VMK	P 16 57 21.66	-0.05	1.9	248.3	157.9	

INPUT DATA FOR FAULT PLANE SOLUTION

STN	DIST. KM	AZIMUTH DEGREES		OMEGA(PZ) METER-SEC		OMEGA(SZ) METER-SEC
MUG	110.	105.8	+	0.13E-08		0.64E-08
HAK	126.	136.2		0.44E-09	+	0.17E-08
LJV	166.	136.2		0.74E-09		0.27E-08
KPM	182.	126.1		0.73E-09		0.22E-08
KLX	242.	139.5		0.53E-09		0.27E-08
VMK	248.	158.0		0.37E-09		0.12E-08

DYNAMIC SOURCE PARAMETERS

SIZE MEASURES
SEISMIC MOMENT: 0.916E+12 Nm
LOCAL MAGNITUDE: 2.0

SHEAR WAVE CORNER FREQUENCY RANGE AT CLOSE DISTANCES (130km)
5.0Hz -10.6Hz (7.6Hz)

FAULT RADIUS RANGE 65m - 138m (90m)

STRESS DROP RANGE 0.15MPa - 1.45MPa (0.54MPa)

RANGE OF THE PEAK SLIP AT THE FAULT 0.7mm - 3.0mm (1.6mm)

THE ORIENTATION OF THE RELAXED STRESS

	AZIMUTH	DIP
P-AXIS	30.	-58. degrees
T-AXIS	86.	19.

THE HORIZONTAL DEVIATORIC STRESS AS GIVEN BY THE P- AND T-AXES
THE AZIMUTH OF COMPRESSION 2 degrees
THE RELATIVE SIZE 0.51

THE TWO POSSIBLE FAULT PLANES

	STRIKE	DIP	SLIP
PLANE A	210.	147.	221. degrees
PLANE B	156.	69.	64.

THE NORMAL DIRECTIONS OF THE FAULT PLANES

	AZIMUTH	DIP
PLANE A	120.	57. degrees
PLANE B	246.	21.

STATISTICAL INFORMATION

OF 2 FIRST MOTION POLARITY OBSERVATIONS
AT LEAST 2 ARE REQUIRED TO FIT

THE OPTIMUM MECHANISM HAS 0 POLARITY MISFITS

AMPLITUDES FOR P AND S AT 6 STATIONS ARE USED
ONLY MECHANISMS GIVING AN ESTIMATED STANDARD
DEVIATION OF THE AMPLITUDE ERROR FACTOR OF LESS
THAN 1.60 FOR SINGLE P-WAVE OBSERVATIONS ARE
TAKEN AS ACCEPTABLE AND INCLUDED IN THE FIGURES

19.36 % OF ALL MECHANISMS ARE ACCEPTABLE
25.7 % ACCEPTABLE DUE TO FIRST MOTION OBSERVATIONS
75.3 % OF THESE FITTED ALSO THE AMPLITUDES
THE PART OF WELL FITTING PLANES IS 88.5%

THE AMPLITUDE FIT OF THE OPTIMAL MECHANISM
GIVES A MEAN ERROR FACTOR OF 1.20
THIS CORRESPONDS TO A STANDARD DEVIATION FACTOR OF 1.25
FOR SINGLE P-WAVE OBSERVATIONS

THE DOUBLE COUPLE SOLUTION IS SIGNIFICANT
AT 32 % LEVEL
(F-VALUE: F(11, 8) = 1.41)

THE MEASURE OF THE MISFIT TO AN EARTHQUAKE SPECTRUM
P-WAVES 0.28
S-WAVES 0.24

-AXIS ORIENTATIONS
EQUAL AREA PROJECTION I36316565
LOWER HEMISPHERE

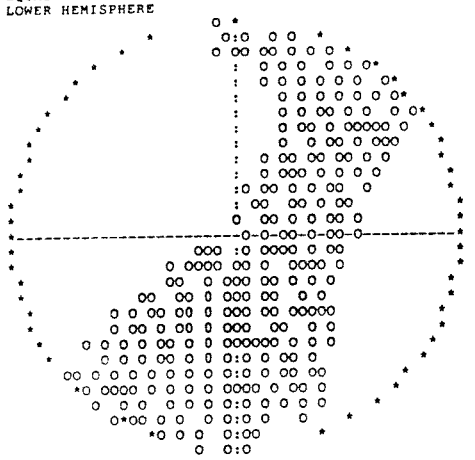

T-AXIS ORIENTATIONS
EQUAL AREA PROJECTION I36316565
LOWER HEMISPHERE

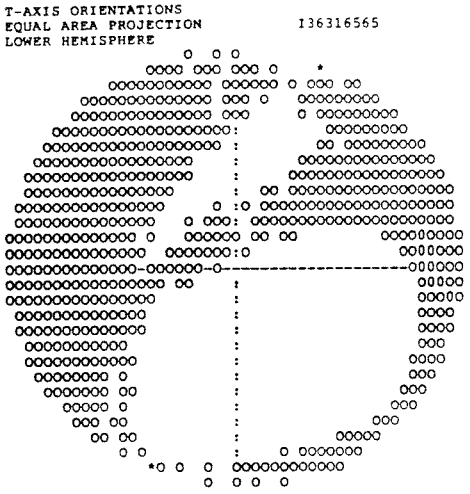

HORIZONTAL DEVIATORIC STRESS
RELATIVE SIZE AND I36316565
ORIENTATION OF COMPRESSION

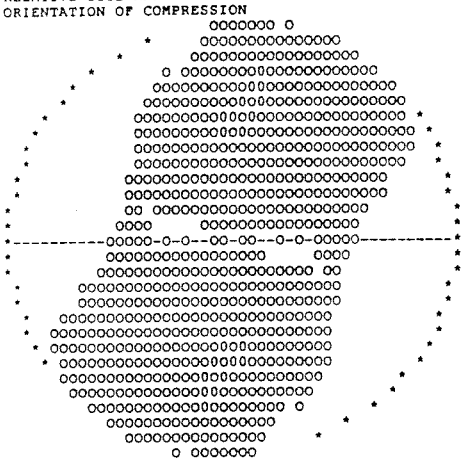

FAULT PLANE ORIENTATIONS
GIVEN BY NORMAL VECTORS
EQUAL AREA PROJECTION I36316565
LOWER HEMISPHERE

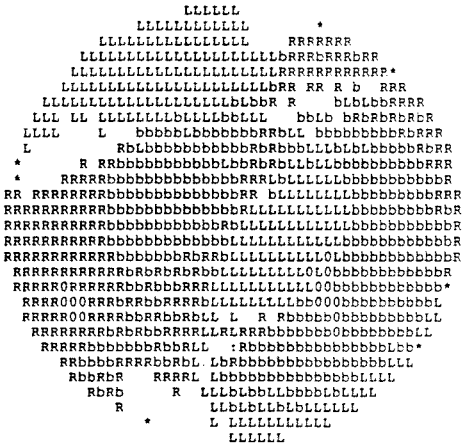

ORIGIN TIME 87 12 30 03H 24M 52.3S +/- 0.62S
LATITUDE 65.391 +/- 0.034 DEG.
LONGITUDE 22.947 +/- 0.052
FOCAL DEPTH 11.6 +/- 3.0 KM

STA	ARR. TIME	RES.	WEIGHT	DIST.	AZIMUTH	
VMK	P 03 25 4.00	-0.02	37.3	70.8	297.8	P DOWN
VMK	S 03 25 12.76	0.14	2.6	70.8	297.8	
KLX	P 03 25 4.81	0.01	35.4	75.7	2.9	
KLX	S 03 25 13.84	-0.14	2.4	75.7	2.9	
LJV	P 03 25 15.79	0.04	18.8	145.6	346.3	
KPM	S 03 25 34.51	-0.02	1.0	151.2	359.6	
HAK	P 03 25 21.18	-0.10	6.4	182.5	340.5	

INPUT DATA FOR FAULT PLANE SOLUTION

STN	DIST. KM	AZIMUTH DEGREES	OMEGA(PZ) METER-SEC	OMEGA(SZ) METER-SEC
VMK	66.	295.6	- 0.22E-09	0.24E-09
KLX	72.	5.5	0.14E-09	0.32E-09
LJV	141.	347.0	0.27E-09	0.85E-09
KPM	148.	0.4	0.15E-09	0.11E-08
HAK	177.	340.9	0.14E-09	0.32E-09
MUG	230.	351.0	0.20E-09	0.88E-09

DYNAMIC SOURCE PARAMETERS

SIZE MEASURES
SEISMIC MOMENT: 0.144E+12 Nm
LOCAL MAGNITUDE: 1.2

SHEAR WAVE CORNER FREQUENCY RANGE AT CLOSE DISTANCES (130km)
11.0Hz -17.3Hz (14.1Hz)

FAULT RADIUS RANGE 39m - 62m (48m)

STRESS DROP RANGE 0.26MPa - 1.00MPa (0.54MPa)

RANGE OF THE PEAK SLIP AT THE FAULT 0.5mm - 1.3mm (0.8mm)

THE ORIENTATION OF THE RELAXED STRESS

	AZIMUTH	DIP	
P-AXIS	147.	-1.	degrees
T-AXIS	231.	84.	

THE HORIZONTAL DEVIATORIC STRESS AS GIVEN BY THE P- AND T-AXES
THE AZIMUTH OF COMPRESSION -33 degrees
THE RELATIVE SIZE 0.51

THE TWO POSSIBLE FAULT PLANES

	STRIKE	DIP	SLIP	
PLANE A	51.	135.	99.	degrees
PLANE B	243.	134.	82.	

THE NORMAL DIRECTIONS OF THE FAULT PLANES

	AZIMUTH	DIP	
PLANE A	321.	45.	degrees
PLANE B	153.	44.	

STATISTICAL INFORMATION

OF 1 FIRST MOTION POLARITY OBSERVATIONS
AT LEAST 1 ARE REQUIRED TO FIT

THE OPTIMUM MECHANISM HAS 0 POLARITY MISFITS

AMPLITUDES FOR P AND S AT 6 STATIONS ARE USED
ONLY MECHANISMS GIVING AN ESTIMATED STANDARD
DEVIATION OF THE AMPLITUDE ERROR FACTOR OF LESS
THAN 1.60 FOR SINGLE P-WAVE OBSERVATIONS ARE
TAKEN AS ACCEPTABLE AND INCLUDED IN THE FIGURES

3.21 % OF ALL MECHANISMS ARE ACCEPTABLE
50.0 % ACCEPTABLE DUE TO FIRST MOTION OBSERVATIONS
6.5 % OF THESE FITTED ALSO THE AMPLITUDES
THE PART OF WELL FITTING PLANES IS 37.8%

THE AMPLITUDE FIT OF THE OPTIMAL MECHANISM
GIVES A MEAN ERROR FACTOR OF 1.31
THIS CORRESPONDS TO A STANDARD DEVIATION FACTOR OF 1.40
FOR SINGLE P-WAVE OBSERVATIONS

THE DOUBLE COUPLE SOLUTION IS SIGNIFICANT
AT 8 % LEVEL
(F-VALUE: F(11, 8) = 2.69)

THE MEASURE OF THE MISFIT TO AN EARTHQUAKE SPECTRUM

P-WAVES	0.24
S-WAVES	0.27

-AXIS ORIENTATIONS
EQUAL AREA PROJECTION
LOWER HEMISPHERE

I36403250

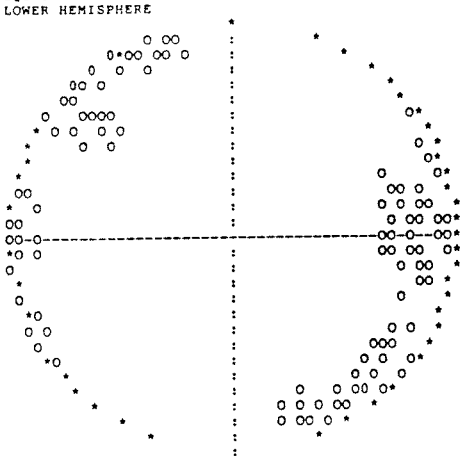

T-AXIS ORIENTATIONS
EQUAL AREA PROJECTION
LOWER HEMISPHERE

I36403250

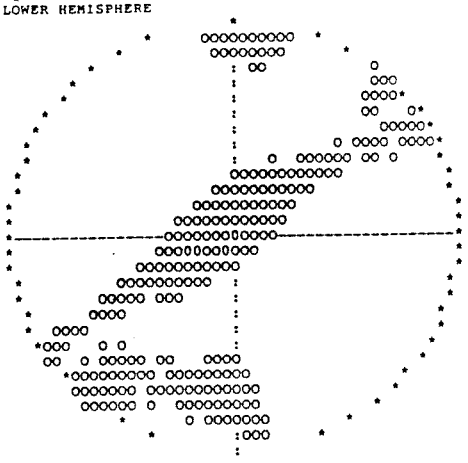

HORIZONTAL DEVIATORIC STRESS
RELATIVE SIZE AND
ORIENTATION OF COMPRESSION

I36403250

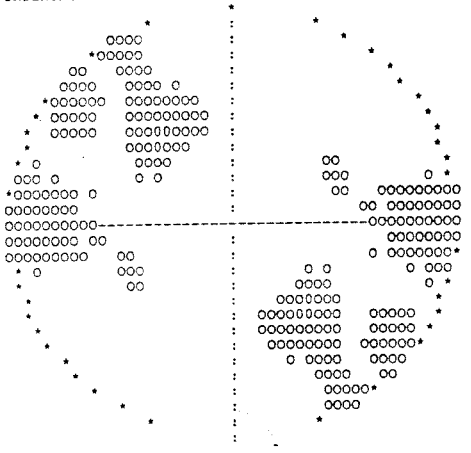

FAULT PLANE ORIENTATIONS
GIVEN BY NORMAL VECTORS
EQUAL AREA PROJECTION
LOWER HEMISPHERE

I36403250

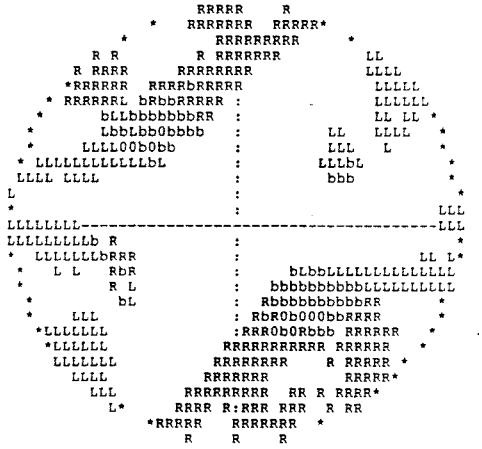

ORIGIN TIME 88 01 04 14H 43M 35.8S +/- 0.59S
LATITUDE 65.280 +/- 0.034 DEG.
LONGITUDE 22.528 +/- 0.036
FOCAL DEPTH 4.5 +/- 3.3 KM

STA	ARR.	TIME	RES.	WEIGHT	DIST.	AZIMUTH	
VMK	P	14 43 46.05	0.03	41.0	62.5	316.1	P DOWN
VMK	S	14 43 53.49	-0.10	3.0	62.5	316.1	
KLX	P	14 43 50.62	-0.04	30.2	91.0	14.5	
KLX	S	14 44 1.85	0.22	2.0	91.0	14.5	
LJV	P	14 44 0.85	-0.09	17.5	154.5	354.0	
LJV	S	14 44 19.56	0.03	1.0	154.5	354.0	
KPM	P	14 44 2.78	0.15	16.1	165.7	5.8	
HAK	P	14 44 5.99	-0.11	6.1	188.9	347.0	

INPUT DATA FOR FAULT PLANE SOLUTION

STN	DIST. KM	AZIMUTH DEGREES		OMEGA(PZ) METER-SEC	OMEGA(SZ) METER-SEC
VMK	63.	316.1	-	0.13E-09	0.11E-09
KLX	91.	14.5		0.82E-10	0.19E-09
LJV	154.	354.0		0.90E-10	0.25E-09
KPM	166.	5.7		0.97E-10	0.22E-09
HAK	189.	347.0		0.90E-10	0.15E-09

DYNAMIC SOURCE PARAMETERS

SIZE MEASURES
SEISMIC MOMENT: 0.104E+12 Nm
LOCAL MAGNITUDE: 1.0

SHEAR WAVE CORNER FREQUENCY RANGE AT CLOSE DISTANCES (130km)
13.0Hz -23.2Hz (17.6Hz)

FAULT RADIUS RANGE 29m - 53m (39m)

STRESS DROP RANGE 0.30MPa - 1.73MPa (0.76MPa)

RANGE OF THE PEAK SLIP AT THE FAULT 0.5mm - 1.7mm (1.0mm)

THE ORIENTATION OF THE RELAXED STRESS

	AZIMUTH	DIP	
P-AXIS	164.	-1.	degrees
T-AXIS	254.	16.	

THE HORIZONTAL DEVIATORIC STRESS AS GIVEN BY THE P- AND T-AXES
THE AZIMUTH OF COMPRESSION -16 degrees
THE RELATIVE SIZE 0.96

THE TWO POSSIBLE FAULT PLANES

	STRIKE	DIP	SLIP	
PLANE A	30.	102.	169.	degrees
PLANE B	-62.	101.	12.	

THE NORMAL DIRECTIONS OF THE FAULT PLANES

	AZIMUTH	DIP	
PLANE A	300.	12.	degrees
PLANE B	208.	11.	

STATISTICAL INFORMATION

OF 1 FIRST MOTION POLARITY OBSERVATIONS
AT LEAST 1 ARE REQUIRED TO FIT

THE OPTIMUM MECHANISM HAS 0 POLARITY MISFITS

AMPLITUDES FOR P AND S AT 5 STATIONS ARE USED
ONLY MECHANISMS GIVING AN ESTIMATED STANDARD
DEVIATION OF THE AMPLITUDE ERROR FACTOR OF LESS
THAN 1.60 FOR SINGLE P-WAVE OBSERVATIONS ARE
TAKEN AS ACCEPTABLE AND INCLUDED IN THE FIGURES

5.76 % OF ALL MECHANISMS ARE ACCEPTABLE
50.0 % ACCEPTABLE DUE TO FIRST MOTION OBSERVATIONS
11.4 % OF THESE FITTED ALSO THE AMPLITUDES
THE PART OF WELL FITTING PLANES IS 47.9%

THE AMPLITUDE FIT OF THE OPTIMAL MECHANISM
GIVES A MEAN ERROR FACTOR OF 1.20
THIS CORRESPONDS TO A STANDARD DEVIATION FACTOR OF 1.27
FOR SINGLE P-WAVE OBSERVATIONS

THE DOUBLE COUPLE SOLUTION IS SIGNIFICANT
AT 1 % LEVEL
(F-VALUE: F(9, 6) = 6.98)

THE MEASURE OF THE MISFIT TO AN EARTHQUAKE SPECTRUM

P-WAVES	0.29
S-WAVES	0.20

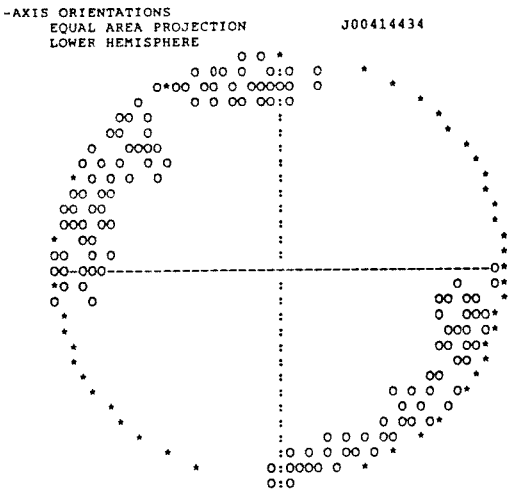
-AXIS ORIENTATIONS
EQUAL AREA PROJECTION
LOWER HEMISPHERE
J00414434

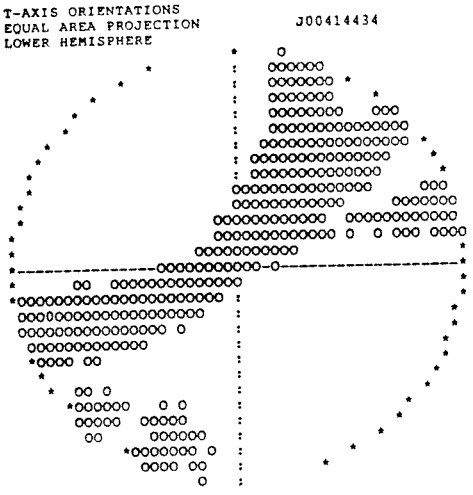
T-AXIS ORIENTATIONS
EQUAL AREA PROJECTION
LOWER HEMISPHERE
J00414434

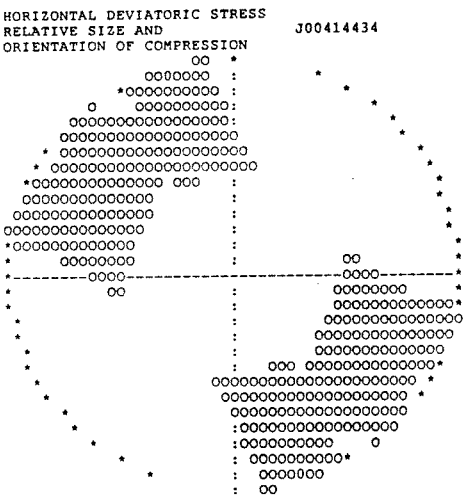
HORIZONTAL DEVIATORIC STRESS
RELATIVE SIZE AND
ORIENTATION OF COMPRESSION
J00414434

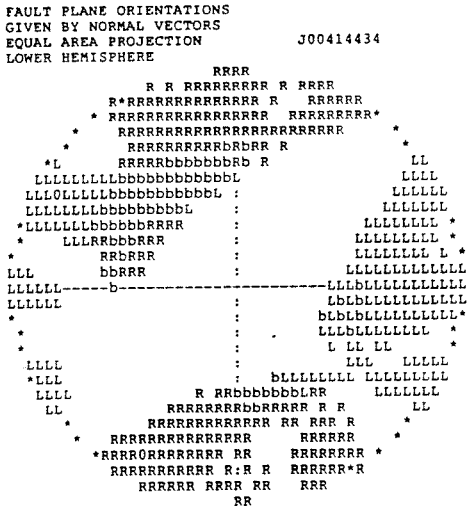
FAULT PLANE ORIENTATIONS
GIVEN BY NORMAL VECTORS
EQUAL AREA PROJECTION
LOWER HEMISPHERE
J00414434

ORIGIN TIME 88 01 08 08H 14M 23.2S +/- 0.41S
LATITUDE 67.537 +/- 0.022 DEG.
LONGITUDE 21.575 +/- 0.093
FOCAL DEPTH 26.5 +/- 3.3 KM

STA	ARR. TIME	RES.	WEIGHT	DIST.	AZIMUTH	
MUG	P 08 14 28.58	0.00	69.9	21.8	112.3	P UP
MUG	S 08 14 32.67	0.04	6.3	21.8	112.3	
HAK	P 08 14 34.72	0.01	38.3	68.4	180.6	P UP
HAK	S 08 14 43.32	-0.02	2.7	68.4	180.6	
LJV	P 08 14 39.61	-0.04	27.2	101.8	165.1	P DOWN
LJV	S 08 14 52.08	0.08	1.7	101.8	165.1	
VMK	P 08 14 54.39	0.16	2.4	207.3	179.8	
VMK	S 08 15 17.79	0.00	0.1	207.3	179.8	

INPUT DATA FOR FAULT PLANE SOLUTION

STN	DIST. KM	AZIMUTH DEGREES		OMEGA(PZ) METER-SEC	OMEGA(SZ) METER-SEC
HAK	67.	181.5	+	0.35E-09	0.40E-08
LJV	100.	165.4	-	0.38E-09	0.38E-08
VMK	205.	180.2		0.28E-09	0.33E-08
MUG	20.	108.6	+	0.00E+00	0.00E+00

DYNAMIC SOURCE PARAMETERS

SIZE MEASURES
SEISMIC MOMENT: 0.111E+13 Nm
LOCAL MAGNITUDE: 2.0

SHEAR WAVE CORNER FREQUENCY RANGE AT CLOSE DISTANCES (130km)
7.3Hz -14.4Hz (10.6Hz)

FAULT RADIUS RANGE 47m - 94m (65m)

STRESS DROP RANGE 0.58MPa - 4.43MPa (1.77MPa)

RANGE OF THE PEAK SLIP AT THE FAULT 1.4mm - 5.3mm (2.9mm)

THE ORIENTATION OF THE RELAXED STRESS

	AZIMUTH	DIP	
P-AXIS	107.	5.	degrees
T-AXIS	183.	-69.	

THE HORIZONTAL DEVIATORIC STRESS AS GIVEN BY THE P- AND T-AXES
THE AZIMUTH OF COMPRESSION -74 degrees
THE RELATIVE SIZE 0.55

THE TWO POSSIBLE FAULT PLANES

	STRIKE	DIP	SLIP	
PLANE A	-4.	44.	240.	degrees
PLANE B	215.	53.	-65.	

THE NORMAL DIRECTIONS OF THE FAULT PLANES

	AZIMUTH	DIP	
PLANE A	86.	46.	degrees
PLANE B	305.	37.	

STATISTICAL INFORMATION

OF 3 FIRST MOTION POLARITY OBSERVATIONS
AT LEAST 3 ARE REQUIRED TO FIT

THE OPTIMUM MECHANISM HAS 0 POLARITY MISFITS

AMPLITUDES FOR P AND S AT 3 STATIONS ARE USED
ONLY MECHANISMS GIVING AN ESTIMATED STANDARD
DEVIATION OF THE AMPLITUDE ERROR FACTOR OF LESS
THAN 1.60 FOR SINGLE P-WAVE OBSERVATIONS ARE
TAKEN AS ACCEPTABLE AND INCLUDED IN THE FIGURES

0.35 % OF ALL MECHANISMS ARE ACCEPTABLE
3.6 % ACCEPTABLE DUE TO FIRST MOTION OBSERVATIONS
9.8 % OF THESE FITTED ALSO THE AMPLITUDES
THE PART OF WELL FITTING PLANES IS 6.8%

THE AMPLITUDE FIT OF THE OPTIMAL MECHANISM
GIVES A MEAN ERROR FACTOR OF 1.24
THIS CORRESPONDS TO A STANDARD DEVIATION FACTOR OF 1.46
FOR SINGLE P-WAVE OBSERVATIONS

THE DOUBLE COUPLE SOLUTION IS SIGNIFICANT
AT 41 % LEVEL
(F-VALUE: F(5, 2) = 1.79)

THE MEASURE OF THE MISFIT TO AN EARTHQUAKE SPECTRUM
P-WAVES 0.25
S-WAVES 0.26

-AXIS ORIENTATIONS
EQUAL AREA PROJECTION
LOWER HEMISPHERE
J00808142

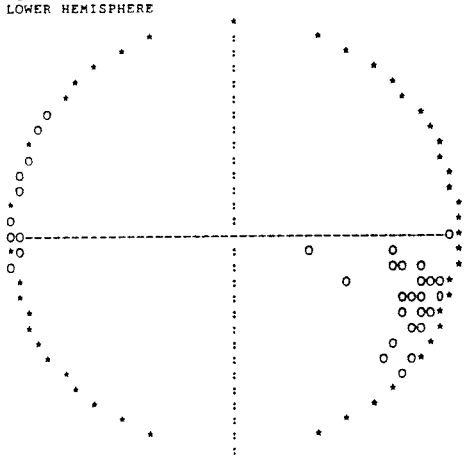

T-AXIS ORIENTATIONS
EQUAL AREA PROJECTION
LOWER HEMISPHERE
J00808142

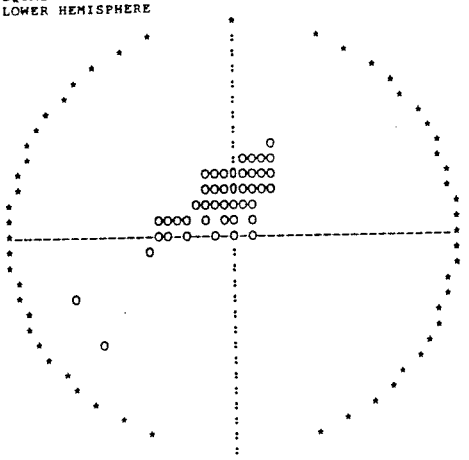

HORIZONTAL DEVIATORIC STRESS
RELATIVE SIZE AND
ORIENTATION OF COMPRESSION
J00808142

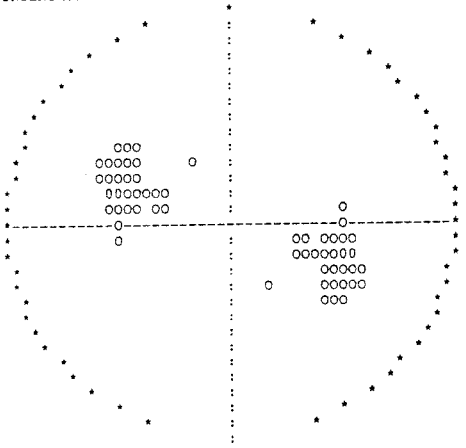

FAULT PLANE ORIENTATIONS
GIVEN BY NORMAL VECTORS
EQUAL AREA PROJECTION
LOWER HEMISPHERE
J00808142

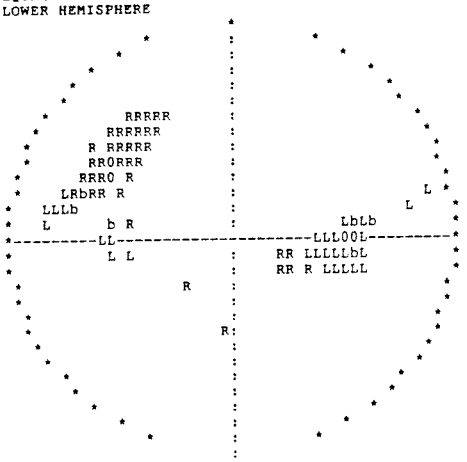

EF. TIME: 104930 REF.GROUP: 0
ORIGIN TIME 88 01 10 10H 49M 38.1S +/- 0.23S
LATITUDE 67.454 +/- 0.014 DEG.
LONGITUDE 22.341 +/- 0.038
FOCAL DEPTH 4.0 +/- 4.3 KM

STA		ARR. TIME	RES.	WEIGHT	DIST.	AZIMUTH	
MUG	P	10 49 40.30	0.01	80.5	12.7	274.3	P UP
MUG	S	10 49 41.78	-0.15	7.8	12.7	274.3	
HAK	P	10 49 49.35	0.07	38.5	68.1	210.2	
HAK	S	10 49 57.53	0.01	2.7	68.1	210.2	
KPM	P	10 49 51.52	0.00	33.2	81.8	162.3	
KPM	S	10 50 1.14	-0.24	2.2	81.8	162.3	
LJV	S	10 50 3.37	-0.22	2.0	89.6	184.9	
KLX	P	10 50 3.78	-0.05	17.1	157.8	168.6	

INPUT DATA FOR FAULT PLANE SOLUTION

STN	DIST. KM	AZIMUTH DEGREES		OMEGA(PZ) METER-SEC	OMEGA(SZ) METER-SEC
MUG	13.	276.1	+	0.30E-08	0.82E-08
HAK	68.	210.3		0.13E-09	0.32E-09
KPM	81.	162.2		0.15E-09	0.73E-09
LJV	89.	184.9		0.11E-09	0.75E-09
KLX	157.	168.5		0.26E-09	0.68E-09

DYNAMIC SOURCE PARAMETERS

SIZE MEASURES
SEISMIC MOMENT: 0.397E+12 Nm
LOCAL MAGNITUDE: 1.6

SHEAR WAVE CORNER FREQUENCY RANGE AT CLOSE DISTANCES (130km)
7.0Hz -12.0Hz (9.4Hz)

FAULT RADIUS RANGE 57m - 98m (73m)

STRESS DROP RANGE 0.18MPa - 0.91MPa (0.44MPa)

RANGE OF THE PEAK SLIP AT THE FAULT 0.6mm - 1.7mm (1.0mm)

THE ORIENTATION OF THE RELAXED STRESS

	AZIMUTH	DIP
P-AXIS	141.	-41. degrees
T-AXIS	80.	30.

THE HORIZONTAL DEVIATORIC STRESS AS GIVEN BY THE P- AND T-AXES
THE AZIMUTH OF COMPRESSION -22 degrees
THE RELATIVE SIZE 0.58

THE TWO POSSIBLE FAULT PLANES

	STRIKE	DIP	SLIP
PLANE A	118.	144.	-11. degrees
PLANE B	199.	84.	125.

THE NORMAL DIRECTIONS OF THE FAULT PLANES

	AZIMUTH	DIP
PLANE A	28.	54. degrees
PLANE B	289.	6.

STATISTICAL INFORMATION

OF 1 FIRST MOTION POLARITY OBSERVATIONS
AT LEAST 1 ARE REQUIRED TO FIT

THE OPTIMUM MECHANISM HAS 0 POLARITY MISFITS

AMPLITUDES FOR P AND S AT 5 STATIONS ARE USED
ONLY MECHANISMS GIVING AN ESTIMATED STANDARD
DEVIATION OF THE AMPLITUDE ERROR FACTOR OF LESS
THAN 1.60 FOR SINGLE P-WAVE OBSERVATIONS ARE
TAKEN AS ACCEPTABLE AND INCLUDED IN THE FIGURES

1.00 % OF ALL MECHANISMS ARE ACCEPTABLE
50.0 % ACCEPTABLE DUE TO FIRST MOTION OBSERVATIONS
1.9 % OF THESE FITTED ALSO THE AMPLITUDES
THE PART OF WELL FITTING PLANES IS 18.1%

THE AMPLITUDE FIT OF THE OPTIMAL MECHANISM
GIVES A MEAN ERROR FACTOR OF 1.26
THIS CORRESPONDS TO A STANDARD DEVIATION FACTOR OF 1.35
FOR SINGLE P-WAVE OBSERVATIONS

THE DOUBLE COUPLE SOLUTION IS SIGNIFICANT
AT 13 % LEVEL
(F-VALUE: F(9, 6) = 2.60)

THE MEASURE OF THE MISFIT TO AN EARTHQUAKE SPECTRUM
P-WAVES 0.24
S-WAVES 0.23

-AXIS ORIENTATIONS
EQUAL AREA PROJECTION
LOWER HEMISPHERE
J01010493

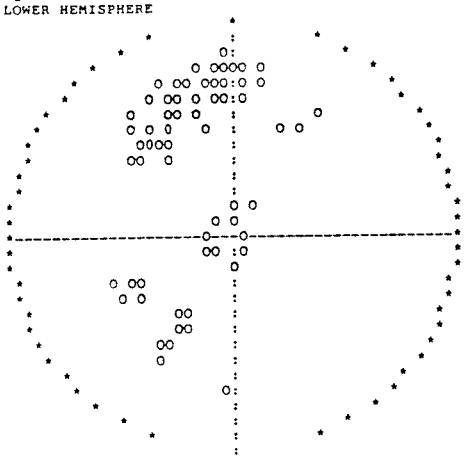

T-AXIS ORIENTATIONS
EQUAL AREA PROJECTION
LOWER HEMISPHERE
J01010493

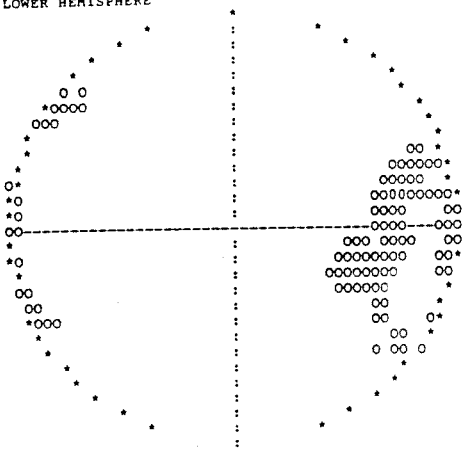

HORIZONTAL DEVIATORIC STRESS
RELATIVE SIZE AND
ORIENTATION OF COMPRESSION
J01010493

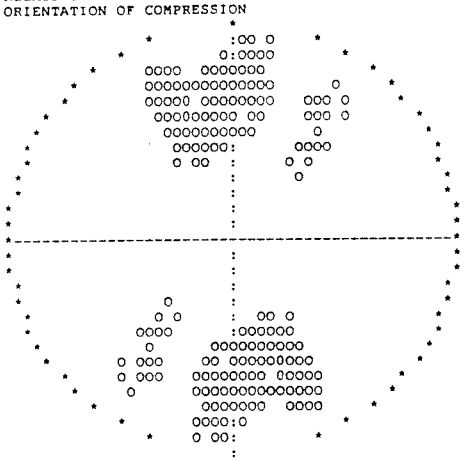

FAULT PLANE ORIENTATIONS
GIVEN BY NORMAL VECTORS
EQUAL AREA PROJECTION
LOWER HEMISPHERE
J01010493

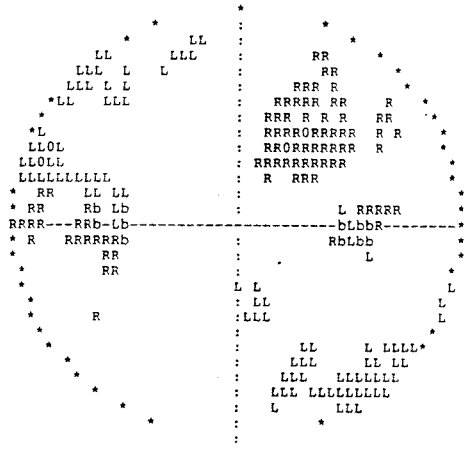

ORIGIN TIME 88 01 18 06H 34M 36.0S +/- 0.44S
LATITUDE 67.247 +/- 0.013 DEG.
LONGITUDE 23.723 +/- 0.076
FOCAL DEPTH 15.8 +/- 2.5 KM

STA	ARR. TIME	RES.	WEIGHT	DIST.	AZIMUTH	
KPM P	06 34 46.92	-0.01	39.6	65.6	213.4	
KPM S	06 34 55.03	0.04	2.8	65.6	213.4	
MUG P	06 34 48.60	0.01	35.2	76.1	289.1	P DOWN
LJV P	06 34 51.58	-0.02	29.1	95.0	226.5	
LJV S	06 35 3.17	0.07	1.9	95.0	226.5	
KLX P	06 34 57.65	0.02	20.3	135.3	193.4	

INPUT DATA FOR FAULT PLANE SOLUTION

STN	DIST. KM	AZIMUTH DEGREES	OMEGA(PZ) METER-SEC	OMEGA(SZ) METER-SEC
KPM	69.	215.8	0.79E-10	0.15E-09
MUG	80.	287.3	- 0.14E-09	0.13E-09
LJV	99.	227.7	0.30E-10	0.19E-09
KLX	138.	195.1	0.11E-09	0.14E-09

DYNAMIC SOURCE PARAMETERS

SIZE MEASURES
SEISMIC MOMENT: 0.109E+12 Nm
LOCAL MAGNITUDE: 1.0

SHEAR WAVE CORNER FREQUENCY RANGE AT CLOSE DISTANCES (130km)
9.0Hz -12.7Hz (10.9Hz)

FAULT RADIUS RANGE 54m - 76m (63m)

STRESS DROP RANGE 0.11MPa - 0.30MPa (0.19MPa)

RANGE OF THE PEAK SLIP AT THE FAULT 0.3mm - 0.5mm (0.4mm)

```
THE ORIENTATION OF THE RELAXED STRESS
        AZIMUTH   DIP
P-AXIS    100.   -18. degrees
T-AXIS    186.    11.

THE HORIZONTAL DEVIATORIC STRESS AS GIVEN BY THE P- AND T-AXES
THE AZIMUTH OF COMPRESSION -82 degrees
THE RELATIVE SIZE 0.93

THE TWO POSSIBLE FAULT PLANES
          STRIKE   DIP   SLIP
PLANE A   -38.   111.   185. degrees
PLANE B   234.    85.    21.

THE NORMAL DIRECTIONS OF THE FAULT PLANES
         AZIMUTH   DIP
PLANE A   232.    21. degrees
PLANE B   324.     5.



STATISTICAL INFORMATION

OF  1 FIRST MOTION POLARITY OBSERVATIONS
AT LEAST  1 ARE REQUIRED TO FIT

THE OPTIMUM MECHANISM HAS  0 POLARITY MISFITS

AMPLITUDES FOR P AND S AT  4 STATIONS ARE USED
ONLY MECHANISMS GIVING AN ESTIMATED STANDARD
DEVIATION OF THE AMPLITUDE ERROR FACTOR OF LESS
THAN 1.60 FOR SINGLE P-WAVE OBSERVATIONS ARE
TAKEN AS ACCEPTABLE AND INCLUDED IN THE FIGURES

 0.13 % OF ALL MECHANISMS ARE ACCEPTABLE
 50.0 % ACCEPTABLE DUE TO FIRST MOTION OBSERVATIONS
  0.3 % OF THESE FITTED ALSO THE AMPLITUDES
THE PART OF WELL FITTING PLANES IS  3.1%

THE AMPLITUDE FIT OF THE OPTIMAL MECHANISM
GIVES A MEAN ERROR FACTOR OF 1.46
THIS CORRESPONDS TO A STANDARD DEVIATION FACTOR OF 1.71
FOR SINGLE P-WAVE OBSERVATIONS

THE DOUBLE COUPLE SOLUTION IS SIGNIFICANT
AT 14 % LEVEL
(F-VALUE: F( 7, 4) =  3.17)

THE MEASURE OF THE MISFIT TO AN EARTHQUAKE SPECTRUM
P-WAVES  0.43
S-WAVES  0.27
```

-AXIS ORIENTATIONS
EQUAL AREA PROJECTION
LOWER HEMISPHERE

J01806344

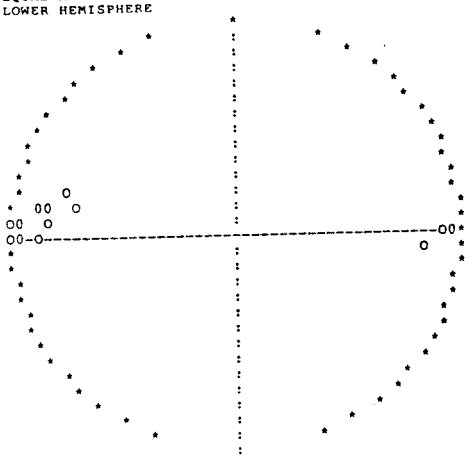

T-AXIS ORIENTATIONS
EQUAL AREA PROJECTION
LOWER HEMISPHERE

J01806344

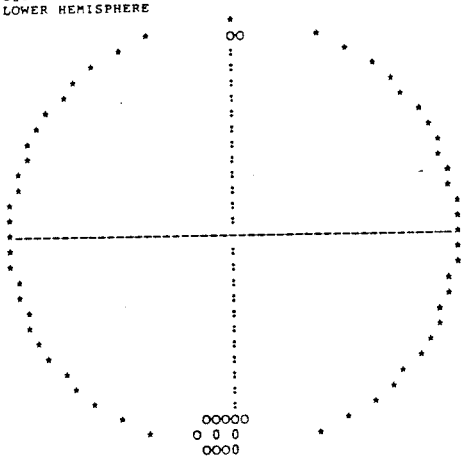

HORIZONTAL DEVIATORIC STRESS
RELATIVE SIZE AND
ORIENTATION OF COMPRESSION

J01806344

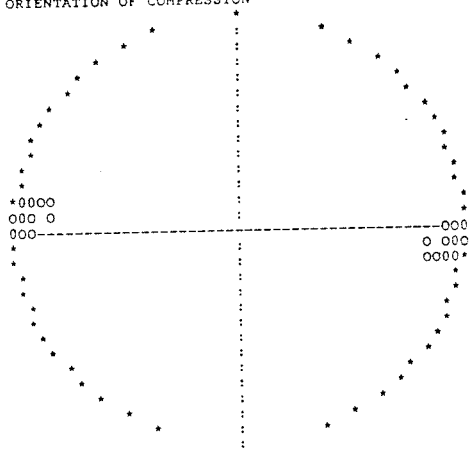

FAULT PLANE ORIENTATIONS
GIVEN BY NORMAL VECTORS
EQUAL AREA PROJECTION
LOWER HEMISPHERE

J01806344

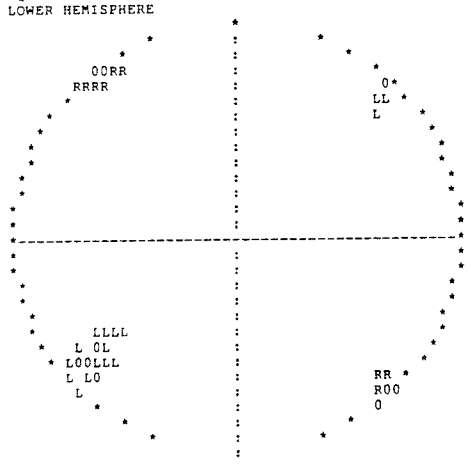

ORIGIN TIME 88 01 31 05H 02M 12.2S +/- 0.53S
LATITUDE 66.756 +/- 0.015 DEG.
LONGITUDE 19.195 +/- 0.086
FOCAL DEPTH 24.8 +/- 4.7 KM

STA		ARR. TIME	RES.	WEIGHT	DIST.	AZIMUTH	
HAK	P	05 02 29.11	-0.13	26.3	105.7	78.7	P DOWN
HAK	S	05 02 41.83	-0.18	1.7	105.7	78.7	
LJV	P	05 02 33.25	0.10	20.9	131.9	93.6	P DOWN
LJV	S	05 02 49.13	0.24	1.3	131.9	93.6	
MUG	P	05 02 35.46	0.08	18.6	146.9	56.2	
MUG	S	05 02 53.01	0.18	1.1	146.9	56.2	
VMK	P	05 02 37.56	0.00	16.6	161.4	137.0	P DOWN
VMK	S	05 02 56.73	0.07	1.0	161.4	137.0	
KPM	P	05 02 37.89	-0.01	16.4	163.7	88.3	P DOWN
KLX	P	05 02 41.00	-0.04	6.1	188.0	112.4	P DOWN

INPUT DATA FOR FAULT PLANE SOLUTION

STN	DIST. KM	AZIMUTH DEGREES	OMEGA(PZ) METER-SEC	OMEGA(SZ) METER-SEC
HAK	105.	78.9	- 0.44E-09	0.13E-08
LJV	132.	93.8	- 0.11E-08	0.39E-08
MUG	146.	56.3	0.11E-08	0.28E-08
VMK	162.	137.1	- 0.44E-09	0.12E-08
KPM	163.	88.5	- 0.63E-09	0.16E-08
KLX	188.	112.5	- 0.47E-09	0.15E-08

DYNAMIC SOURCE PARAMETERS

SIZE MEASURES
SEISMIC MOMENT: 0.119E+13 Nm
LOCAL MAGNITUDE: 2.1

SHEAR WAVE CORNER FREQUENCY RANGE AT CLOSE DISTANCES (130km)
11.0Hz -30.0Hz (15.9Hz)

FAULT RADIUS RANGE 23m - 62m (43m)

STRESS DROP RANGE 2.11MPa - 42.87MPa (6.38MPa)

RANGE OF THE PEAK SLIP AT THE FAULT 3.3mm - 24.8mm (7.0mm)

THE ORIENTATION OF THE RELAXED STRESS

	AZIMUTH	DIP
P-AXIS	115.	-12. degrees
T-AXIS	24.	-6.

THE HORIZONTAL DEVIATORIC STRESS AS GIVEN BY THE P- AND T-AXES
THE AZIMUTH OF COMPRESSION -66 degrees
THE RELATIVE SIZE 0.97

THE TWO POSSIBLE FAULT PLANES

	STRIKE	DIP	SLIP
PLANE A	70.	94.	-13. degrees
PLANE B	159.	77.	176.

THE NORMAL DIRECTIONS OF THE FAULT PLANES

	AZIMUTH	DIP
PLANE A	340.	4. degrees
PLANE B	249.	13.

STATISTICAL INFORMATION

OF 5 FIRST MOTION POLARITY OBSERVATIONS
AT LEAST 5 ARE REQUIRED TO FIT

THE OPTIMUM MECHANISM HAS 0 POLARITY MISFITS

AMPLITUDES FOR P AND S AT 6 STATIONS ARE USED
ONLY MECHANISMS GIVING AN ESTIMATED STANDARD
DEVIATION OF THE AMPLITUDE ERROR FACTOR OF LESS
THAN 1.60 FOR SINGLE P-WAVE OBSERVATIONS ARE
TAKEN AS ACCEPTABLE AND INCLUDED IN THE FIGURES

1.84 % OF ALL MECHANISMS ARE ACCEPTABLE
12.7 % ACCEPTABLE DUE TO FIRST MOTION OBSERVATIONS
14.5 % OF THESE FITTED ALSO THE AMPLITUDES
THE PART OF WELL FITTING PLANES IS 20.9%

THE AMPLITUDE FIT OF THE OPTIMAL MECHANISM
GIVES A MEAN ERROR FACTOR OF 1.30
THIS CORRESPONDS TO A STANDARD DEVIATION FACTOR OF 1.38
FOR SINGLE P-WAVE OBSERVATIONS

THE DOUBLE COUPLE SOLUTION IS SIGNIFICANT
AT 17 % LEVEL
(F-VALUE: F(11, 8) = 1.97)

THE MEASURE OF THE MISFIT TO AN EARTHQUAKE SPECTRUM
P-WAVES 0.28
S-WAVES 0.23

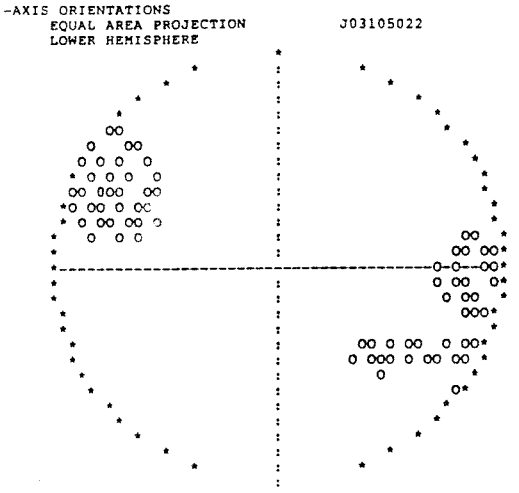
-AXIS ORIENTATIONS
EQUAL AREA PROJECTION
LOWER HEMISPHERE
J03105022

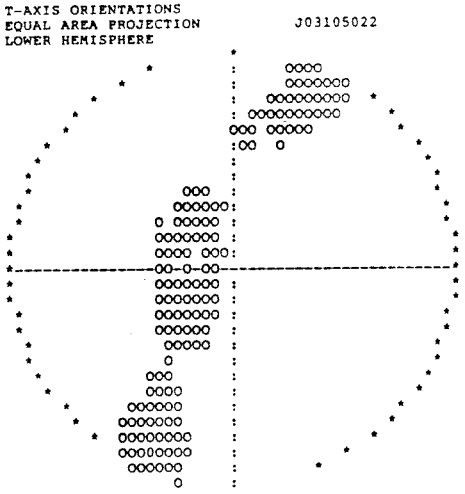
T-AXIS ORIENTATIONS
EQUAL AREA PROJECTION
LOWER HEMISPHERE
J03105022

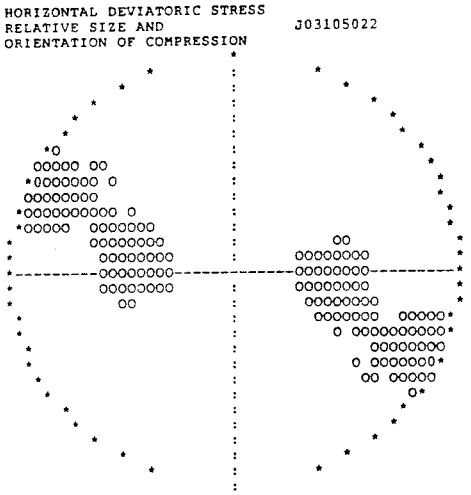
HORIZONTAL DEVIATORIC STRESS
RELATIVE SIZE AND
ORIENTATION OF COMPRESSION
J03105022

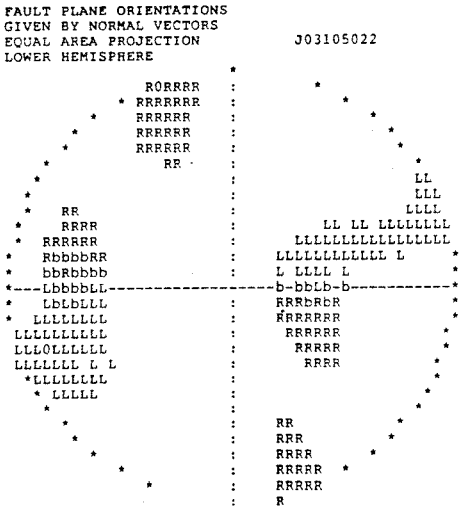
FAULT PLANE ORIENTATIONS
GIVEN BY NORMAL VECTORS
EQUAL AREA PROJECTION
LOWER HEMISPHERE
J03105022

ORIGIN TIME 88 02 02 11H 13M 21.1S +/- 0.37S
LATITUDE 67.491 +/- 0.020 DEG.
LONGITUDE 21.889 +/- 0.043
FOCAL DEPTH 6.8 +/- 2.5 KM

STA	ARR. TIME	RES.	WEIGHT	DIST.	AZIMUTH	
MUG	P 11 13 22.70	0.00	87.8	7.5	115.8	P UP
MUG	S 11 13 23.99	0.06	9.0	7.5	115.8	
HAK	P 11 13 31.63	-0.09	39.9	64.9	192.8	P DOWN
HAK	S 11 13 39.46	-0.12	2.9	64.9	192.8	
KPM	P 11 13 36.22	-0.12	29.6	93.3	151.3	
KPM	S 11 13 47.21	-0.37	1.9	93.3	151.3	
LJV	P 11 13 36.75	0.26	29.3	94.2	172.5	
LJV	S 11 13 47.92	0.07	1.9	94.2	172.5	
VMK	P 11 13 53.35	0.02	2.5	202.7	183.9	

INPUT DATA FOR FAULT PLANE SOLUTION

STN	DIST. KM	AZIMUTH DEGREES	OMEGA(PZ) METER-SEC	OMEGA(SZ) METER-SEC
HAK	65.	192.9	- 0.19E-09	0.25E-09
KPM	93.	151.3	0.14E-09	0.58E-09
LJV	94.	172.5	0.11E-09	0.55E-09
MUG	7.	115.3	+ 0.00E+00	0.00E+00

DYNAMIC SOURCE PARAMETERS

SIZE MEASURES
SEISMIC MOMENT: 0.167E+12 Nm
LOCAL MAGNITUDE: 1.2

SHEAR WAVE CORNER FREQUENCY RANGE AT CLOSE DISTANCES (130km)
10.8Hz -16.5Hz (13.6Hz)

FAULT RADIUS RANGE 41m - 63m (50m)

STRESS DROP RANGE 0.28MPa - 1.00MPa (0.56MPa)

RANGE OF THE PEAK SLIP AT THE FAULT 0.6mm - 1.3mm (0.9mm)

THE ORIENTATION OF THE RELAXED STRESS

	AZIMUTH	DIP	
P-AXIS	44.	5.	degrees
T-AXIS	-31.	-71.	

THE HORIZONTAL DEVIATORIC STRESS AS GIVEN BY THE P- AND T-AXES
THE AZIMUTH OF COMPRESSION 45 degrees
THE RELATIVE SIZE 0.54

THE TWO POSSIBLE FAULT PLANES

	STRIKE	DIP	SLIP	
PLANE A	-27.	43.	-62.	degrees
PLANE B	117.	53.	246.	

THE NORMAL DIRECTIONS OF THE FAULT PLANES

	AZIMUTH	DIP	
PLANE A	63.	47.	degrees
PLANE B	207.	37.	

STATISTICAL INFORMATION

OF 2 FIRST MOTION POLARITY OBSERVATIONS
AT LEAST 2 ARE REQUIRED TO FIT

THE OPTIMUM MECHANISM HAS 0 POLARITY MISFITS

AMPLITUDES FOR P AND S AT 3 STATIONS ARE USED
ONLY MECHANISMS GIVING AN ESTIMATED STANDARD
DEVIATION OF THE AMPLITUDE ERROR FACTOR OF LESS
THAN 1.60 FOR SINGLE P-WAVE OBSERVATIONS ARE
TAKEN AS ACCEPTABLE AND INCLUDED IN THE FIGURES

6.95 % OF ALL MECHANISMS ARE ACCEPTABLE
32.8 % ACCEPTABLE DUE TO FIRST MOTION OBSERVATIONS
21.2 % OF THESE FITTED ALSO THE AMPLITUDES
THE PART OF WELL FITTING PLANES IS 54.0%

THE AMPLITUDE FIT OF THE OPTIMAL MECHANISM
GIVES A MEAN ERROR FACTOR OF 1.14
THIS CORRESPONDS TO A STANDARD DEVIATION FACTOR OF 1.25
FOR SINGLE P-WAVE OBSERVATIONS

THE DOUBLE COUPLE SOLUTION IS SIGNIFICANT
AT 15 % LEVEL
(F-VALUE: F(5, 2) = 6.59)

THE MEASURE OF THE MISFIT TO AN EARTHQUAKE SPECTRUM

P-WAVES	0.17
S-WAVES	0.24

-AXIS ORIENTATIONS
EQUAL AREA PROJECTION
LOWER HEMISPHERE
J03311132

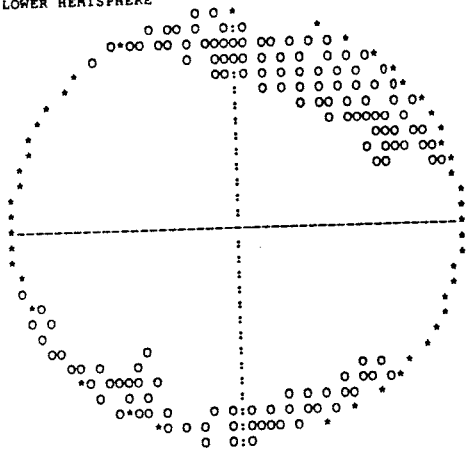

T-AXIS ORIENTATIONS
EQUAL AREA PROJECTION
LOWER HEMISPHERE
J03311132

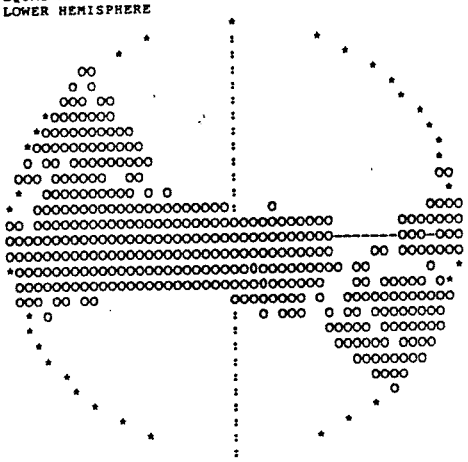

HORIZONTAL DEVIATORIC STRESS
RELATIVE SIZE AND
ORIENTATION OF COMPRESSION
J03311132

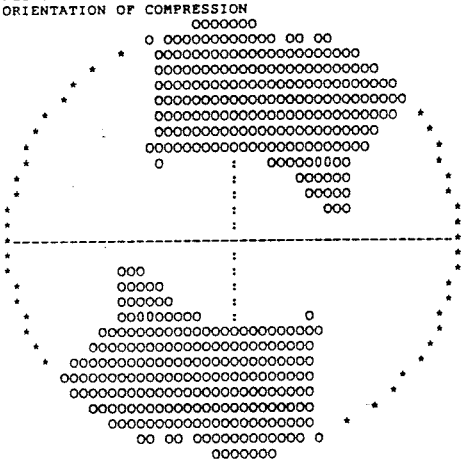

FAULT PLANE ORIENTATIONS
GIVEN BY NORMAL VECTORS
EQUAL AREA PROJECTION
LOWER HEMISPHERE
J03311132

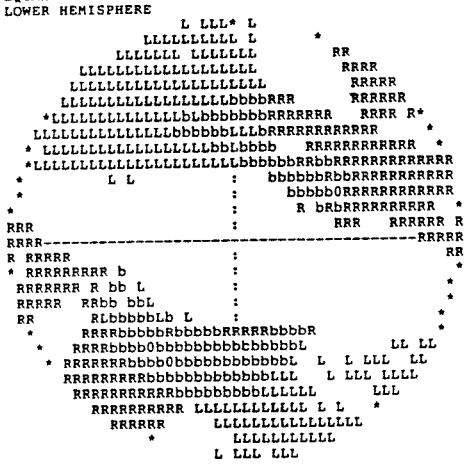

ORIGIN TIME 88 02 06 14H 51M 34.2S +/- 0.42S
LATITUDE 67.560 +/- 0.024 DEG.
LONGITUDE 22.210 +/- 0.050
FOCAL DEPTH 12.0 +/- 2.0 KM

STA	ARR. TIME	RES.	WEIGHT	DIST.	AZIMUTH	
MUG	P 14 51 37.07	0.01	80.1	13.1	213.0	P UP
MUG	S 14 51 39.22	0.03	7.8	13.1	213.0	
HAK	P 14 51 46.68	-0.06	35.1	76.4	201.9	
HAK	S 14 51 56.07	0.06	2.4	76.4	201.9	
KPM	P 14 51 49.64	-0.07	29.1	94.8	161.2	P DOWN
KPM	S 14 52 1.35	0.20	1.9	94.8	161.2	
KLX	P 14 52 1.63	0.32	6.9	170.6	167.4	

INPUT DATA FOR FAULT PLANE SOLUTION

STN	DIST. KM	AZIMUTH DEGREES		OMEGA(PZ) METER-SEC	OMEGA(SZ) METER-SEC
MUG	13.	212.9	+	0.22E-09	0.87E-09
HAK	76.	201.9		0.52E-10	0.14E-09
KPM	95.	161.1	-	0.87E-10	0.24E-09
LJV	101.	181.1		0.89E-10	0.27E-09
KLX	171.	167.4		0.95E-10	0.23E-09

DYNAMIC SOURCE PARAMETERS

SIZE MEASURES
SEISMIC MOMENT: 0.789E+11 Nm
LOCAL MAGNITUDE: 0.9

SHEAR WAVE CORNER FREQUENCY RANGE AT CLOSE DISTANCES (130km)
10.7Hz -16.7Hz (13.7Hz)

FAULT RADIUS RANGE 41m - 64m (50m)

STRESS DROP RANGE 0.13MPa - 0.49MPa (0.27MPa)

RANGE OF THE PEAK SLIP AT THE FAULT 0.3mm - 0.6mm (0.4mm)

THE ORIENTATION OF THE RELAXED STRESS

	AZIMUTH	DIP
P-AXIS	170.	-1. degrees
T-AXIS	80.	25.

THE HORIZONTAL DEVIATORIC STRESS AS GIVEN BY THE P- AND T-AXES
THE AZIMUTH OF COMPRESSION -10 degrees
THE RELATIVE SIZE 0.91

THE TWO POSSIBLE FAULT PLANES

	STRIKE	DIP	SLIP
PLANE A	122.	108.	18. degrees
PLANE B	218.	107.	161.

THE NORMAL DIRECTIONS OF THE FAULT PLANES

	AZIMUTH	DIP
PLANE A	32.	18. degrees
PLANE B	128.	17.

STATISTICAL INFORMATION

OF 2 FIRST MOTION POLARITY OBSERVATIONS
AT LEAST 2 ARE REQUIRED TO FIT

THE OPTIMUM MECHANISM HAS 0 POLARITY MISFITS

AMPLITUDES FOR P AND S AT 5 STATIONS ARE USED
ONLY MECHANISMS GIVING AN ESTIMATED STANDARD
DEVIATION OF THE AMPLITUDE ERROR FACTOR OF LESS
THAN 1.60 FOR SINGLE P-WAVE OBSERVATIONS ARE
TAKEN AS ACCEPTABLE AND INCLUDED IN THE FIGURES

5.22 % OF ALL MECHANISMS ARE ACCEPTABLE
27.2 % ACCEPTABLE DUE TO FIRST MOTION OBSERVATIONS
19.2 % OF THESE FITTED ALSO THE AMPLITUDES
THE PART OF WELL FITTING PLANES IS 46.9%

THE AMPLITUDE FIT OF THE OPTIMAL MECHANISM
GIVES A MEAN ERROR FACTOR OF 1.19
THIS CORRESPONDS TO A STANDARD DEVIATION FACTOR OF 1.25
FOR SINGLE P-WAVE OBSERVATIONS

THE DOUBLE COUPLE SOLUTION IS SIGNIFICANT
AT 10 % LEVEL
(F-VALUE: F(9, 6) = 2.84)

THE MEASURE OF THE MISFIT TO AN EARTHQUAKE SPECTRUM
P-WAVES 0.27
S-WAVES 0.22

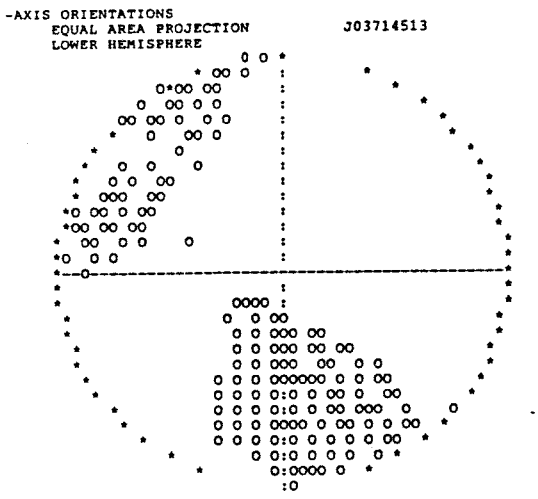
-AXIS ORIENTATIONS
EQUAL AREA PROJECTION
LOWER HEMISPHERE
J03714513

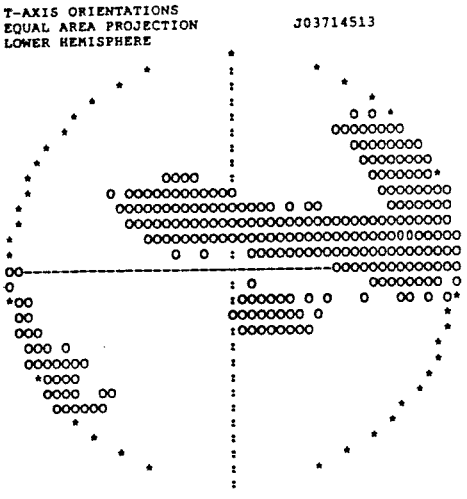
T-AXIS ORIENTATIONS
EQUAL AREA PROJECTION
LOWER HEMISPHERE
J03714513

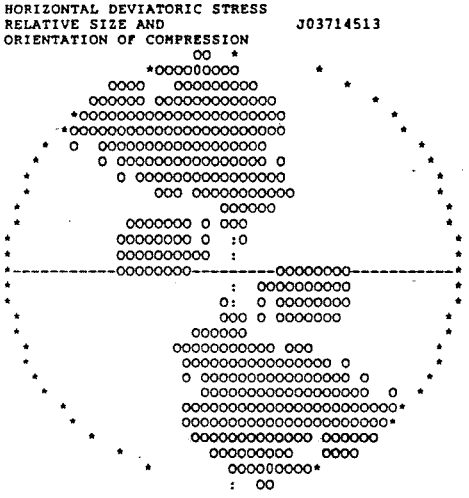
HORIZONTAL DEVIATORIC STRESS
RELATIVE SIZE AND
ORIENTATION OF COMPRESSION
J03714513

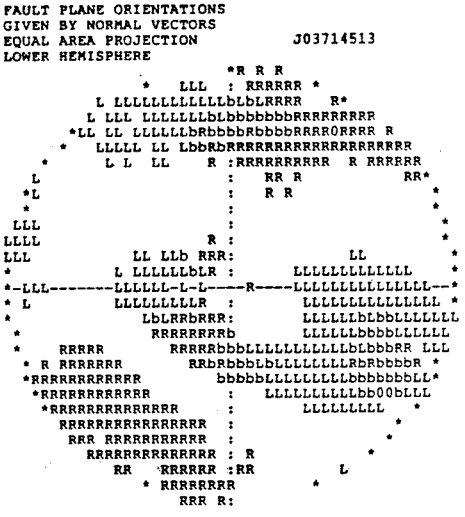
FAULT PLANE ORIENTATIONS
GIVEN BY NORMAL VECTORS
EQUAL AREA PROJECTION
LOWER HEMISPHERE
J03714513

ORIGIN TIME 88 02 06 20H 15M 44.0S +/- 0.86S
LATITUDE 67.651 +/- 0.037 DEG.
LONGITUDE 19.363 +/- 0.112
FOCAL DEPTH 4.9 +/- 4.5 KM

STA	ARR.	TIME	RES.	WEIGHT	DIST.	AZIMUTH
MUG	P	20 16 3.02	0.01	23.9	116.4	99.3
MUG	S	20 16 16.81	-0.19	1.5	116.4	99.3
HAK	P	20 16 4.35	-0.04	22.2	124.9	129.6
LJV	P	20 16 10.69	0.01	16.2	165.0	131.2
LJV	S	20 16 31.07	0.43	0.9	165.0	131.2
KPM	P	20 16 13.47	0.07	6.3	183.2	121.5
KPM	S	20 16 35.08	-0.36	0.4	183.2	121.5
KLX	P	20 16 20.89	-0.15	2.0	239.3	136.0

INPUT DATA FOR FAULT PLANE SOLUTION

STN	DIST. KM	AZIMUTH DEGREES	OMEGA(PZ) METER-SEC	OMEGA(SZ) METER-SEC
MUG	116.	99.7	0.16E-09	0.10E-08
LJV	165.	131.5	0.25E-09	0.58E-09
KPM	183.	121.8	0.18E-09	0.93E-09
KLX	240.	136.2	0.28E-09	0.62E-09
VMK	242.	155.0	0.85E-10	0.20E-09

DYNAMIC SOURCE PARAMETERS

SIZE MEASURES
SEISMIC MOMENT: 0.202E+12 Nm
LOCAL MAGNITUDE: 1.3

SHEAR WAVE CORNER FREQUENCY RANGE AT CLOSE DISTANCES (130km)
4.6Hz - 9.3Hz (6.7Hz)

FAULT RADIUS RANGE 74m - 150m (102m)

STRESS DROP RANGE 0.03MPa - 0.22MPa (0.08MPa)

RANGE OF THE PEAK SLIP AT THE FAULT 0.1mm - 0.5mm (0.3mm)

THE ORIENTATION OF THE RELAXED STRESS

	AZIMUTH	DIP	
P-AXIS	49.	5.	degrees
T-AXIS	-35.	-47.	

THE HORIZONTAL DEVIATORIC STRESS AS GIVEN BY THE P- AND T-AXES
THE AZIMUTH OF COMPRESSION 51 degrees
THE RELATIVE SIZE 0.72

THE TWO POSSIBLE FAULT PLANES

	STRIKE	DIP	SLIP	
PLANE A	-4.	54.	-34.	degrees
PLANE B	107.	63.	221.	

THE NORMAL DIRECTIONS OF THE FAULT PLANES

	AZIMUTH	DIP	
PLANE A	86.	36.	degrees
PLANE B	197.	27.	

STATISTICAL INFORMATION

OF 0 FIRST MOTION POLARITY OBSERVATIONS
AT LEAST 0 ARE REQUIRED TO FIT

THE OPTIMUM MECHANISM HAS 0 POLARITY MISFITS

AMPLITUDES FOR P AND S AT 5 STATIONS ARE USED
ONLY MECHANISMS GIVING AN ESTIMATED STANDARD
DEVIATION OF THE AMPLITUDE ERROR FACTOR OF LESS
THAN 1.60 FOR SINGLE P-WAVE OBSERVATIONS ARE
TAKEN AS ACCEPTABLE AND INCLUDED IN THE FIGURES

34.91 % OF ALL MECHANISMS ARE ACCEPTABLE
100.0 % ACCEPTABLE DUE TO FIRST MOTION OBSERVATIONS
34.9 % OF THESE FITTED ALSO THE AMPLITUDES
THE PART OF WELL FITTING PLANES IS 83.3%

THE AMPLITUDE FIT OF THE OPTIMAL MECHANISM
GIVES A MEAN ERROR FACTOR OF 1.35
THIS CORRESPONDS TO A STANDARD DEVIATION FACTOR OF 1.48
FOR SINGLE P-WAVE OBSERVATIONS

THE DOUBLE COUPLE SOLUTION IS SIGNIFICANT
AT 32 % LEVEL
(F-VALUE: F(9, 6) = 1.49)

THE MEASURE OF THE MISFIT TO AN EARTHQUAKE SPECTRUM
P-WAVES 0.18
S-WAVES 0.24

-AXIS ORIENTATIONS
EQUAL AREA PROJECTION J03720160
LOWER HEMISPHERE

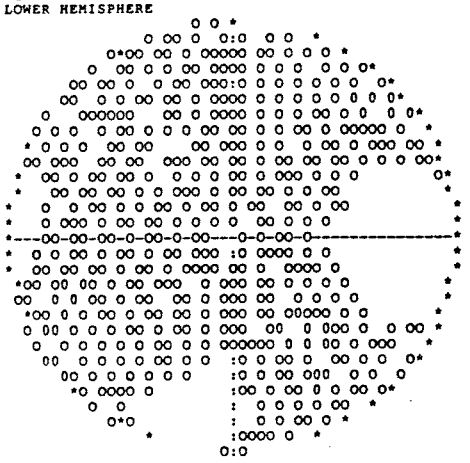

T-AXIS ORIENTATIONS
EQUAL AREA PROJECTION J03720160
LOWER HEMISPHERE

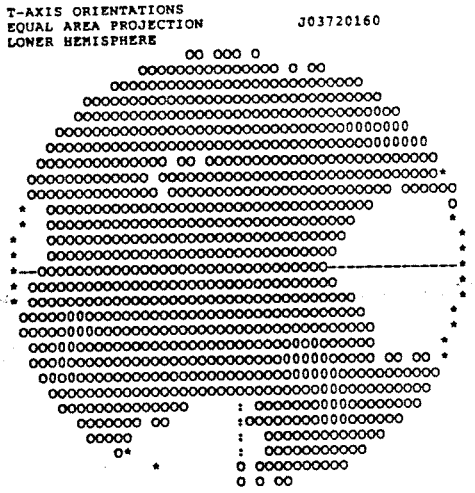

HORIZONTAL DEVIATORIC STRESS
RELATIVE SIZE AND J03720160
ORIENTATION OF COMPRESSION

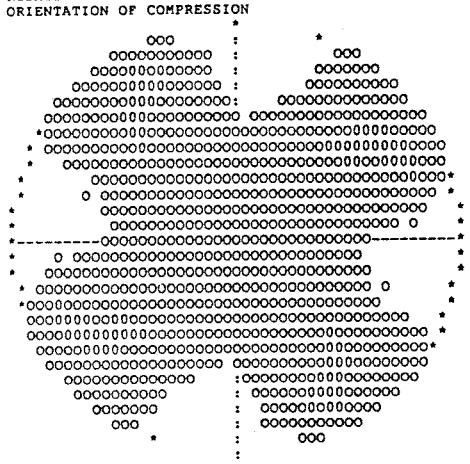

FAULT PLANE ORIENTATIONS
GIVEN BY NORMAL VECTORS
EQUAL AREA PROJECTION J03720160
LOWER HEMISPHERE

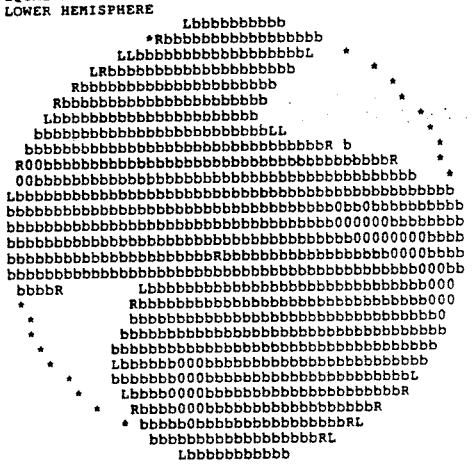

ORIGIN TIME 88 02 07 19H 22M 56.2S +/- 0.42S
LATITUDE 66.071 +/- 0.013 DEG.
LONGITUDE 23.517 +/- 0.071
FOCAL DEPTH 6.7 +/- 5.0 KM

STA		ARR. TIME	RES.	WEIGHT	DIST.	AZIMUTH	
KLX	P	19 23 0.01	0.00	69.6	22.1	269.2	P DOWN
KLX	S	19 23 2.82	0.01	6.3	22.1	269.2	
KPM	P	19 23 9.52	-0.02	33.4	81.2	340.5	P DOWN
KPM	S	19 23 19.17	-0.17	2.3	81.2	340.5	
LJV	P	19 23 10.84	0.04	30.9	89.0	317.7	
VMK	P	19 23 12.33	0.00	28.1	98.4	244.6	
VMK	S	19 23 24.03	-0.15	1.8	98.4	244.6	

INPUT DATA FOR FAULT PLANE SOLUTION

STN	DIST. KM	AZIMUTH DEGREES	OMEGA(PZ) METER-SEC	OMEGA(SZ) METER-SEC
KLX	22.	269.5	- 0.57E-10	0.54E-09
KPM	81.	340.8	- 0.32E-10	0.16E-09
LJV	89.	317.9	0.37E-10	0.84E-10
VMK	98.	244.5	0.23E-10	0.98E-10
HAK	129.	318.5	0.42E-10	0.91E-10

DYNAMIC SOURCE PARAMETERS

SIZE MEASURES
SEISMIC MOMENT: 0.368E+11 Nm
LOCAL MAGNITUDE: 0.6

SHEAR WAVE CORNER FREQUENCY RANGE AT CLOSE DISTANCES (130km)
3.4Hz - 6.5Hz (4.9Hz)

FAULT RADIUS RANGE 106m - 202m (140m)

STRESS DROP RANGE 0.00MPa - 0.01MPa (0.01MPa)

RANGE OF THE PEAK SLIP AT THE FAULT 0.0mm - 0.0mm (0.0mm)

THE ORIENTATION OF THE RELAXED STRESS

	AZIMUTH	DIP
P-AXIS	138.	-12. degrees
T-AXIS	193.	70.

THE HORIZONTAL DEVIATORIC STRESS AS GIVEN BY THE P- AND T-AXES
THE AZIMUTH OF COMPRESSION -45 degrees
THE RELATIVE SIZE 0.50

THE TWO POSSIBLE FAULT PLANES

	STRIKE	DIP	SLIP
PLANE A	28.	144.	119. degrees
PLANE B	242.	121.	71.

THE NORMAL DIRECTIONS OF THE FAULT PLANES

	AZIMUTH	DIP
PLANE A	298.	54. degrees
PLANE B	152.	31.

STATISTICAL INFORMATION

OF 2 FIRST MOTION POLARITY OBSERVATIONS
AT LEAST 2 ARE REQUIRED TO FIT

THE OPTIMUM MECHANISM HAS 0 POLARITY MISFITS

AMPLITUDES FOR P AND S AT 5 STATIONS ARE USED
ONLY MECHANISMS GIVING AN ESTIMATED STANDARD
DEVIATION OF THE AMPLITUDE ERROR FACTOR OF LESS
THAN 1.60 FOR SINGLE P-WAVE OBSERVATIONS ARE
TAKEN AS ACCEPTABLE AND INCLUDED IN THE FIGURES

1.98 % OF ALL MECHANISMS ARE ACCEPTABLE
19.1 % ACCEPTABLE DUE TO FIRST MOTION OBSERVATIONS
10.3 % OF THESE FITTED ALSO THE AMPLITUDES
THE PART OF WELL FITTING PLANES IS 33.6%

THE AMPLITUDE FIT OF THE OPTIMAL MECHANISM
GIVES A MEAN ERROR FACTOR OF 1.32
THIS CORRESPONDS TO A STANDARD DEVIATION FACTOR OF 1.43
FOR SINGLE P-WAVE OBSERVATIONS

THE DOUBLE COUPLE SOLUTION IS SIGNIFICANT
AT 30 % LEVEL
(F-VALUE: F(9, 6) = 1.56)

THE MEASURE OF THE MISFIT TO AN EARTHQUAKE SPECTRUM

P-WAVES	0.21
S-WAVES	0.25

-AXIS ORIENTATIONS
EQUAL AREA PROJECTION
LOWER HEMISPHERE

J03819230

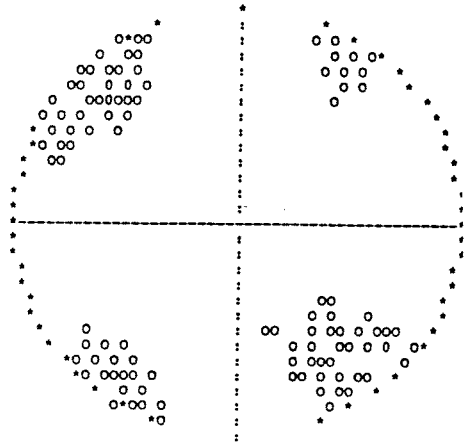

T-AXIS ORIENTATIONS
EQUAL AREA PROJECTION
LOWER HEMISPHERE

J03819230

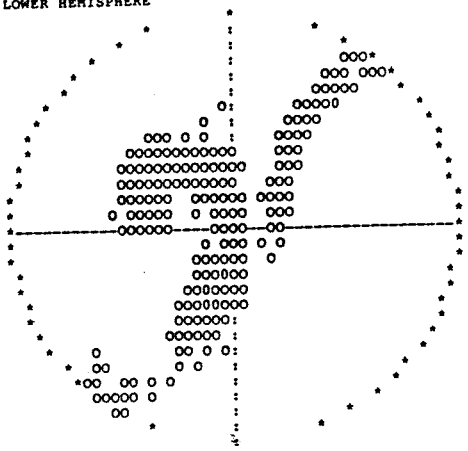

HORIZONTAL DEVIATORIC STRESS
RELATIVE SIZE AND
ORIENTATION OF COMPRESSION

J03819230

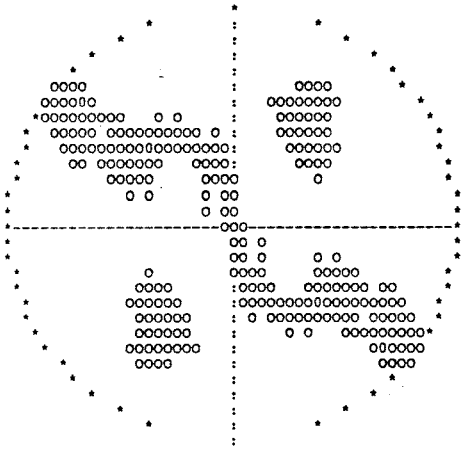

FAULT PLANE ORIENTATIONS
GIVEN BY NORMAL VECTORS
EQUAL AREA PROJECTION
LOWER HEMISPHERE

J03819230

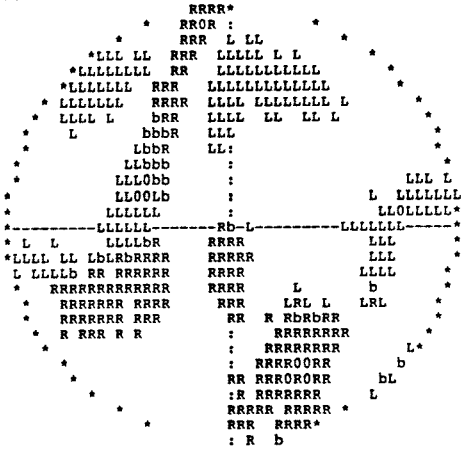

ORIGIN TIME 88 02 08 07H 48M 44.4S +/- 0.54S
LATITUDE 67.703 +/- 0.031 DEG.
LONGITUDE 23.358 +/- 0.061
FOCAL DEPTH 6.7 +/- 23.3 KM

STA	ARR.	TIME	RES.	WEIGHT	DIST.	AZIMUTH
MUG	P	07 48 54.54	-0.03	41.2	62.1	245.0
MUG	S	07 49 2.39	0.29	3.0	62.1	245.0
KPM	P	07 49 1.96	0.00	25.8	107.6	190.7
KPM	S	07 49 14.87	-0.05	1.6	107.6	190.7
HAK	S	07 49 17.28	-0.12	1.5	116.5	222.6
HAK	P	07 49 3.39	-0.01	23.9	116.5	222.6
LJV	P	07 49 5.33	0.07	21.6	128.0	204.4
LJV	S	07 49 20.18	-0.45	1.3	128.0	204.4

INPUT DATA FOR FAULT PLANE SOLUTION

STN	DIST. KM	AZIMUTH DEGREES	OMEGA(PZ) METER-SEC	OMEGA(SZ) METER-SEC
MUG	64.	243.8	0.39E-09	0.75E-09
KPM	110.	191.0	0.88E-10	0.37E-09
HAK	119.	222.3	0.90E-10	0.33E-09
LJV	130.	204.4	0.95E-10	0.42E-09
KLX	185.	184.9	0.20E-09	0.38E-09
VMK	241.	200.0	0.85E-10	0.22E-09

DYNAMIC SOURCE PARAMETERS

SIZE MEASURES
SEISMIC MOMENT: 0.237E+12 Nm
LOCAL MAGNITUDE: 1.4

SHEAR WAVE CORNER FREQUENCY RANGE AT CLOSE DISTANCES (130km)
13.4Hz -30.0Hz (19.2Hz)

FAULT RADIUS RANGE 23m - 51m (35m)

STRESS DROP RANGE 0.76MPa - 8.52MPa (2.23MPa)

RANGE OF THE PEAK SLIP AT THE FAULT 1.3mm - 6.3mm (2.6mm)

THE ORIENTATION OF THE RELAXED STRESS

	AZIMUTH	DIP	
P-AXIS	166.	-18.	degrees
T-AXIS	82.	16.	

THE HORIZONTAL DEVIATORIC STRESS AS GIVEN BY THE P- AND T-AXES
THE AZIMUTH OF COMPRESSION -10 degrees
THE RELATIVE SIZE 0.91

THE TWO POSSIBLE FAULT PLANES

	STRIKE	DIP	SLIP
PLANE A	124.	114.	-1. degrees
PLANE B	214.	89.	155.

THE NORMAL DIRECTIONS OF THE FAULT PLANES

	AZIMUTH	DIP	
PLANE A	34.	24.	degrees
PLANE B	304.	1.	

STATISTICAL INFORMATION

OF 0 FIRST MOTION POLARITY OBSERVATIONS
AT LEAST 0 ARE REQUIRED TO FIT

THE OPTIMUM MECHANISM HAS 0 POLARITY MISFITS

AMPLITUDES FOR P AND S AT 6 STATIONS ARE USED
ONLY MECHANISMS GIVING AN ESTIMATED STANDARD
DEVIATION OF THE AMPLITUDE ERROR FACTOR OF LESS
THAN 1.60 FOR SINGLE P-WAVE OBSERVATIONS ARE
TAKEN AS ACCEPTABLE AND INCLUDED IN THE FIGURES

4.26 % OF ALL MECHANISMS ARE ACCEPTABLE
100.0 % ACCEPTABLE DUE TO FIRST MOTION OBSERVATIONS
4.3 % OF THESE FITTED ALSO THE AMPLITUDES
THE PART OF WELL FITTING PLANES IS 30.0%

THE AMPLITUDE FIT OF THE OPTIMAL MECHANISM
GIVES A MEAN ERROR FACTOR OF 1.33
THIS CORRESPONDS TO A STANDARD DEVIATION FACTOR OF 1.42
FOR SINGLE P-WAVE OBSERVATIONS

THE DOUBLE COUPLE SOLUTION IS SIGNIFICANT
AT 4 % LEVEL
(F-VALUE: F(11, 8) = 3.24)

THE MEASURE OF THE MISFIT TO AN EARTHQUAKE SPECTRUM
P-WAVES 0.25
S-WAVES 0.22

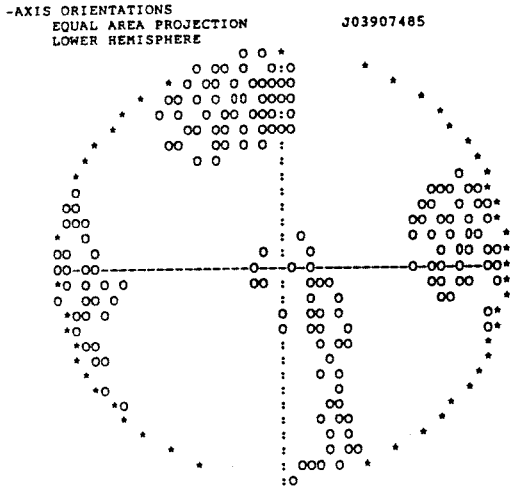
-AXIS ORIENTATIONS
EQUAL AREA PROJECTION
LOWER HEMISPHERE
J03907485

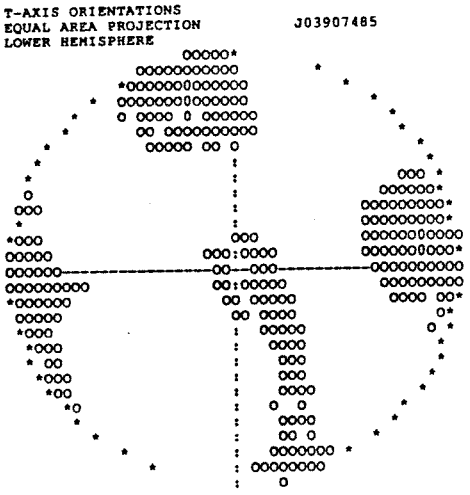
T-AXIS ORIENTATIONS
EQUAL AREA PROJECTION
LOWER HEMISPHERE
J03907485

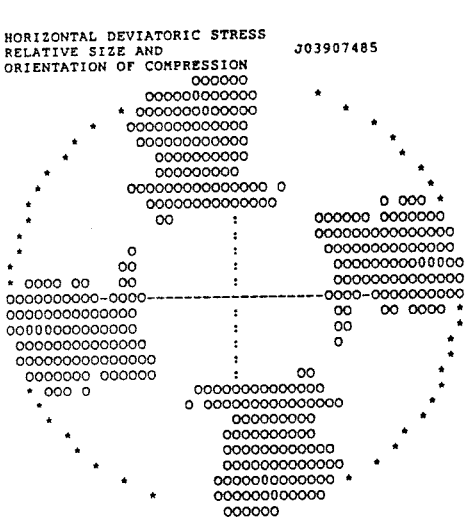
HORIZONTAL DEVIATORIC STRESS
RELATIVE SIZE AND
ORIENTATION OF COMPRESSION
J03907485

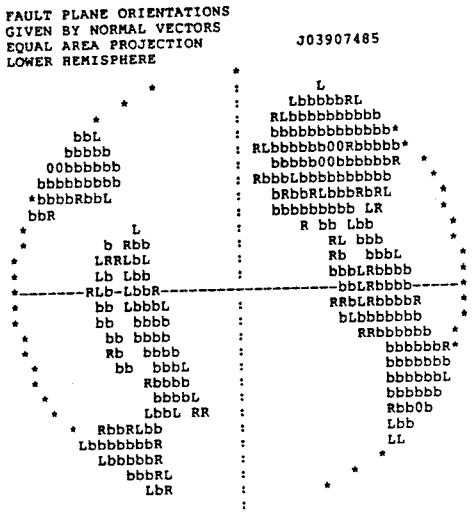
FAULT PLANE ORIENTATIONS
GIVEN BY NORMAL VECTORS
EQUAL AREA PROJECTION
LOWER HEMISPHERE
J03907485

ORIGIN TIME 88 02 19 23H 03M 4.8S +/- 0.42S
LATITUDE 66.631 +/- 0.016 DEG.
LONGITUDE 22.782 +/- 0.024
FOCAL DEPTH 6.9 +/- 7.0 KM

STA	ARR. TIME	RES.	WEIGHT	DIST.	AZIMUTH	
KPM P	23 03 7.52	0.03	78.2	14.6	21.2	P UP
KPM S	23 03 9.32	-0.21	7.5	14.6	21.2	
LJV P	23 03 9.41	-0.02	64.3	27.5	275.2	
LJV S	23 03 13.04	0.13	5.6	27.5	275.2	
HAK S	23 03 22.71	-0.07	2.9	63.1	301.6	
KLX S	23 03 23.01	-0.08	2.9	64.2	170.0	

INPUT DATA FOR FAULT PLANE SOLUTION

STN	DIST. KM	AZIMUTH DEGREES		OMEGA(PZ) METER-SEC	OMEGA(SZ) METER-SEC
KPM	14.	23.1	+	0.55E-10	0.26E-09
LJV	27.	273.7		0.12E-09	0.26E-09

DYNAMIC SOURCE PARAMETERS

SIZE MEASURES
SEISMIC MOMENT: 0.531E+11 Nm
LOCAL MAGNITUDE: 0.7

SHEAR WAVE CORNER FREQUENCY RANGE AT CLOSE DISTANCES (130km)
 3.2Hz - 6.4Hz (4.7Hz)

FAULT RADIUS RANGE 107m - 215m (146m)

STRESS DROP RANGE 0.00MPa - 0.02MPa (0.01MPa)

RANGE OF THE PEAK SLIP AT THE FAULT 0.0mm - 0.1mm (0.0mm)

THE ORIENTATION OF THE RELAXED STRESS

	AZIMUTH	DIP	
P-AXIS	150.	-12.	degrees
T-AXIS	63.	14.	

THE HORIZONTAL DEVIATORIC STRESS AS GIVEN BY THE P- AND T-AXES
THE AZIMUTH OF COMPRESSION -28 degrees
THE RELATIVE SIZE 0.95

THE TWO POSSIBLE FAULT PLANES

	STRIKE	DIP	SLIP	
PLANE A	106.	108.	1.	degrees
PLANE B	197.	91.	162.	

THE NORMAL DIRECTIONS OF THE FAULT PLANES

	AZIMUTH	DIP	
PLANE A	16.	18.	degrees
PLANE B	107.	1.	

STATISTICAL INFORMATION

OF 1 FIRST MOTION POLARITY OBSERVATIONS
AT LEAST 1 ARE REQUIRED TO FIT

THE OPTIMUM MECHANISM HAS 0 POLARITY MISFITS

AMPLITUDES FOR P AND S AT 2 STATIONS ARE USED
ONLY MECHANISMS GIVING AN ESTIMATED STANDARD
DEVIATION OF THE AMPLITUDE ERROR FACTOR OF LESS
THAN 1.60 FOR SINGLE P-WAVE OBSERVATIONS ARE
TAKEN AS ACCEPTABLE AND INCLUDED IN THE FIGURES

3.36 % OF ALL MECHANISMS ARE ACCEPTABLE
50.0 % ACCEPTABLE DUE TO FIRST MOTION OBSERVATIONS
6.8 % OF THESE FITTED ALSO THE AMPLITUDES
THE PART OF WELL FITTING PLANES IS 42.7%

THE AMPLITUDE FIT OF THE OPTIMAL MECHANISM
GIVES A MEAN ERROR FACTOR OF 1.06

THE MEASURE OF THE MISFIT TO AN EARTHQUAKE SPECTRUM
P-WAVES 0.42
S-WAVES 0.28

-AXIS ORIENTATIONS
EQUAL AREA PROJECTION J05023030
LOWER HEMISPHERE

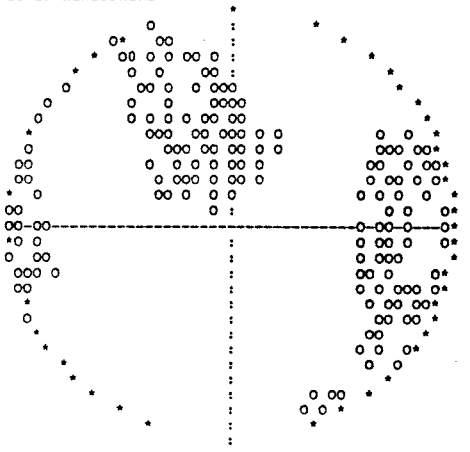

T-AXIS ORIENTATIONS
EQUAL AREA PROJECTION J05023030
LOWER HEMISPHERE

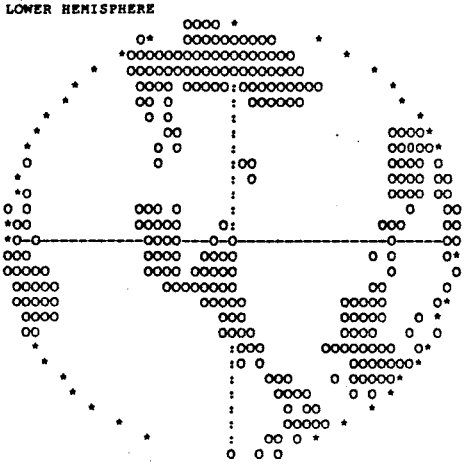

HORIZONTAL DEVIATORIC STRESS
RELATIVE SIZE AND J05023030
ORIENTATION OF COMPRESSION

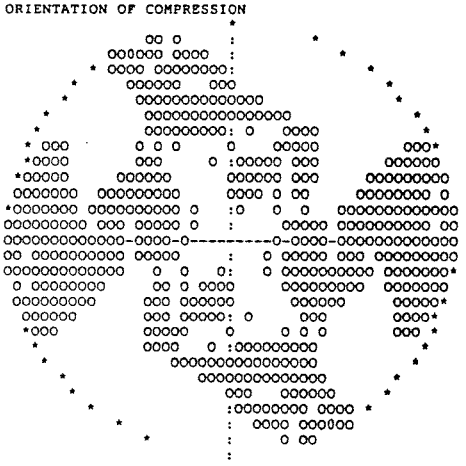

FAULT PLANE ORIENTATIONS
GIVEN BY NORMAL VECTORS
EQUAL AREA PROJECTION J05023030
LOWER HEMISPHERE

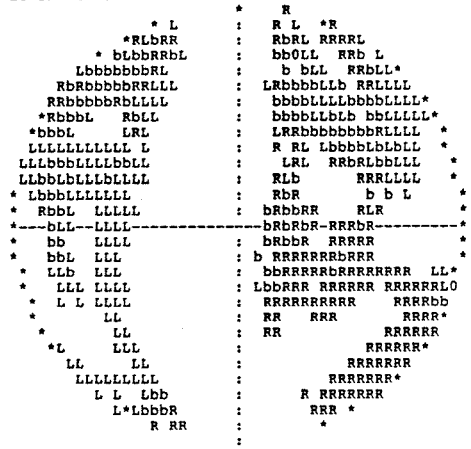

ORIGIN TIME 88 02 25 12H 49M 9.3S +/- 0.41S
LATITUDE 66.701 +/- 0.026 DEG.
LONGITUDE 21.993 +/- 0.031
FOCAL DEPTH 24.6 +/- 2.9 KM

STA	ARR. TIME	RES.	WEIGHT	DIST.	AZIMUTH	
LJV P	12 49 13.49	0.00	85.2	9.2	123.5	P UP
LJV S	12 49 16.60	0.00	8.6	9.2	123.5	
HAK P	12 49 15.65	0.00	60.7	31.5	322.9	
KPM P	12 49 16.86	0.00	53.6	40.7	80.9	
KPM S	12 49 22.48	-0.01	4.3	40.7	80.9	

INPUT DATA FOR FAULT PLANE SOLUTION

STN	DIST. KM	AZIMUTH DEGREES		OMEGA(PZ) METER-SEC	OMEGA(SZ) METER-SEC
LJV	18.	145.2	+	0.45E-10	0.83E-10
KPM	43.	94.7		0.22E-10	0.29E-10

DYNAMIC SOURCE PARAMETERS

SIZE MEASURES
SEISMIC MOMENT: 0.115E+11 Nm
LOCAL MAGNITUDE: 0.1

SHEAR WAVE CORNER FREQUENCY RANGE AT CLOSE DISTANCES (130km)
 5.5Hz -10.8Hz (8.0Hz)

FAULT RADIUS RANGE 63m - 125m (86m)

STRESS DROP RANGE 0.00MPa - 0.02MPa (0.01MPa)

RANGE OF THE PEAK SLIP AT THE FAULT 0.0mm - 0.0mm (0.0mm)

THE ORIENTATION OF THE RELAXED STRESS

	AZIMUTH	DIP
P-AXIS	70.	-18. degrees
T-AXIS	5.	53.

THE HORIZONTAL DEVIATORIC STRESS AS GIVEN BY THE P- AND T-AXES
THE AZIMUTH OF COMPRESSION 76 degrees
THE RELATIVE SIZE 0.58

THE TWO POSSIBLE FAULT PLANES

	STRIKE	DIP	SLIP
PLANE A	18.	142.	34. degrees
PLANE B	136.	111.	123.

THE NORMAL DIRECTIONS OF THE FAULT PLANES

	AZIMUTH	DIP
PLANE A	288.	52. degrees
PLANE B	46.	21.

STATISTICAL INFORMATION

OF 1 FIRST MOTION POLARITY OBSERVATIONS
AT LEAST 1 ARE REQUIRED TO FIT

THE OPTIMUM MECHANISM HAS 0 POLARITY MISFITS

AMPLITUDES FOR P AND S AT 2 STATIONS ARE USED
ONLY MECHANISMS GIVING AN ESTIMATED STANDARD
DEVIATION OF THE AMPLITUDE ERROR FACTOR OF LESS
THAN 1.60 FOR SINGLE P-WAVE OBSERVATIONS ARE
TAKEN AS ACCEPTABLE AND INCLUDED IN THE FIGURES

3.33 % OF ALL MECHANISMS ARE ACCEPTABLE
50.0 % ACCEPTABLE DUE TO FIRST MOTION OBSERVATIONS
6.7 % OF THESE FITTED ALSO THE AMPLITUDES
THE PART OF WELL FITTING PLANES IS 39.4%

THE AMPLITUDE FIT OF THE OPTIMAL MECHANISM
GIVES A MEAN ERROR FACTOR OF 1.03

THE MEASURE OF THE MISFIT TO AN EARTHQUAKE SPECTRUM
P-WAVES 0.30
S-WAVES 0.23

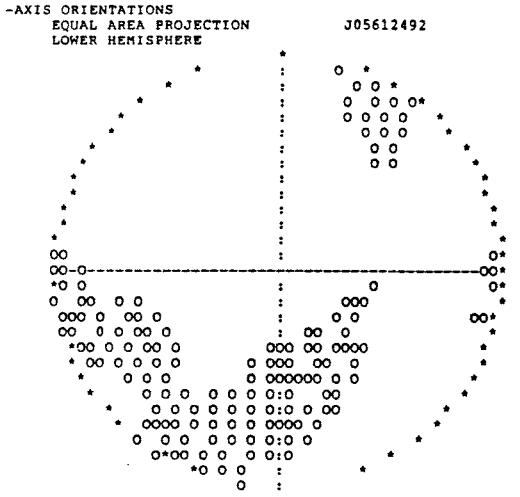
-AXIS ORIENTATIONS
EQUAL AREA PROJECTION
LOWER HEMISPHERE
J05612492

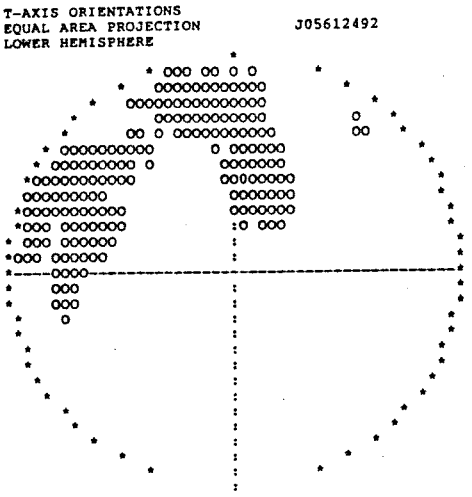
T-AXIS ORIENTATIONS
EQUAL AREA PROJECTION
LOWER HEMISPHERE
J05612492

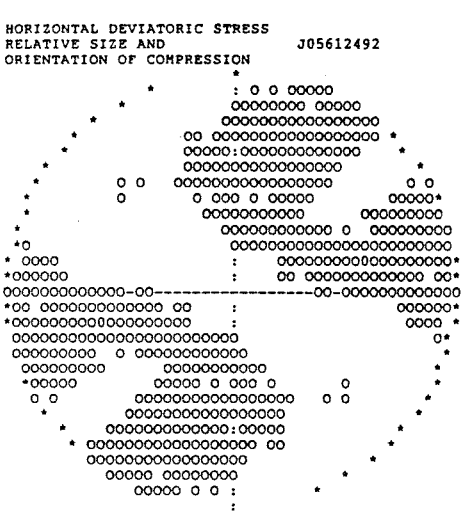
HORIZONTAL DEVIATORIC STRESS
RELATIVE SIZE AND
ORIENTATION OF COMPRESSION
J05612492

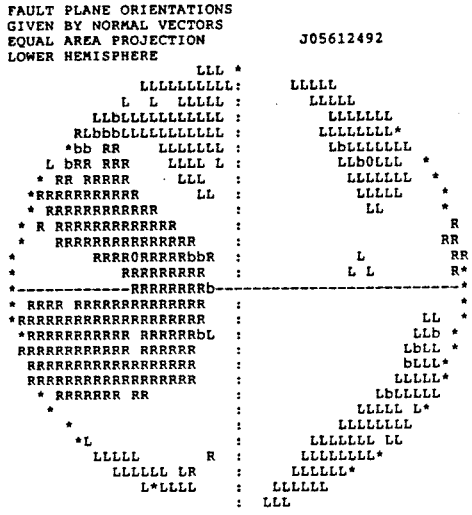
FAULT PLANE ORIENTATIONS
GIVEN BY NORMAL VECTORS
EQUAL AREA PROJECTION
LOWER HEMISPHERE
J05612492

ORIGIN TIME 88 02 27 06H 37M 1.8S +/- 0.81S
LATITUDE 64.885 +/- 0.047 DEG.
LONGITUDE 21.032 +/- 0.121
FOCAL DEPTH 21.6 +/- 4.5 KM

STA	ARR. TIME	RES.	WEIGHT	DIST.	AZIMUTH	
VMK	P 06 37 16.87	0.00	29.8	92.6	16.0	P DOWN
VMK	S 06 37 28.07	-0.06	1.9	92.6	16.0	
KLX	P 06 37 27.17	0.01	16.6	161.4	34.2	P UP
KLX	S 06 37 46.33	0.08	1.0	161.4	34.2	
LJV	P 06 37 33.07	0.11	2.5	204.4	14.2	
LJV	S 06 37 57.05	0.48	0.1	204.4	14.2	
KPM	P 06 37 35.33	-0.26	2.2	225.8	21.5	
HAK	P 06 37 36.18	0.18	2.1	229.1	5.8	
HAK	S 06 38 1.75	-0.13	0.1	229.1	5.8	
MUG	P 06 37 43.56	-0.13	1.5	291.5	8.6	

INPUT DATA FOR FAULT PLANE SOLUTION

STN	DIST. KM	AZIMUTH DEGREES		OMEGA(PZ) METER-SEC	OMEGA(SZ) METER-SEC
VMK	92.	16.5	-	0.19E-09	0.18E-08
KLX	161.	34.5	+	0.58E-09	0.48E-08

DYNAMIC SOURCE PARAMETERS

SIZE MEASURES
SEISMIC MOMENT: 0.171E+13 Nm
LOCAL MAGNITUDE: 2.2

SHEAR WAVE CORNER FREQUENCY RANGE AT CLOSE DISTANCES (130km)
11.6Hz -22.3Hz (15.5Hz)

FAULT RADIUS RANGE 30m - 59m (44m)

STRESS DROP RANGE 3.55MPa - 25.21MPa (8.46MPa)

RANGE OF THE PEAK SLIP AT THE FAULT 5.3mm - 19.7mm (9.5mm)

THE ORIENTATION OF THE RELAXED STRESS

	AZIMUTH	DIP	
P-AXIS	125.	51.	degrees
T-AXIS	95.	-35.	

THE HORIZONTAL DEVIATORIC STRESS AS GIVEN BY THE P- AND T-AXES
THE AZIMUTH OF COMPRESSION -13 degrees
THE RELATIVE SIZE 0.29

THE TWO POSSIBLE FAULT PLANES

	STRIKE	DIP	SLIP	
PLANE A	136.	17.	29.	degrees
PLANE B	198.	98.	255.	

THE NORMAL DIRECTIONS OF THE FAULT PLANES

	AZIMUTH	DIP	
PLANE A	226.	73.	degrees
PLANE B	108.	8.	

STATISTICAL INFORMATION

OF 2 FIRST MOTION POLARITY OBSERVATIONS
AT LEAST 2 ARE REQUIRED TO FIT

THE OPTIMUM MECHANISM HAS 0 POLARITY MISFITS

AMPLITUDES FOR P AND S AT 2 STATIONS ARE USED
ONLY MECHANISMS GIVING AN ESTIMATED STANDARD
DEVIATION OF THE AMPLITUDE ERROR FACTOR OF LESS
THAN 1.60 FOR SINGLE P-WAVE OBSERVATIONS ARE
TAKEN AS ACCEPTABLE AND INCLUDED IN THE FIGURES

1.57 % OF ALL MECHANISMS ARE ACCEPTABLE
9.6 % ACCEPTABLE DUE TO FIRST MOTION OBSERVATIONS
16.3 % OF THESE FITTED ALSO THE AMPLITUDES
THE PART OF WELL FITTING PLANES IS 26.9%

THE AMPLITUDE FIT OF THE OPTIMAL MECHANISM
GIVES A MEAN ERROR FACTOR OF 1.17

THE MEASURE OF THE MISFIT TO AN EARTHQUAKE SPECTRUM
P-WAVES 0.50
S-WAVES 0.22

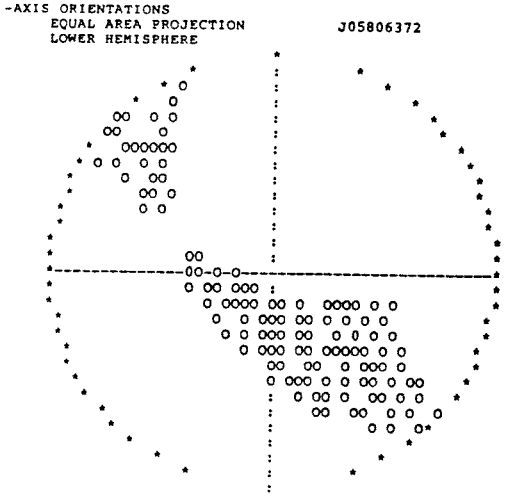
-AXIS ORIENTATIONS
EQUAL AREA PROJECTION
LOWER HEMISPHERE
J05806372

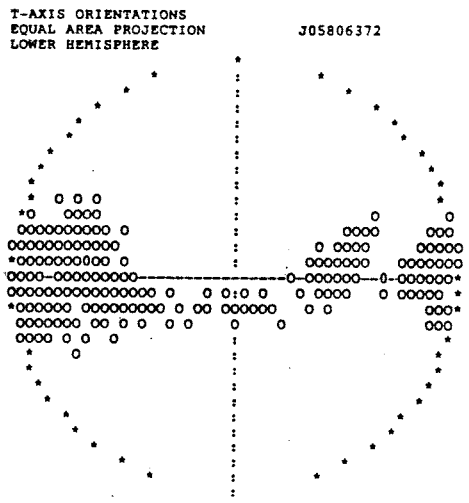
T-AXIS ORIENTATIONS
EQUAL AREA PROJECTION
LOWER HEMISPHERE
J05806372

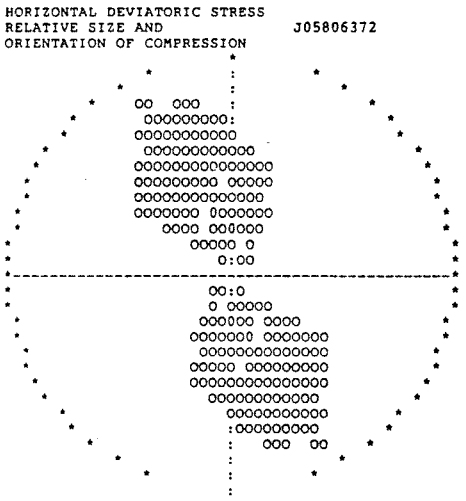
HORIZONTAL DEVIATORIC STRESS
RELATIVE SIZE AND
ORIENTATION OF COMPRESSION
J05806372

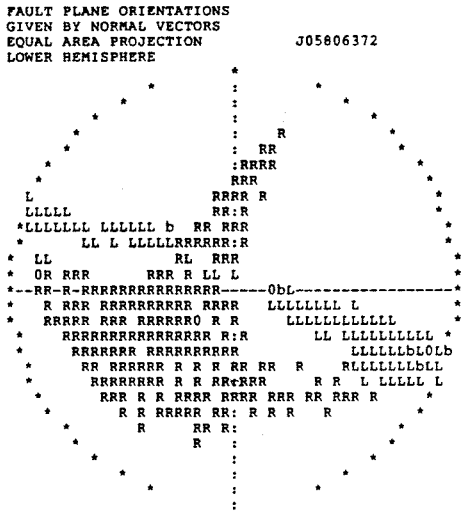
FAULT PLANE ORIENTATIONS
GIVEN BY NORMAL VECTORS
EQUAL AREA PROJECTION
LOWER HEMISPHERE
J05806372

ORIGIN TIME 88 02 27 06H 37M 1.8S +/- 0.81S
LATITUDE 64.885 +/- 0.047 DEG.
LONGITUDE 21.032 +/- 0.121
FOCAL DEPTH 21.6 +/- 4.5 KM

STA	ARR. TIME	RES.	WEIGHT	DIST.	AZIMUTH	
VMK P	06 37 16.87	0.00	29.8	92.6	16.0	P DOWN
VMK S	06 37 28.07	-0.06	1.9	92.6	16.0	
KLX P	06 37 27.17	0.01	16.6	161.4	34.2	P UP
KLX S	06 37 46.33	0.08	1.0	161.4	34.2	
LJV P	06 37 33.07	0.11	2.5	204.4	14.2	
LJV S	06 37 57.05	0.48	0.1	204.4	14.2	
KPM P	06 37 35.33	-0.26	2.2	225.8	21.5	
HAK P	06 37 36.18	0.18	2.1	229.1	5.8	
HAK S	06 38 1.75	-0.13	0.1	229.1	5.8	
MUG P	06 37 43.56	-0.13	1.5	291.5	8.6	

INPUT DATA FOR FAULT PLANE SOLUTION

STN	DIST. KM	AZIMUTH DEGREES		OMEGA(PZ) METER-SEC	OMEGA(SZ) METER-SEC
VMK	92.	16.5	-	0.19E-09	0.18E-08
KLX	161.	34.5	+	0.58E-09	0.48E-08

DYNAMIC SOURCE PARAMETERS

SIZE MEASURES
SEISMIC MOMENT: 0.171E+13 Nm
LOCAL MAGNITUDE: 2.2

SHEAR WAVE CORNER FREQUENCY RANGE AT CLOSE DISTANCES (130km)
11.6Hz -22.3Hz (15.5Hz)

FAULT RADIUS RANGE 30m - 59m (44m)

STRESS DROP RANGE 3.55MPa - 25.21MPa (8.46MPa)

RANGE OF THE PEAK SLIP AT THE FAULT 5.3mm - 19.7mm (9.5mm)

THE ORIENTATION OF THE RELAXED STRESS

	AZIMUTH	DIP	
P-AXIS	125.	51.	degrees
T-AXIS	95.	-35.	

THE HORIZONTAL DEVIATORIC STRESS AS GIVEN BY THE P- AND T-AXES
THE AZIMUTH OF COMPRESSION -13 degrees
THE RELATIVE SIZE 0.29

THE TWO POSSIBLE FAULT PLANES

	STRIKE	DIP	SLIP	
PLANE A	136.	17.	29.	degrees
PLANE B	198.	98.	255.	

THE NORMAL DIRECTIONS OF THE FAULT PLANES

	AZIMUTH	DIP	
PLANE A	226.	73.	degrees
PLANE B	108.	8.	

STATISTICAL INFORMATION

OF 2 FIRST MOTION POLARITY OBSERVATIONS
AT LEAST 2 ARE REQUIRED TO FIT

THE OPTIMUM MECHANISM HAS 0 POLARITY MISFITS

AMPLITUDES FOR P AND S AT 2 STATIONS ARE USED
ONLY MECHANISMS GIVING AN ESTIMATED STANDARD
DEVIATION OF THE AMPLITUDE ERROR FACTOR OF LESS
THAN 1.60 FOR SINGLE P-WAVE OBSERVATIONS ARE
TAKEN AS ACCEPTABLE AND INCLUDED IN THE FIGURES

1.57 % OF ALL MECHANISMS ARE ACCEPTABLE
9.6 % ACCEPTABLE DUE TO FIRST MOTION OBSERVATIONS
16.3 % OF THESE FITTED ALSO THE AMPLITUDES
THE PART OF WELL FITTING PLANES IS 26.9%

THE AMPLITUDE FIT OF THE OPTIMAL MECHANISM
GIVES A MEAN ERROR FACTOR OF 1.17

THE MEASURE OF THE MISFIT TO AN EARTHQUAKE SPECTRUM
P-WAVES 0.50
S-WAVES 0.22

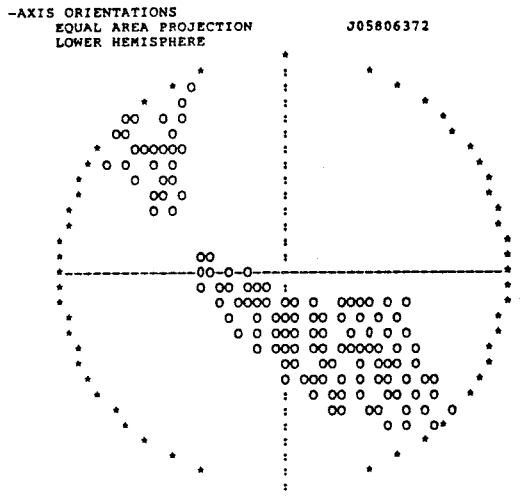
-AXIS ORIENTATIONS
EQUAL AREA PROJECTION
LOWER HEMISPHERE
J05806372

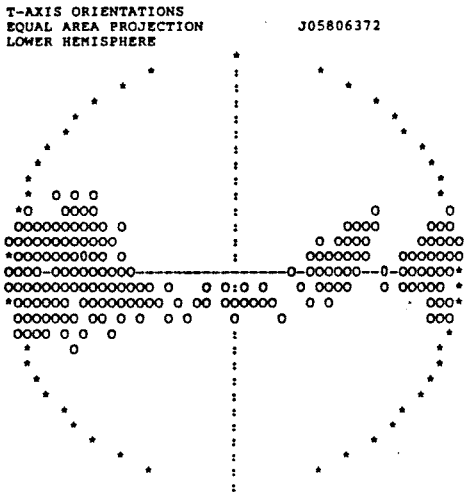
T-AXIS ORIENTATIONS
EQUAL AREA PROJECTION
LOWER HEMISPHERE
J05806372

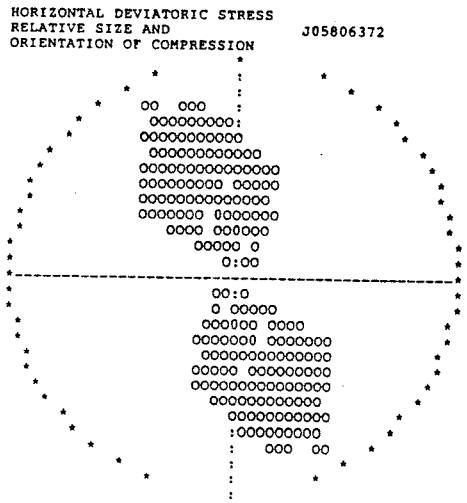
HORIZONTAL DEVIATORIC STRESS
RELATIVE SIZE AND
ORIENTATION OF COMPRESSION
J05806372

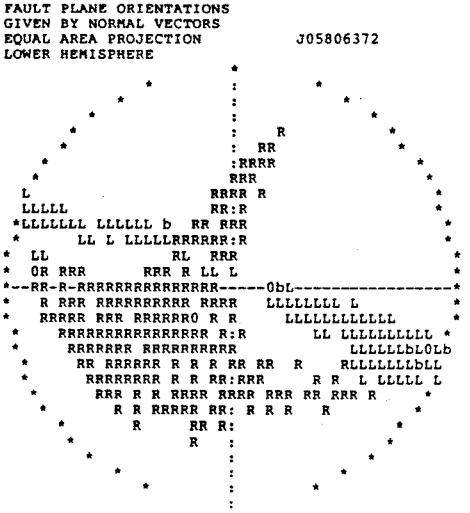
FAULT PLANE ORIENTATIONS
GIVEN BY NORMAL VECTORS
EQUAL AREA PROJECTION
LOWER HEMISPHERE
J05806372

ORIGIN TIME 88 02 29 14H 08M 26.5S +/- 0.33S
LATITUDE 64.690 +/- 0.012 DEG.
LONGITUDE 22.730 +/- 0.027
FOCAL DEPTH 4.9 +/- 4.8 KM

STA	ARR. TIME	RES.	WEIGHT	DIST.	AZIMUTH	
VMK	P 14 08 46.71	0.06	22.6	122.9	334.6	P UP
VMK	S 14 09 1.09	-0.34	1.4	122.9	334.6	
KLX	P 14 08 51.67	-0.04	17.5	154.5	5.1	
UME	P 14 08 51.90	0.02	17.4	155.6	232.2	
UME	S 14 09 10.00	-0.63	1.0	155.6	232.2	
OUL	P 14 08 52.10	0.07	17.2	156.5	72.2	
OUL	S 14 09 10.00	-0.90	1.0	156.5	72.2	
LJV	P 14 09 1.38	-0.03	2.2	221.0	353.5	
KPM	P 14 09 2.53	-0.09	2.1	230.8	1.9	

INPUT DATA FOR FAULT PLANE SOLUTION

STN	DIST. KM	AZIMUTH DEGREES		OMEGA(PZ) METER-SEC	OMEGA(SZ) METER-SEC
VMK	120.	334.2	+	0.82E-09	0.72E-08
KLX	151.	5.3		0.10E-08	0.41E-08
LJV	218.	353.5		0.97E-09	0.30E-08
KPM	227.	2.0		0.90E-09	0.28E-08
HAK	252.	348.4		0.71E-09	0.16E-08

DYNAMIC SOURCE PARAMETERS

SIZE MEASURES
SEISMIC MOMENT: 0.141E+13 Nm
LOCAL MAGNITUDE: 2.1

SHEAR WAVE CORNER FREQUENCY RANGE AT CLOSE DISTANCES (130km)
4.9Hz - 8.6Hz (6.6Hz)

FAULT RADIUS RANGE 80m - 140m (104m)

STRESS DROP RANGE 0.22MPa - 1.19MPa (0.54MPa)

RANGE OF THE PEAK SLIP AT THE FAULT 1.0mm - 3.1mm (1.8mm)

THE ORIENTATION OF THE RELAXED STRESS

	AZIMUTH	DIP	
P-AXIS	47.	62.	degrees
T-AXIS	83.	-23.	

THE HORIZONTAL DEVIATORIC STRESS AS GIVEN BY THE P- AND T-AXES
THE AZIMUTH OF COMPRESSION 0 degrees
THE RELATIVE SIZE 0.40

THE TWO POSSIBLE FAULT PLANES

	STRIKE	DIP	SLIP	
PLANE A	199.	25.	125.	degrees
PLANE B	161.	111.	-75.	

THE NORMAL DIRECTIONS OF THE FAULT PLANES

	AZIMUTH	DIP	
PLANE A	289.	65.	degrees
PLANE B	71.	21.	

STATISTICAL INFORMATION

OF 1 FIRST MOTION POLARITY OBSERVATIONS
AT LEAST 1 ARE REQUIRED TO FIT

THE OPTIMUM MECHANISM HAS 0 POLARITY MISFITS

AMPLITUDES FOR P AND S AT 5 STATIONS ARE USED
ONLY MECHANISMS GIVING AN ESTIMATED STANDARD
DEVIATION OF THE AMPLITUDE ERROR FACTOR OF LESS
THAN 1.60 FOR SINGLE P-WAVE OBSERVATIONS ARE
TAKEN AS ACCEPTABLE AND INCLUDED IN THE FIGURES

31.23 % OF ALL MECHANISMS ARE ACCEPTABLE
50.0 % ACCEPTABLE DUE TO FIRST MOTION OBSERVATIONS
63.9 % OF THESE FITTED ALSO THE AMPLITUDES
THE PART OF WELL FITTING PLANES IS 97.3%

THE AMPLITUDE FIT OF THE OPTIMAL MECHANISM
GIVES A MEAN ERROR FACTOR OF 1.20
THIS CORRESPONDS TO A STANDARD DEVIATION FACTOR OF 1.27
FOR SINGLE P-WAVE OBSERVATIONS

THE DOUBLE COUPLE SOLUTION IS SIGNIFICANT
AT 18 % LEVEL
(F-VALUE: F(9, 6) = 2.14)

THE MEASURE OF THE MISFIT TO AN EARTHQUAKE SPECTRUM
P-WAVES 0.24
S-WAVES 0.25

-AXIS ORIENTATIONS
EQUAL AREA PROJECTION J06014084
LOWER HEMISPHERE

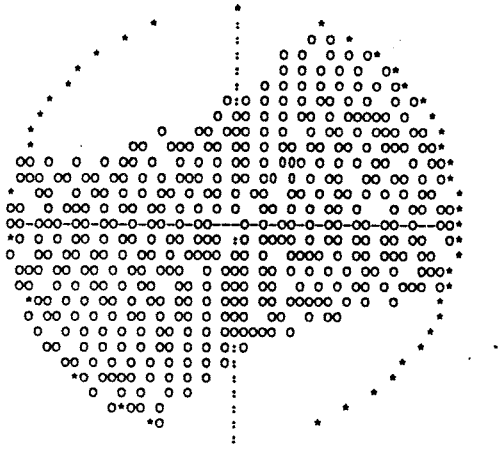

T-AXIS ORIENTATIONS
EQUAL AREA PROJECTION J06014084
LOWER HEMISPHERE

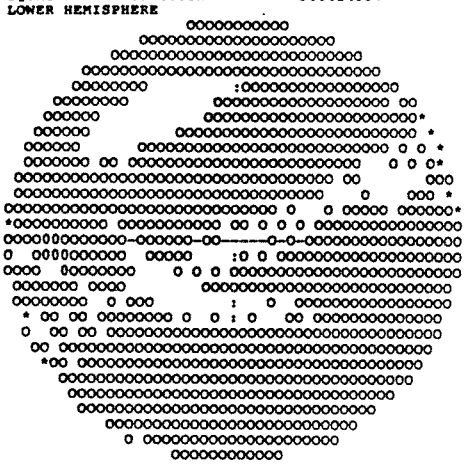

HORIZONTAL DEVIATORIC STRESS
RELATIVE SIZE AND J06014084
ORIENTATION OF COMPRESSION

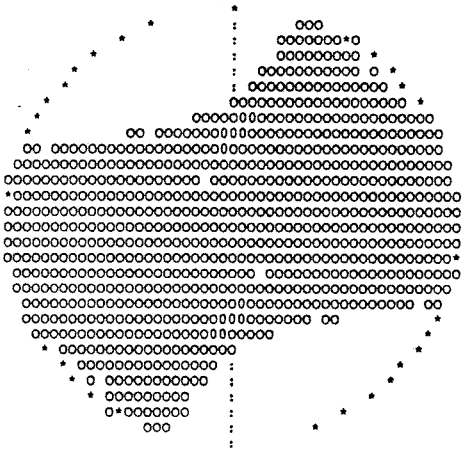

FAULT PLANE ORIENTATIONS
GIVEN BY NORMAL VECTORS
EQUAL AREA PROJECTION J06014084
LOWER HEMISPHERE

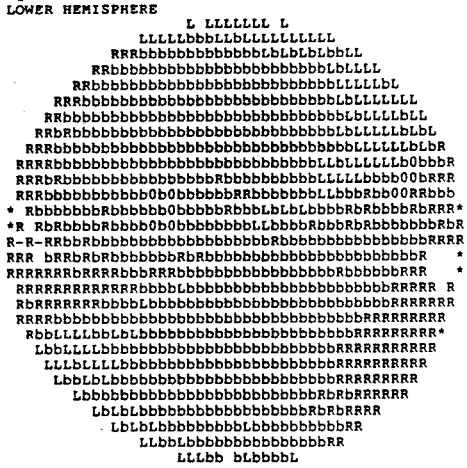

```
ORIGIN TIME 88 03 04   21H 50M 50.5S +/- 0.49S      ***
LATITUDE  65.480  +/- 0.028 DEG.    22.km from n:o 71     ***
LONGITUDE 21.538  +/- 0.048          V Pite}  I30213391 Rg ***
FOCAL DEPTH 11.7  +/-   1.9 KM              ***
VMK

STA  ARR. TIME     RES.  WEIGHT DIST.  AZIMUTH
VMK P 21 50 54.62  0.02  69.2  22.5   5.8       P UP
VMK S 21 50 57.51 -0.14   6.2  22.5   5.8
KLX P 21 51  5.98 -0.04  29.1  94.8  45.6
KLX S 21 51 17.77  0.31   1.9  94.8  45.6
LJV S 21 51 28.67  0.24   1.2 134.2  12.0
LJV P 21 51 12.17 -0.02  20.5 134.2  12.0
```

INPUT DATA FOR FAULT PLANE SOLUTION

STN	DIST. KM	AZIMUTH DEGREES		OMEGA(PZ) METER-SEC	OMEGA(SZ) METER-SEC
VMK	24.	1.9	+	0.18E-09	0.21E-09
KLX	95.	44.5		0.29E-10	0.78E-10
LJV	135.	11.3		0.43E-10	0.16E-09

DYNAMIC SOURCE PARAMETERS

SIZE MEASURES
SEISMIC MOMENT: 0.438E+11 Nm
LOCAL MAGNITUDE: 0.6

SHEAR WAVE CORNER FREQUENCY RANGE AT CLOSE DISTANCES (130km)
4.5Hz -11.9Hz (7.7Hz)

FAULT RADIUS RANGE 57m - 153m (89m)

STRESS DROP RANGE 0.01MPa - 0.10MPa (0.03MPa)

RANGE OF THE PEAK SLIP AT THE FAULT 0.0mm - 0.2mm (0.1mm)

THE ORIENTATION OF THE RELAXED STRESS

	AZIMUTH	DIP
P-AXIS	81.	17. degrees
T-AXIS	172.	3.

THE HORIZONTAL DEVIATORIC STRESS AS GIVEN BY THE P- AND T-AXES
THE AZIMUTH OF COMPRESSION 82 degrees
THE RELATIVE SIZE 0.96

THE TWO POSSIBLE FAULT PLANES

	STRIKE	DIP	SLIP
PLANE A	-54.	80.	166. degrees
PLANE B	218.	104.	-10.

THE NORMAL DIRECTIONS OF THE FAULT PLANES

	AZIMUTH	DIP
PLANE A	36.	10. degrees
PLANE B	128.	14.

STATISTICAL INFORMATION

OF 1 FIRST MOTION POLARITY OBSERVATIONS
AT LEAST 1 ARE REQUIRED TO FIT

THE OPTIMUM MECHANISM HAS 0 POLARITY MISFITS

AMPLITUDES FOR P AND S AT 3 STATIONS ARE USED
ONLY MECHANISMS GIVING AN ESTIMATED STANDARD
DEVIATION OF THE AMPLITUDE ERROR FACTOR OF LESS
THAN 1.60 FOR SINGLE P-WAVE OBSERVATIONS ARE
TAKEN AS ACCEPTABLE AND INCLUDED IN THE FIGURES

7.98 % OF ALL MECHANISMS ARE ACCEPTABLE
50.0 % ACCEPTABLE DUE TO FIRST MOTION OBSERVATIONS
16.3 % OF THESE FITTED ALSO THE AMPLITUDES
THE PART OF WELL FITTING PLANES IS 56.4%

THE AMPLITUDE FIT OF THE OPTIMAL MECHANISM
GIVES A MEAN ERROR FACTOR OF 1.07
THIS CORRESPONDS TO A STANDARD DEVIATION FACTOR OF 1.12
FOR SINGLE P-WAVE OBSERVATIONS

THE DOUBLE COUPLE SOLUTION IS SIGNIFICANT
AT 3 % LEVEL
(F-VALUE: F(5, 2) = 32.84)

THE MEASURE OF THE MISFIT TO AN EARTHQUAKE SPECTRUM
P-WAVES 0.24
S-WAVES 0.28

-AXIS ORIENTATIONS
EQUAL AREA PROJECTION J06421505
LOWER HEMISPHERE

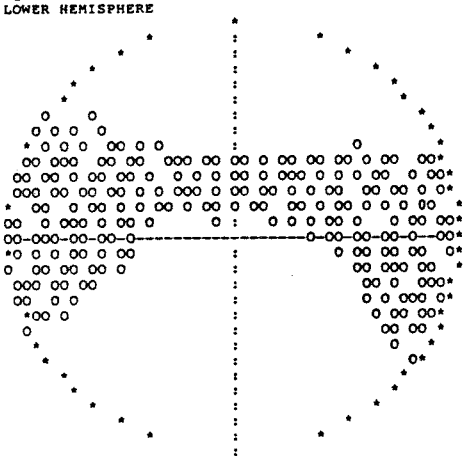

T-AXIS ORIENTATIONS
EQUAL AREA PROJECTION J06421505
LOWER HEMISPHERE

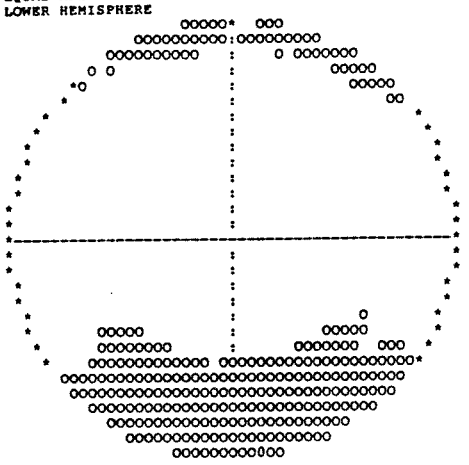

HORIZONTAL DEVIATORIC STRESS
RELATIVE SIZE AND J06421505
ORIENTATION OF COMPRESSION

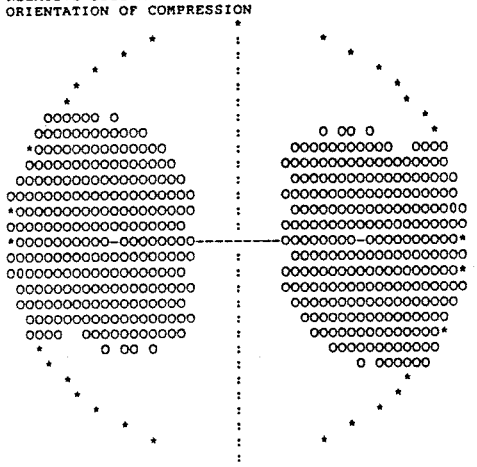

FAULT PLANE ORIENTATIONS
GIVEN BY NORMAL VECTORS
EQUAL AREA PROJECTION J06421505
LOWER HEMISPHERE

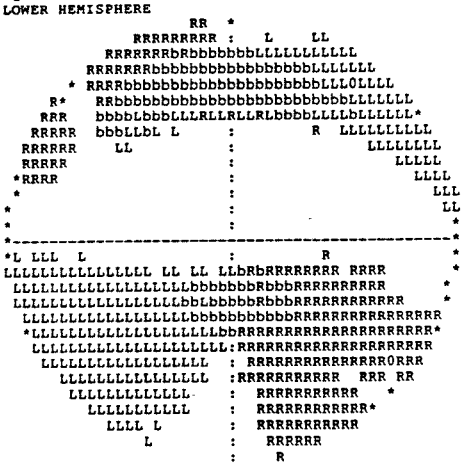

ORIGIN TIME 88 03 07 16H 02M 27.2S +/- 0.10S
LATITUDE 66.313 +/- 0.004 DEG.
LONGITUDE 22.134 +/- 0.019
FOCAL DEPTH 8.1 +/- 6.0 KM

STA	ARR. TIME	RES.	WEIGHT	DIST.	AZIMUTH	
LJV	P 16 02 33.58	0.03	55.4	38.2	2.2	P UP
LJV	S 16 02 38.29	0.03	4.5	38.2	2.2	
KLX	P 16 02 35.37	0.10	48.2	48.9	123.7	
KLX	S 16 02 40.88	-0.36	3.7	48.9	123.7	
KPM	P 16 02 37.01	-0.08	42.1	60.2	34.4	P UP
KPM	S 16 02 44.04	-0.35	3.1	60.2	34.4	
HAK	P 16 02 39.15	0.00	36.5	72.9	339.8	
HAK	S 16 02 47.97	-0.01	2.5	72.9	339.8	
VMK	P 16 02 39.43	-0.03	35.7	74.9	199.6	
VMK	S 16 02 48.18	-0.35	2.5	74.9	199.6	
MUG	P 16 02 48.22	0.08	21.5	128.4	358.3	
MUG	S 16 03 3.37	-0.20	1.3	128.4	358.3	

INPUT DATA FOR FAULT PLANE SOLUTION

STN	DIST. KM	AZIMUTH DEGREES		OMEGA(PZ) METER-SEC	OMEGA(SZ) METER-SEC
LJV	39.	2.4	+	0.38E-09	0.24E-08
KLX	49.	123.3		0.35E-09	0.25E-08
KPM	61.	34.4	+	0.26E-09	0.84E-09
HAK	73.	340.0		0.27E-09	0.12E-08
VMK	75.	199.6		0.23E-09	0.99E-09
MUG	129.	358.4		0.68E-09	0.24E-08

DYNAMIC SOURCE PARAMETERS

SIZE MEASURES
SEISMIC MOMENT: 0.349E+12 Nm
LOCAL MAGNITUDE: 1.5

SHEAR WAVE CORNER FREQUENCY RANGE AT CLOSE DISTANCES (130km)
2.6Hz - 8.1Hz (4.8Hz)

FAULT RADIUS RANGE 85m - 265m (143m)

STRESS DROP RANGE 0.008MPa - 0.247MPa (0.051MPa)

RANGE OF THE PEAK SLIP AT THE FAULT 0.1mm - 0.7mm (0.2mm)

THE ORIENTATION OF THE RELAXED STRESS

	AZIMUTH	DIP	
P-AXIS	121.	63.	degrees
T-AXIS	165.	-20.	

THE HORIZONTAL DEVIATORIC STRESS AS GIVEN BY THE P- AND T-AXES
THE AZIMUTH OF COMPRESSION 82 degrees
THE RELATIVE SIZE 0.45

THE TWO POSSIBLE FAULT PLANES

	STRIKE	DIP	SLIP	
PLANE A	-77.	29.	128.	degrees
PLANE B	241.	113.	-71.	

THE NORMAL DIRECTIONS OF THE FAULT PLANES

	AZIMUTH	DIP	
PLANE A	13.	61.	degrees
PLANE B	151.	23.	

STATISTICAL INFORMATION

OF 2 FIRST MOTION POLARITY OBSERVATIONS
AT LEAST 2 ARE REQUIRED TO FIT

THE OPTIMUM MECHANISM HAS 0 POLARITY MISFITS

AMPLITUDES FOR P AND S AT 6 STATIONS ARE USED
ONLY MECHANISMS GIVING AN ESTIMATED STANDARD
DEVIATION OF THE AMPLITUDE ERROR FACTOR OF LESS
THAN 1.60 FOR SINGLE P-WAVE OBSERVATIONS ARE
TAKEN AS ACCEPTABLE AND INCLUDED IN THE FIGURES

0.83 % OF ALL MECHANISMS ARE ACCEPTABLE
33.7 % ACCEPTABLE DUE TO FIRST MOTION OBSERVATIONS
2.4 % OF THESE FITTED ALSO THE AMPLITUDES
THE PART OF WELL FITTING PLANES IS 21.1%

THE AMPLITUDE FIT OF THE OPTIMAL MECHANISM
GIVES A MEAN ERROR FACTOR OF 1.27
THIS CORRESPONDS TO A STANDARD DEVIATION FACTOR OF 1.34
FOR SINGLE P-WAVE OBSERVATIONS

THE DOUBLE COUPLE SOLUTION IS NOT SIGNIFICANT
NOT EVEN AT 50 % LEVEL
(F-VALUE: F(11, 8) = 0.80)

THE MEASURE OF THE MISFIT TO AN EARTHQUAKE SPECTRUM

P-WAVES	0.26
S-WAVES	0.35

-AXIS ORIENTATIONS
EQUAL AREA PROJECTION J06716023
LOWER HEMISPHERE

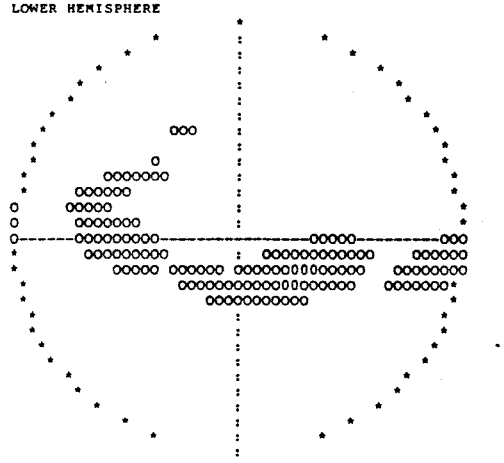

T-AXIS ORIENTATIONS
EQUAL AREA PROJECTION J06716023
LOWER HEMISPHERE

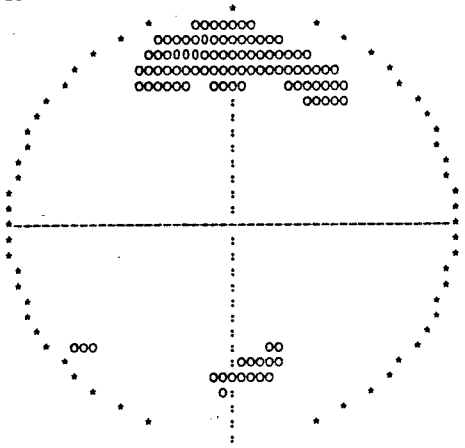

HORIZONTAL DEVIATORIC STRESS
RELATIVE SIZE AND J06716023
ORIENTATION OF COMPRESSION

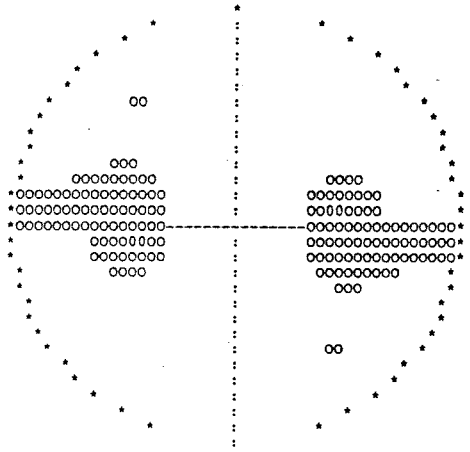

FAULT PLANE ORIENTATIONS
GIVEN BY NORMAL VECTORS
EQUAL AREA PROJECTION J06716023
LOWER HEMISPHERE

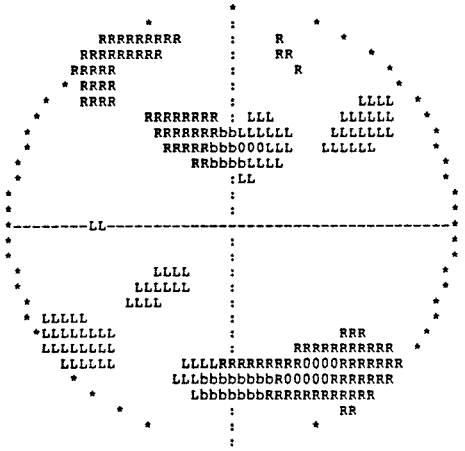

ORIGIN TIME 88 03 18 11H 00M 14.7S +/- 0.32S
LATITUDE 65.767 +/- 0.018 DEG.
LONGITUDE 22.820 +/- 0.044
FOCAL DEPTH 7.3 +/- 3.3 KM

STA	ARR.	TIME	RES.	WEIGHT	DIST.	AZIMUTH	
KLX	P	11 00 20.62	0.04	57.9	34.9	15.9	P UP
KLX	S	11 00 24.82	-0.07	4.8	34.9	15.9	
VMK	P	11 00 24.20	-0.02	43.5	57.5	260.9	P DOWN
VMK	S	11 00 31.12	-0.08	3.2	57.5	260.9	
LJV	P	11 00 31.83	0.16	26.8	103.4	343.8	
LJV	S	11 00 44.33	0.21	1.7	103.4	343.8	
KPM	P	11 00 32.62	-0.19	25.2	110.4	1.9	P UP
KPM	S	11 00 45.26	-0.84	1.6	110.4	1.9	
HAK	P	11 00 37.80	0.04	19.4	141.1	337.0	
HAK	S	11 00 54.60	-0.12	1.1	141.1	337.0	
MUG	S	11 01 8.47	0.00	0.3	192.4	350.1	

INPUT DATA FOR FAULT PLANE SOLUTION

STN	DIST. KM	AZIMUTH DEGREES		OMEGA(PZ) METER-SEC	OMEGA(SZ) METER-SEC
KLX	35.	16.0	+	0.37E-09	0.66E-09
VMK	58.	260.5	-	0.13E-09	0.77E-09
LJV	103.	343.7		0.23E-09	0.50E-09
KPM	110.	1.9	+	0.19E-09	0.74E-09
HAK	141.	336.9		0.18E-09	0.43E-09

DYNAMIC SOURCE PARAMETERS

SIZE MEASURES
SEISMIC MOMENT: 0.147E+12 Nm
LOCAL MAGNITUDE: 1.2

SHEAR WAVE CORNER FREQUENCY RANGE AT CLOSE DISTANCES (130km)
2.9Hz - 6.9Hz (4.8Hz)

FAULT RADIUS RANGE 100m - 237m (143m)

STRESS DROP RANGE 0.00MPa - 0.06MPa (0.02MPa)

RANGE OF THE PEAK SLIP AT THE FAULT 0.0mm - 0.2mm (0.1mm)

THE ORIENTATION OF THE RELAXED STRESS

	AZIMUTH	DIP
P-AXIS	95.	45. degrees
T-AXIS	175.	-10.

THE HORIZONTAL DEVIATORIC STRESS AS GIVEN BY THE P- AND T-AXES
THE AZIMUTH OF COMPRESSION 88 degrees
THE RELATIVE SIZE 0.72

THE TWO POSSIBLE FAULT PLANES

	STRIKE	DIP	SLIP
PLANE A	-56.	51.	151. degrees
PLANE B	233.	112.	-43.

THE NORMAL DIRECTIONS OF THE FAULT PLANES

	AZIMUTH	DIP
PLANE A	34.	39. degrees
PLANE B	143.	22.

STATISTICAL INFORMATION

OF 3 FIRST MOTION POLARITY OBSERVATIONS
AT LEAST 3 ARE REQUIRED TO FIT

THE OPTIMUM MECHANISM HAS 0 POLARITY MISFITS

AMPLITUDES FOR P AND S AT 5 STATIONS ARE USED
ONLY MECHANISMS GIVING AN ESTIMATED STANDARD
DEVIATION OF THE AMPLITUDE ERROR FACTOR OF LESS
THAN 1.60 FOR SINGLE P-WAVE OBSERVATIONS ARE
TAKEN AS ACCEPTABLE AND INCLUDED IN THE FIGURES

2.72 % OF ALL MECHANISMS ARE ACCEPTABLE
24.3 % ACCEPTABLE DUE TO FIRST MOTION OBSERVATIONS
11.2 % OF THESE FITTED ALSO THE AMPLITUDES
THE PART OF WELL FITTING PLANES IS 34.2%

THE AMPLITUDE FIT OF THE OPTIMAL MECHANISM
GIVES A MEAN ERROR FACTOR OF 1.19
THIS CORRESPONDS TO A STANDARD DEVIATION FACTOR OF 1.25
FOR SINGLE P-WAVE OBSERVATIONS

THE DOUBLE COUPLE SOLUTION IS SIGNIFICANT
AT 6 % LEVEL
(F-VALUE: F(9, 6) = 3.75)

THE MEASURE OF THE MISFIT TO AN EARTHQUAKE SPECTRUM
P-WAVES 0.26
S-WAVES 0.25

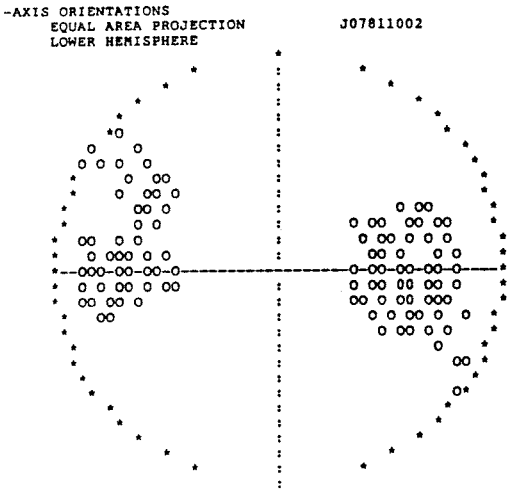
-AXIS ORIENTATIONS
EQUAL AREA PROJECTION
LOWER HEMISPHERE
J07811002

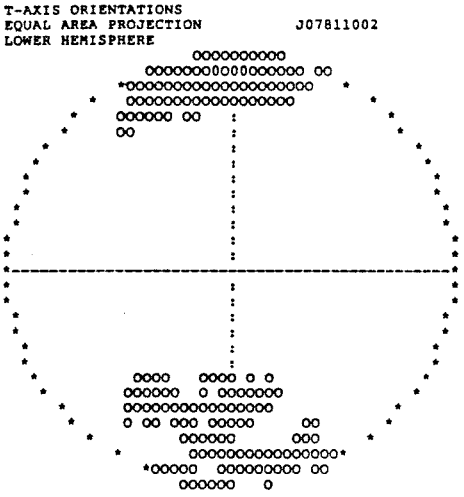
T-AXIS ORIENTATIONS
EQUAL AREA PROJECTION
LOWER HEMISPHERE
J07811002

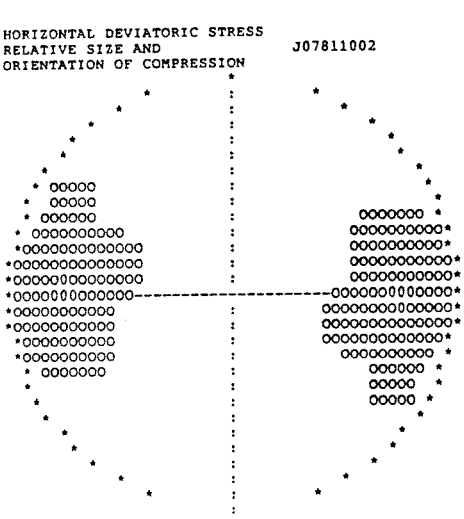
HORIZONTAL DEVIATORIC STRESS
RELATIVE SIZE AND
ORIENTATION OF COMPRESSION
J07811002

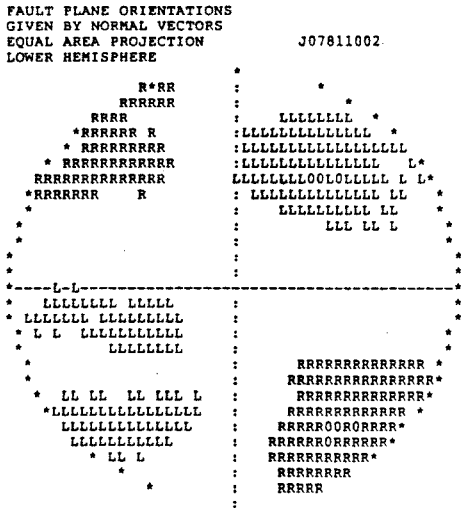
FAULT PLANE ORIENTATIONS
GIVEN BY NORMAL VECTORS
EQUAL AREA PROJECTION
LOWER HEMISPHERE
J07811002

ORIGIN TIME 88 03 22 04H 05M 37.3S +/- 0.31S
LATITUDE 67.486 +/- 0.018 DEG.
LONGITUDE 22.261 +/- 0.043
FOCAL DEPTH 10.5 +/- 2.3 KM

STA	ARR. TIME	RES.	WEIGHT	DIST.	AZIMUTH
MUG P	04 05 39.59	0.01	84.6	9.7	253.8
MUG S	04 05 41.25	-0.05	8.5	9.7	253.8
HAK P	04 05 48.74	-0.01	37.8	69.7	206.2
HAK S	04 05 56.98	-0.22	2.7	69.7	206.2
KPM P	04 05 51.35	-0.07	31.7	86.3	160.8
KPM S	04 06 2.08	0.24	2.1	86.3	160.8
LJV P	04 05 52.61	0.11	29.7	93.0	182.6
LJV S	04 06 3.62	-0.09	1.9	93.0	182.6
KLX P	04 06 3.17	-0.05	16.6	162.1	167.6

INPUT DATA FOR FAULT PLANE SOLUTION

STN	DIST. KM	AZIMUTH DEGREES	OMEGA(PZ) METER-SEC	OMEGA(SZ) METER-SEC
HAK	69.	206.4	0.47E-10	0.15E-09
KPM	86.	160.6	0.82E-10	0.21E-09
LJV	92.	182.6	0.59E-10	0.23E-09
KLX	161.	167.5	0.15E-09	0.41E-09
VMK	203.	188.8	0.63E-10	0.17E-09
MUG	9.	257.7	- 0.00E+00	0.00E+00

DYNAMIC SOURCE PARAMETERS

SIZE MEASURES
SEISMIC MOMENT: 0.799E+11 Nm
LOCAL MAGNITUDE: 0.9

SHEAR WAVE CORNER FREQUENCY RANGE AT CLOSE DISTANCES (130km)
9.3Hz -13.2Hz (11.4Hz)

FAULT RADIUS RANGE 52m - 74m (60m)

STRESS DROP RANGE 0.09MPa - 0.24MPa (0.16MPa)

RANGE OF THE PEAK SLIP AT THE FAULT 0.2mm - 0.4mm (0.3mm)

THE ORIENTATION OF THE RELAXED STRESS

	AZIMUTH	DIP	
P-AXIS	79.	-23.	degrees
T-AXIS	-9.	4.	

THE HORIZONTAL DEVIATORIC STRESS AS GIVEN BY THE P- AND T-AXES
THE AZIMUTH OF COMPRESSION 79 degrees
THE RELATIVE SIZE 0.92

THE TWO POSSIBLE FAULT PLANES

	STRIKE	DIP	SLIP	
PLANE A	37.	109.	-15.	degrees
PLANE B	122.	76.	160.	

THE NORMAL DIRECTIONS OF THE FAULT PLANES

	AZIMUTH	DIP	
PLANE A	307.	19.	degrees
PLANE B	212.	14.	

STATISTICAL INFORMATION

OF 1 FIRST MOTION POLARITY OBSERVATIONS
AT LEAST 1 ARE REQUIRED TO FIT

THE OPTIMUM MECHANISM HAS 0 POLARITY MISFITS

AMPLITUDES FOR P AND S AT 5 STATIONS ARE USED
ONLY MECHANISMS GIVING AN ESTIMATED STANDARD
DEVIATION OF THE AMPLITUDE ERROR FACTOR OF LESS
THAN 1.60 FOR SINGLE P-WAVE OBSERVATIONS ARE
TAKEN AS ACCEPTABLE AND INCLUDED IN THE FIGURES

13.27 % OF ALL MECHANISMS ARE ACCEPTABLE
50.0 % ACCEPTABLE DUE TO FIRST MOTION OBSERVATIONS
26.9 % OF THESE FITTED ALSO THE AMPLITUDES
THE PART OF WELL FITTING PLANES IS 74.7%

THE AMPLITUDE FIT OF THE OPTIMAL MECHANISM
GIVES A MEAN ERROR FACTOR OF 1.23
THIS CORRESPONDS TO A STANDARD DEVIATION FACTOR OF 1.30
FOR SINGLE P-WAVE OBSERVATIONS

THE DOUBLE COUPLE SOLUTION IS SIGNIFICANT
AT 22 % LEVEL
(F-VALUE: F(9, 6) = 1.88)

THE MEASURE OF THE MISFIT TO AN EARTHQUAKE SPECTRUM
P-WAVES 0.18
S-WAVES 0.19

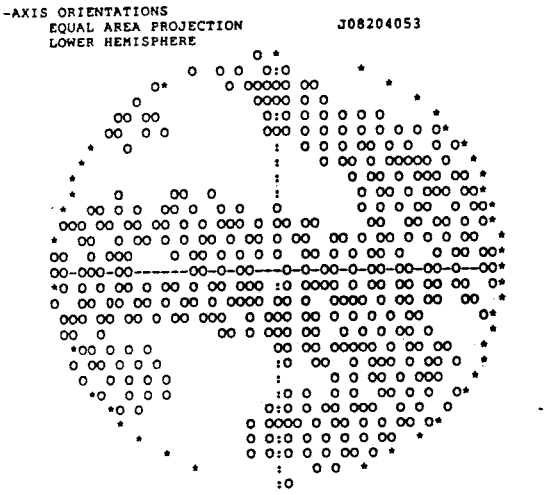
-AXIS ORIENTATIONS
EQUAL AREA PROJECTION
LOWER HEMISPHERE
J08204053

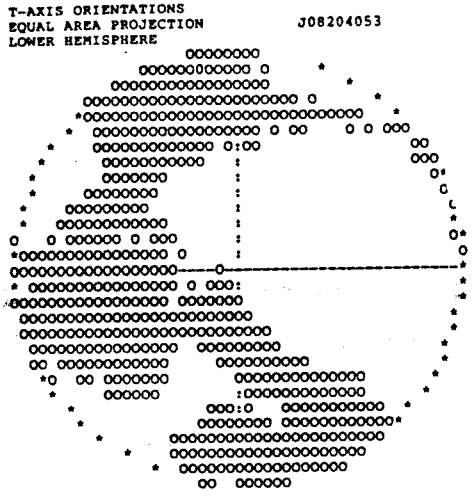
T-AXIS ORIENTATIONS
EQUAL AREA PROJECTION
LOWER HEMISPHERE
J08204053

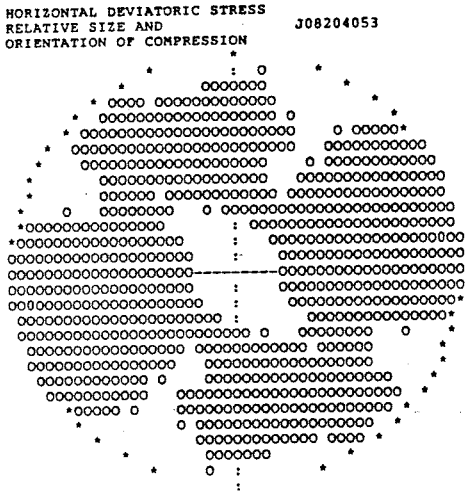
HORIZONTAL DEVIATORIC STRESS
RELATIVE SIZE AND
ORIENTATION OF COMPRESSION
J08204053

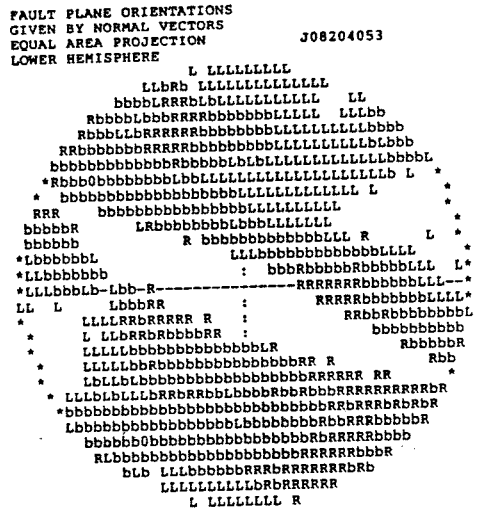
FAULT PLANE ORIENTATIONS
GIVEN BY NORMAL VECTORS
EQUAL AREA PROJECTION
LOWER HEMISPHERE
J08204053

ORIGIN TIME 88 03 22 20H 28M 32.8S +/- 0.10S
LATITUDE 67.463 +/- 0.012 DEG.
LONGITUDE 24.287 +/- 0.013
FOCAL DEPTH 5.4 +/- 3.5 KM

STA		ARR. TIME	RES.	WEIGHT	DIST.	AZIMUTH	
SO	P	20 28 48.00	0.35	30.4	90.5	92.0	
SO	S	20 28 58.50	-0.07	2.0	90.5	92.0	
MUG	P	20 28 48.54	-0.02	28.8	96.1	271.0	P UP
MUG	S	20 28 59.87	-0.27	1.9	96.1	271.0	
KPM	P	20 28 49.15	0.08	27.9	99.3	217.9	
KPM	S	20 29 0.92	-0.11	1.8	99.3	217.9	
SOD	P	20 28 49.00	-0.37	27.4	101.1	94.7	
SOD	S	20 29 1.00	-0.55	1.8	101.1	94.7	
LJV	P	20 28 54.00	0.07	21.4	129.2	226.6	
HAK	P	20 28 54.37	-0.12	20.8	132.6	244.3	
HAK	S	20 29 9.89	-0.53	1.2	132.6	244.3	
KLX	P	20 28 59.62	0.03	16.2	165.4	200.1	
KIR	P	20 29 0.50	0.25	7.0	169.8	286.2	
KIR	S	20 29 20.10	-0.67	0.4	169.8	286.2	
VMK	P	20 29 8.73	-0.31	2.1	232.4	212.3	

INPUT DATA FOR FAULT PLANE SOLUTION

STN	DIST. KM	AZIMUTH DEGREES		OMEGA(PZ) METER-SEC	OMEGA(SZ) METER-SEC
MUG	95.	270.5	+	0.14E-08	0.44E-08
KPM	99.	216.9		0.48E-09	0.25E-08
LJV	129.	225.9		0.54E-09	0.33E-08
HAK	132.	243.7		0.46E-09	0.14E-08
KLX	166.	199.5		0.98E-09	0.31E-08
VMK	232.	211.9		0.25E-09	0.12E-08

DYNAMIC SOURCE PARAMETERS

SIZE MEASURES
SEISMIC MOMENT: 0.949E+12 Nm
LOCAL MAGNITUDE: 2.0

SHEAR WAVE CORNER FREQUENCY RANGE AT CLOSE DISTANCES (130km)
9.1Hz -16.2Hz (11.8Hz)

FAULT RADIUS RANGE 42m - 75m (58m)

STRESS DROP RANGE 0.95MPa - 5.37MPa (2.08MPa)

RANGE OF THE PEAK SLIP AT THE FAULT 2.3mm - 7.3mm (3.9mm)

THE ORIENTATION OF THE RELAXED STRESS

	AZIMUTH	DIP
P-AXIS	167.	28. degrees
T-AXIS	123.	-54.

THE HORIZONTAL DEVIATORIC STRESS AS GIVEN BY THE P- AND T-AXES
THE AZIMUTH OF COMPRESSION -1 degrees
THE RELATIVE SIZE 0.42

THE TWO POSSIBLE FAULT PLANES

	STRIKE	DIP	SLIP
PLANE A	119.	26.	-33. degrees
PLANE B	239.	76.	248.

THE NORMAL DIRECTIONS OF THE FAULT PLANES

	AZIMUTH	DIP
PLANE A	209.	64. degrees
PLANE B	329.	14.

STATISTICAL INFORMATION

OF 1 FIRST MOTION POLARITY OBSERVATIONS
AT LEAST 1 ARE REQUIRED TO FIT

THE OPTIMUM MECHANISM HAS 0 POLARITY MISFITS

AMPLITUDES FOR P AND S AT 6 STATIONS ARE USED
ONLY MECHANISMS GIVING AN ESTIMATED STANDARD
DEVIATION OF THE AMPLITUDE ERROR FACTOR OF LESS
THAN 1.60 FOR SINGLE P-WAVE OBSERVATIONS ARE
TAKEN AS ACCEPTABLE AND INCLUDED IN THE FIGURES

11.35 % OF ALL MECHANISMS ARE ACCEPTABLE
50.0 % ACCEPTABLE DUE TO FIRST MOTION OBSERVATIONS
21.9 % OF THESE FITTED ALSO THE AMPLITUDES
THE PART OF WELL FITTING PLANES IS 63.1%

THE AMPLITUDE FIT OF THE OPTIMAL MECHANISM
GIVES A MEAN ERROR FACTOR OF 1.23
THIS CORRESPONDS TO A STANDARD DEVIATION FACTOR OF 1.29
FOR SINGLE P-WAVE OBSERVATIONS

THE DOUBLE COUPLE SOLUTION IS SIGNIFICANT
AT 4 % LEVEL
(F-VALUE: F(11, 8) = 3.32)

THE MEASURE OF THE MISFIT TO AN EARTHQUAKE SPECTRUM
P-WAVES 0.24
S-WAVES 0.22

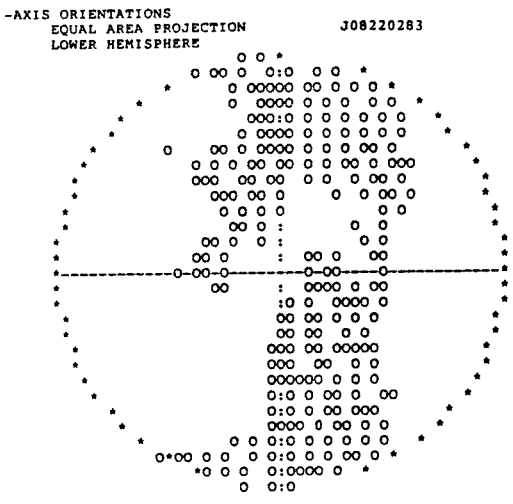
-AXIS ORIENTATIONS
EQUAL AREA PROJECTION
LOWER HEMISPHERE
J08220283

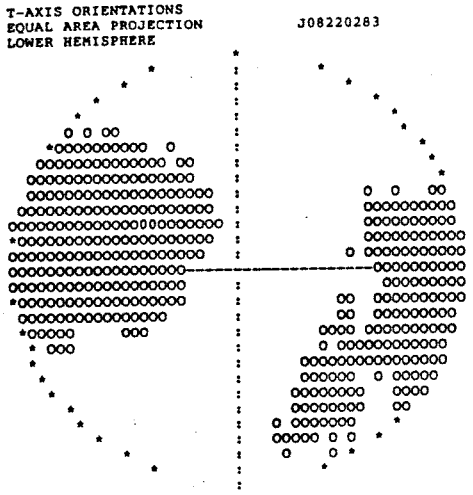
T-AXIS ORIENTATIONS
EQUAL AREA PROJECTION
LOWER HEMISPHERE
J08220283

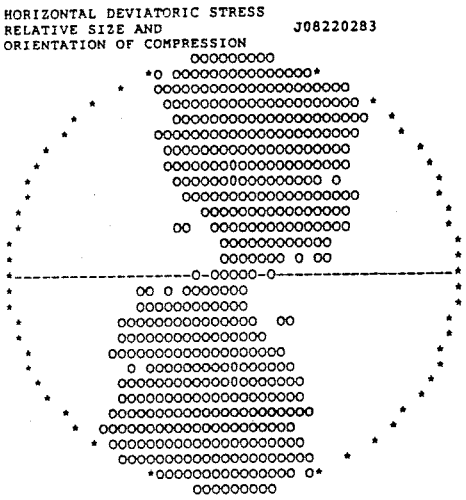
HORIZONTAL DEVIATORIC STRESS
RELATIVE SIZE AND
ORIENTATION OF COMPRESSION
J08220283

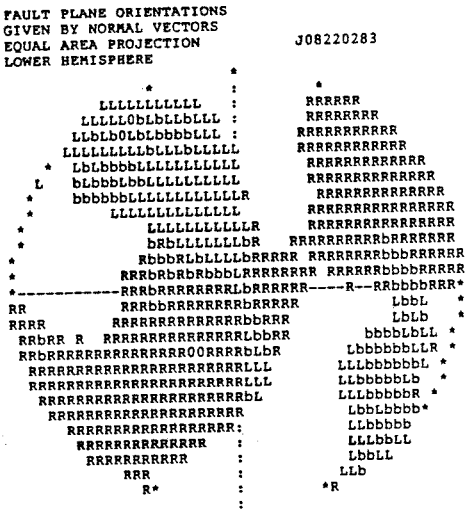
FAULT PLANE ORIENTATIONS
GIVEN BY NORMAL VECTORS
EQUAL AREA PROJECTION
LOWER HEMISPHERE
J08220283

ORIGIN TIME 88 03 22 23H 58M 36.0S +/- 0.62S
LATITUDE 65.426 +/- 0.038 DEG.
LONGITUDE 22.609 +/- 0.042
FOCAL DEPTH 9.1 +/- 3.2 KM

STA	ARR. TIME	RES.	WEIGHT	DIST.	AZIMUTH
VMK	P 23 58 45.14	0.00	44.7	55.2	301.5
VMK	S 23 58 51.82	-0.05	3.3	55.2	301.5
KLX	P 23 58 48.22	0.00	36.0	74.3	14.9
KLX	S 23 58 57.22	0.02	2.5	74.3	14.9
KPM	P 23 59 0.06	-0.05	18.2	149.1	5.0
HAK	P 23 59 3.97	0.13	6.8	174.0	344.7

INPUT DATA FOR FAULT PLANE SOLUTION

STN	DIST. KM	AZIMUTH DEGREES	OMEGA(PZ) METER-SEC	OMEGA(SZ) METER-SEC
VMK	54.	301.8	0.54E-10	0.15E-09
KLX	74.	16.0	0.69E-10	0.11E-09
HAK	173.	345.0	0.11E-09	0.15E-09

DYNAMIC SOURCE PARAMETERS

SIZE MEASURES
SEISMIC MOMENT: 0.926E+11 Nm
LOCAL MAGNITUDE: 1.0

SHEAR WAVE CORNER FREQUENCY RANGE AT CLOSE DISTANCES (130km)
13.1Hz -30.0Hz (18.8Hz)

FAULT RADIUS RANGE 23m - 52m (36m)

STRESS DROP RANGE 0.28MPa - 3.33MPa (0.82MPa)

RANGE OF THE PEAK SLIP AT THE FAULT 0.5mm - 2.4mm (1.0mm)

THE ORIENTATION OF THE RELAXED STRESS

	AZIMUTH	DIP	
P-AXIS	84.	5.	degrees
T-AXIS	173.	-10.	

THE HORIZONTAL DEVIATORIC STRESS AS GIVEN BY THE P- AND T-AXES
THE AZIMUTH OF COMPRESSION 83 degrees
THE RELATIVE SIZE 0.98

THE TWO POSSIBLE FAULT PLANES

	STRIKE	DIP	SLIP	
PLANE A	-51.	79.	184.	degrees
PLANE B	218.	86.	-11.	

THE NORMAL DIRECTIONS OF THE FAULT PLANES

	AZIMUTH	DIP	
PLANE A	39.	11.	degrees
PLANE B	308.	4.	

STATISTICAL INFORMATION

OF 0 FIRST MOTION POLARITY OBSERVATIONS
AT LEAST 0 ARE REQUIRED TO FIT

THE OPTIMUM MECHANISM HAS 0 POLARITY MISFITS

AMPLITUDES FOR P AND S AT 3 STATIONS ARE USED
ONLY MECHANISMS GIVING AN ESTIMATED STANDARD
DEVIATION OF THE AMPLITUDE ERROR FACTOR OF LESS
THAN 1.60 FOR SINGLE P-WAVE OBSERVATIONS ARE
TAKEN AS ACCEPTABLE AND INCLUDED IN THE FIGURES

3.61 % OF ALL MECHANISMS ARE ACCEPTABLE
100.0 % ACCEPTABLE DUE TO FIRST MOTION OBSERVATIONS
3.6 % OF THESE FITTED ALSO THE AMPLITUDES
THE PART OF WELL FITTING PLANES IS 28.3%

THE AMPLITUDE FIT OF THE OPTIMAL MECHANISM
GIVES A MEAN ERROR FACTOR OF 1.18
THIS CORRESPONDS TO A STANDARD DEVIATION FACTOR OF 1.32
FOR SINGLE P-WAVE OBSERVATIONS

THE DOUBLE COUPLE SOLUTION IS SIGNIFICANT
AT 18 % LEVEL
(F-VALUE: F(5, 2) = 5.28)

THE MEASURE OF THE MISFIT TO AN EARTHQUAKE SPECTRUM
P-WAVES 0.33
S-WAVES 0.26

-AXIS ORIENTATIONS
EQUAL AREA PROJECTION J08223584
LOWER HEMISPHERE

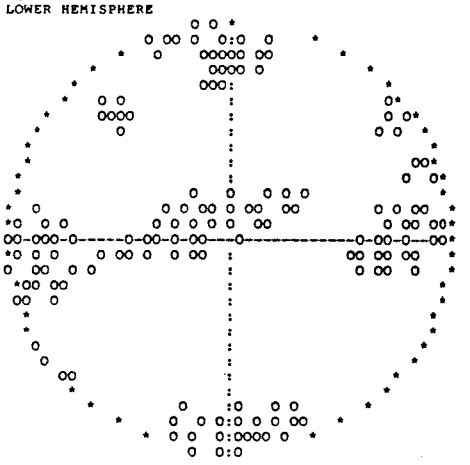

T-AXIS ORIENTATIONS
EQUAL AREA PROJECTION J08223584
LOWER HEMISPHERE

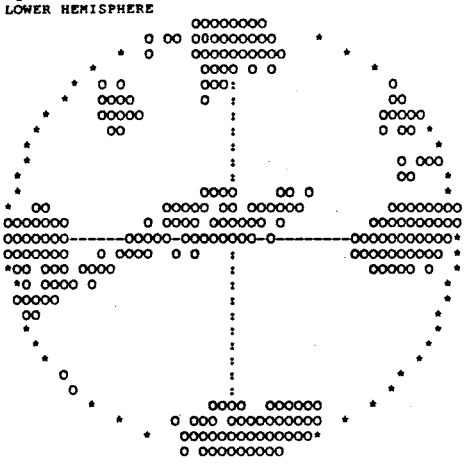

HORIZONTAL DEVIATORIC STRESS
RELATIVE SIZE AND J08223584
ORIENTATION OF COMPRESSION

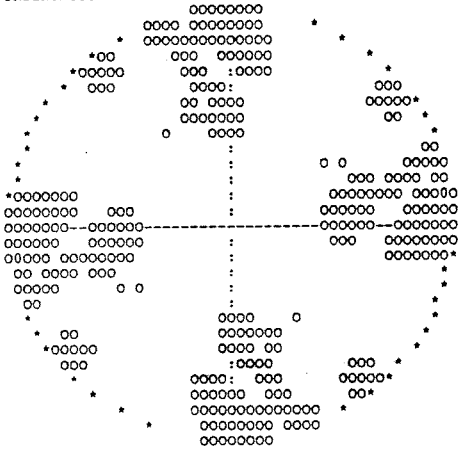

FAULT PLANE ORIENTATIONS
GIVEN BY NORMAL VECTORS
EQUAL AREA PROJECTION J08223584
LOWER HEMISPHERE

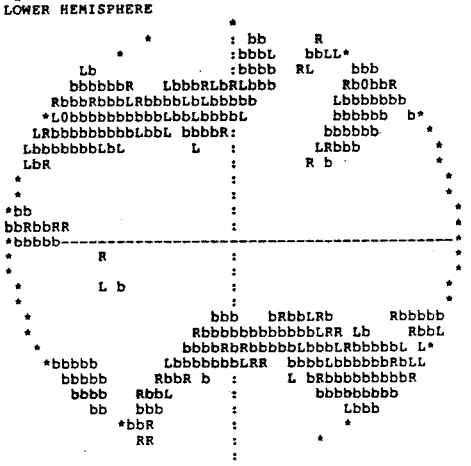

ORIGIN TIME 88 03 29 06H 07M 37.5S +/- 0.99S
LATITUDE 67.952 +/- 0.046 DEG.
LONGITUDE 19.390 +/- 0.128
FOCAL DEPTH 12.8 +/- 12.9 KM

STA	ARR. TIME	RES.	WEIGHT	DIST.	AZIMUTH	
MUG P	06 07 57.77	-0.02	22.3	124.5	114.8	P DOWN
MUG S	06 08 13.16	0.37	1.4	124.5	114.8	
HAK P	06 08 1.21	0.02	18.5	147.2	140.2	
HAK S	06 08 18.67	-0.11	1.1	147.2	140.2	
LJV P	06 08 7.13	-0.08	6.2	187.5	139.3	
KPM P	06 08 9.17	0.11	2.5	201.3	130.0	

INPUT DATA FOR FAULT PLANE SOLUTION

STN	DIST. KM	AZIMUTH DEGREES	OMEGA(PZ) METER-SEC	OMEGA(SZ) METER-SEC
MUG	125.	114.6	- 0.12E-08	0.35E-08
HAK	148.	139.9	0.37E-09	0.11E-08
LJV	188.	139.1	0.45E-09	0.31E-08
KPM	202.	129.8	0.57E-09	0.27E-08

DYNAMIC SOURCE PARAMETERS

SIZE MEASURES
SEISMIC MOMENT: 0.793E+12 Nm
LOCAL MAGNITUDE: 1.9

SHEAR WAVE CORNER FREQUENCY RANGE AT CLOSE DISTANCES (130km)
4.8Hz - 8.8Hz (6.6Hz)

FAULT RADIUS RANGE 78m - 143m (104m)

STRESS DROP RANGE 0.12MPa - 0.72MPa (0.30MPa)

RANGE OF THE PEAK SLIP AT THE FAULT 0.5mm - 1.8mm (1.0mm)

THE ORIENTATION OF THE RELAXED STRESS

	AZIMUTH	DIP	
P-AXIS	87.	40.	degrees
T-AXIS	79.	-50.	

THE HORIZONTAL DEVIATORIC STRESS AS GIVEN BY THE P- AND T-AXES
THE AZIMUTH OF COMPRESSION -78 degrees
THE RELATIVE SIZE 0.11

THE TWO POSSIBLE FAULT PLANES

	STRIKE	DIP	SLIP	
PLANE A	29.	7.	-55.	degrees
PLANE B	173.	85.	266.	

THE NORMAL DIRECTIONS OF THE FAULT PLANES

	AZIMUTH	DIP	
PLANE A	119.	83.	degrees
PLANE B	263.	5.	

STATISTICAL INFORMATION

OF 1 FIRST MOTION POLARITY OBSERVATIONS
AT LEAST 1 ARE REQUIRED TO FIT

THE OPTIMUM MECHANISM HAS 0 POLARITY MISFITS

AMPLITUDES FOR P AND S AT 4 STATIONS ARE USED
ONLY MECHANISMS GIVING AN ESTIMATED STANDARD
DEVIATION OF THE AMPLITUDE ERROR FACTOR OF LESS
THAN 1.60 FOR SINGLE P-WAVE OBSERVATIONS ARE
TAKEN AS ACCEPTABLE AND INCLUDED IN THE FIGURES

28.99 % OF ALL MECHANISMS ARE ACCEPTABLE
50.0 % ACCEPTABLE DUE TO FIRST MOTION OBSERVATIONS
59.1 % OF THESE FITTED ALSO THE AMPLITUDES
THE PART OF WELL FITTING PLANES IS 93.6%

THE AMPLITUDE FIT OF THE OPTIMAL MECHANISM
GIVES A MEAN ERROR FACTOR OF 1.18
THIS CORRESPONDS TO A STANDARD DEVIATION FACTOR OF 1.27
FOR SINGLE P-WAVE OBSERVATIONS

THE DOUBLE COUPLE SOLUTION IS SIGNIFICANT
AT 19 % LEVEL
(F-VALUE: F(7, 4) = 2.60)

THE MEASURE OF THE MISFIT TO AN EARTHQUAKE SPECTRUM
P-WAVES 0.26
S-WAVES 0.21

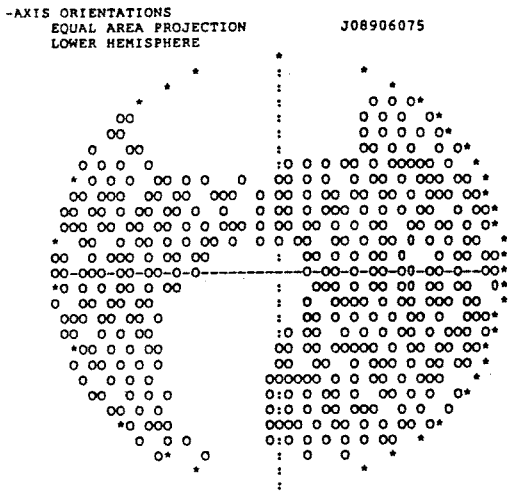
-AXIS ORIENTATIONS
EQUAL AREA PROJECTION
LOWER HEMISPHERE
J08906075

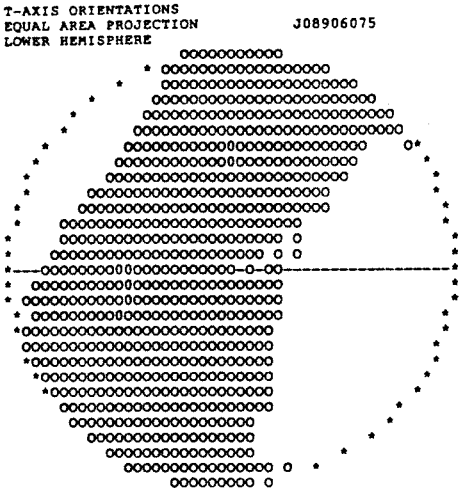
T-AXIS ORIENTATIONS
EQUAL AREA PROJECTION
LOWER HEMISPHERE
J08906075

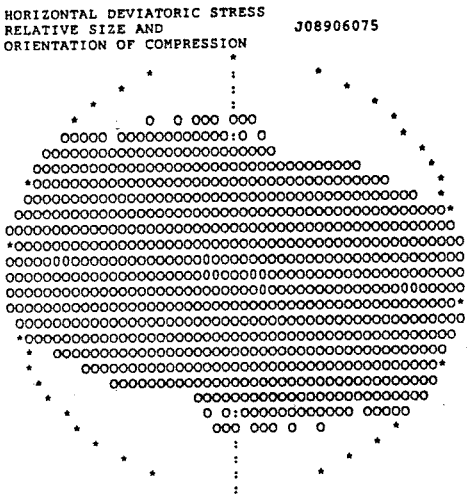
HORIZONTAL DEVIATORIC STRESS
RELATIVE SIZE AND
ORIENTATION OF COMPRESSION
J08906075

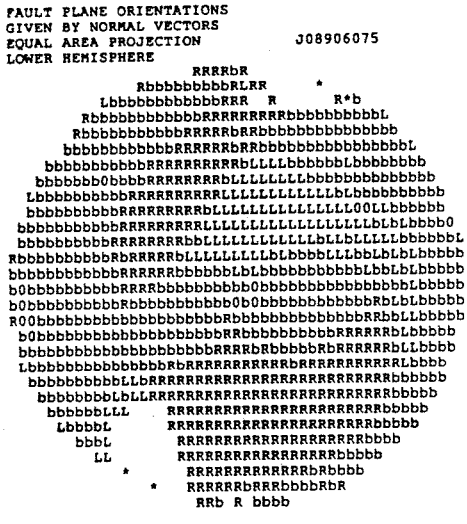
FAULT PLANE ORIENTATIONS
GIVEN BY NORMAL VECTORS
EQUAL AREA PROJECTION
LOWER HEMISPHERE
J08906075

ORIGIN TIME 88 03 30 02H 21M 12.1S +/- 1.04S
LATITUDE 65.220 +/- 0.068 DEG.
LONGITUDE 20.032 +/- 0.126
FOCAL DEPTH 8.0 +/- 6.5 KM

STA	ARR. TIME	RES.	WEIGHT	DIST.	AZIMUTH	
VMK	P 02 21 26.59	0.00	31.0	88.7	53.9	P UP
VMK	S 02 21 37.27	-0.02	2.0	88.7	53.9	
KLX	P 02 21 38.96	-0.03	7.1	167.5	54.3	
LJV	P 02 21 42.08	0.11	6.2	187.4	30.3	
HAK	P 02 21 44.03	-0.20	2.5	202.6	19.3	

INPUT DATA FOR FAULT PLANE SOLUTION

STN	DIST. KM	AZIMUTH DEGREES		OMEGA(PZ) METER-SEC	OMEGA(SZ) METER-SEC
VMK	89.	53.9	+	0.41E-09	0.22E-08
KLX	168.	54.3		0.11E-08	0.73E-08
LJV	188.	30.3		0.13E-08	0.40E-08
HAK	203.	19.3		0.49E-09	0.10E-08
KPM	216.	36.0		0.45E-09	0.23E-08

DYNAMIC SOURCE PARAMETERS

SIZE MEASURES
SEISMIC MOMENT: 0.125E+13 Nm
LOCAL MAGNITUDE: 2.1

SHEAR WAVE CORNER FREQUENCY RANGE AT CLOSE DISTANCES (130km)
8.8Hz -12.9Hz (10.8Hz)

FAULT RADIUS RANGE 53m - 78m (63m)

STRESS DROP RANGE 1.13MPa - 3.57MPa (2.09MPa)

RANGE OF THE PEAK SLIP AT THE FAULT 2.8mm - 6.1mm (4.3mm)

THE ORIENTATION OF THE RELAXED STRESS

	AZIMUTH	DIP	
P-AXIS	111.	-69.	degrees
T-AXIS	103.	20.	

THE HORIZONTAL DEVIATORIC STRESS AS GIVEN BY THE P- AND T-AXES
THE AZIMUTH OF COMPRESSION 12 degrees
THE RELATIVE SIZE 0.38

THE TWO POSSIBLE FAULT PLANES

	STRIKE	DIP	SLIP
PLANE A	189.	155.	-84. degrees
PLANE B	196.	66.	93.

THE NORMAL DIRECTIONS OF THE FAULT PLANES

	AZIMUTH	DIP	
PLANE A	99.	65.	degrees
PLANE B	286.	24.	

STATISTICAL INFORMATION

OF 1 FIRST MOTION POLARITY OBSERVATIONS
AT LEAST 1 ARE REQUIRED TO FIT

THE OPTIMUM MECHANISM HAS 0 POLARITY MISFITS

AMPLITUDES FOR P AND S AT 5 STATIONS ARE USED
ONLY MECHANISMS GIVING AN ESTIMATED STANDARD
DEVIATION OF THE AMPLITUDE ERROR FACTOR OF LESS
THAN 1.60 FOR SINGLE P-WAVE OBSERVATIONS ARE
TAKEN AS ACCEPTABLE AND INCLUDED IN THE FIGURES

28.75 % OF ALL MECHANISMS ARE ACCEPTABLE
50.0 % ACCEPTABLE DUE TO FIRST MOTION OBSERVATIONS
56.9 % OF THESE FITTED ALSO THE AMPLITUDES
THE PART OF WELL FITTING PLANES IS 93.0%

THE AMPLITUDE FIT OF THE OPTIMAL MECHANISM
GIVES A MEAN ERROR FACTOR OF 1.34
THIS CORRESPONDS TO A STANDARD DEVIATION FACTOR OF 1.46
FOR SINGLE P-WAVE OBSERVATIONS

THE DOUBLE COUPLE SOLUTION IS NOT SIGNIFICANT
NOT EVEN AT 50 % LEVEL
(F-VALUE: F(9, 6) = 0.93)

THE MEASURE OF THE MISFIT TO AN EARTHQUAKE SPECTRUM
P-WAVES 0.26
S-WAVES 0.27

-AXIS ORIENTATIONS
EQUAL AREA PROJECTION J09002213
LOWER HEMISPHERE

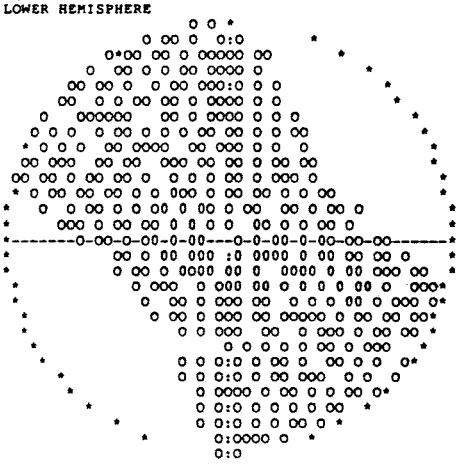

T-AXIS ORIENTATIONS
EQUAL AREA PROJECTION J09002213
LOWER HEMISPHERE

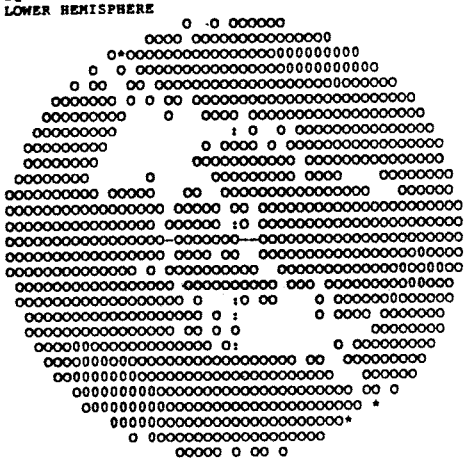

HORIZONTAL DEVIATORIC STRESS
RELATIVE SIZE AND J09002213
ORIENTATION OF COMPRESSION

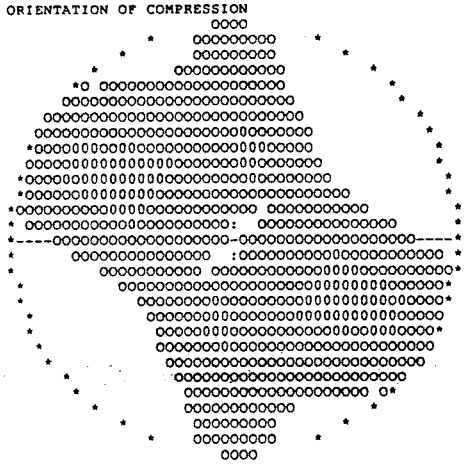

FAULT PLANE ORIENTATIONS
GIVEN BY NORMAL VECTORS
EQUAL AREA PROJECTION J09002213
LOWER HEMISPHERE

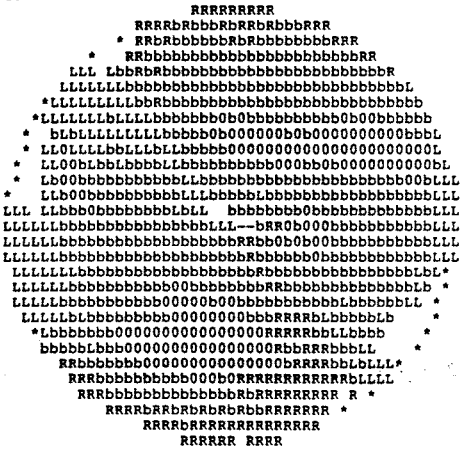

ORIGIN TIME 88 03 30 12H 06M 35.0S +/- 0.33S
LATITUDE 67.518 +/- 0.019 DEG.
LONGITUDE 22.413 +/- 0.045
FOCAL DEPTH 8.9 +/- 3.2 KM

STA	ARR. TIME	RES.	WEIGHT	DIST.	AZIMUTH	
MUG	P 12 06 38.14	0.00	75.2	17.0	248.4	P UP
MUG	S 12 06 40.43	-0.03	7.1	17.0	248.4	
HAK	P 12 06 47.47	-0.02	35.3	75.9	209.5	
HAK	S 12 06 56.75	0.08	2.4	75.9	209.5	
KPM	P 12 06 49.38	-0.03	31.2	87.9	165.7	
KPM	S 12 07 0.01	-0.01	2.1	87.9	165.7	
LJV	P 12 06 51.02	0.12	28.5	97.1	186.5	
LJV	S 12 07 2.22	-0.38	1.8	97.1	186.5	
KLX	P 12 07 1.35	-0.05	16.3	164.3	170.2	

INPUT DATA FOR FAULT PLANE SOLUTION

STN	DIST. KM	AZIMUTH DEGREES	OMEGA(PZ) METER-SEC	OMEGA(SZ) METER-SEC
HAK	76.	209.4	0.12E-09	0.34E-09
KPM	88.	165.7	0.19E-09	0.52E-09
LJV	97.	186.4	0.18E-09	0.10E-08
KLX	165.	170.1	0.26E-09	0.43E-09
VMK	209.	190.5	0.81E-10	0.40E-09
MUG	17.	247.6	+ 0.00E+00	0.00E+00

DYNAMIC SOURCE PARAMETERS

SIZE MEASURES
SEISMIC MOMENT: 0.270E+12 Nm
LOCAL MAGNITUDE: 1.4

SHEAR WAVE CORNER FREQUENCY RANGE AT CLOSE DISTANCES (130km)
6.6Hz - 9.1Hz (7.9Hz)

FAULT RADIUS RANGE 75m - 104m (87m)

STRESS DROP RANGE 0.10MPa - 0.27MPa (0.18MPa)

RANGE OF THE PEAK SLIP AT THE FAULT 0.3mm - 0.7mm (0.5mm)

THE ORIENTATION OF THE RELAXED STRESS

	AZIMUTH	DIP	
P-AXIS	149.	11.	degrees
T-AXIS	63.	-19.	

THE HORIZONTAL DEVIATORIC STRESS AS GIVEN BY THE P- AND T-AXES
THE AZIMUTH OF COMPRESSION -28 degrees
THE RELATIVE SIZE 0.93

THE TWO POSSIBLE FAULT PLANES

	STRIKE	DIP	SLIP
PLANE A	105.	69.	-6. degrees
PLANE B	197.	84.	202.

THE NORMAL DIRECTIONS OF THE FAULT PLANES

	AZIMUTH	DIP	
PLANE A	195.	21.	degrees
PLANE B	287.	6.	

STATISTICAL INFORMATION

OF 1 FIRST MOTION POLARITY OBSERVATIONS
AT LEAST 1 ARE REQUIRED TO FIT

THE OPTIMUM MECHANISM HAS 0 POLARITY MISFITS

AMPLITUDES FOR P AND S AT 5 STATIONS ARE USED
ONLY MECHANISMS GIVING AN ESTIMATED STANDARD
DEVIATION OF THE AMPLITUDE ERROR FACTOR OF LESS
THAN 1.60 FOR SINGLE P-WAVE OBSERVATIONS ARE
TAKEN AS ACCEPTABLE AND INCLUDED IN THE FIGURES

9.61 % OF ALL MECHANISMS ARE ACCEPTABLE
50.0 % ACCEPTABLE DUE TO FIRST MOTION OBSERVATIONS
18.8 % OF THESE FITTED ALSO THE AMPLITUDES
THE PART OF WELL FITTING PLANES IS 58.0%

THE AMPLITUDE FIT OF THE OPTIMAL MECHANISM
GIVES A MEAN ERROR FACTOR OF 1.25
THIS CORRESPONDS TO A STANDARD DEVIATION FACTOR OF 1.34
FOR SINGLE P-WAVE OBSERVATIONS

THE DOUBLE COUPLE SOLUTION IS SIGNIFICANT
AT 17 % LEVEL
(F-VALUE: F(9, 6) = 2.26)

THE MEASURE OF THE MISFIT TO AN EARTHQUAKE SPECTRUM
P-WAVES 0.22
S-WAVES 0.21

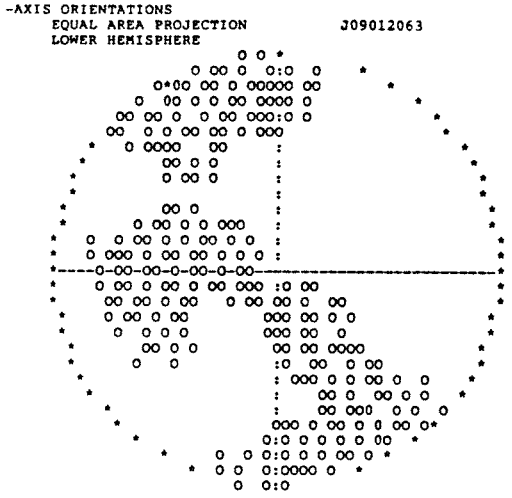
-AXIS ORIENTATIONS
EQUAL AREA PROJECTION
LOWER HEMISPHERE
J09012063

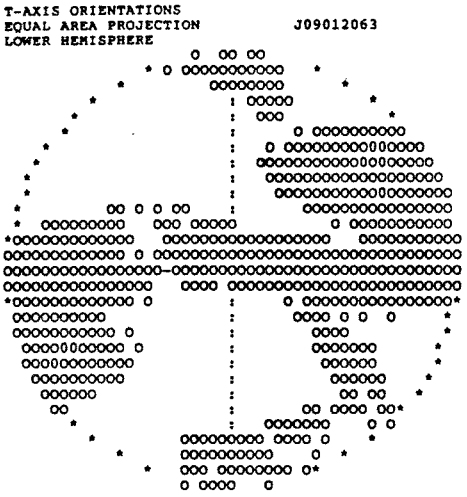
T-AXIS ORIENTATIONS
EQUAL AREA PROJECTION
LOWER HEMISPHERE
J09012063

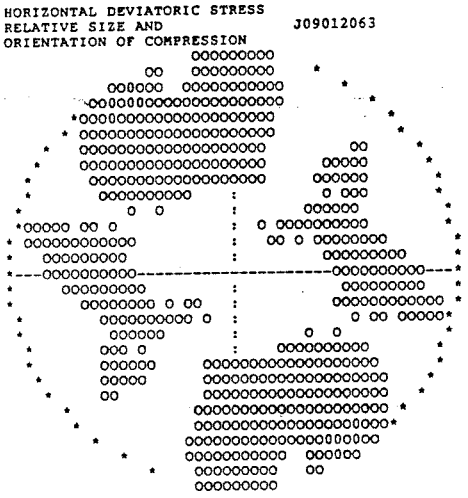
HORIZONTAL DEVIATORIC STRESS
RELATIVE SIZE AND
ORIENTATION OF COMPRESSION
J09012063

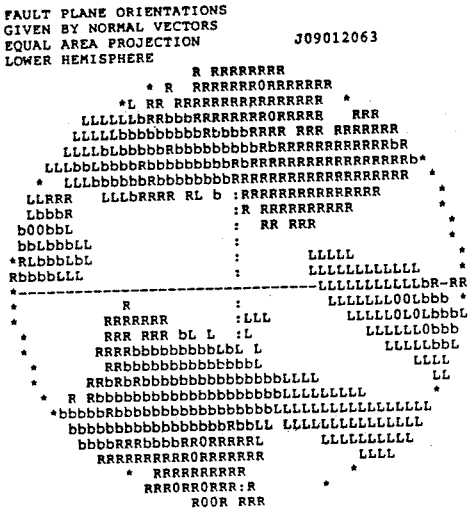
FAULT PLANE ORIENTATIONS
GIVEN BY NORMAL VECTORS
EQUAL AREA PROJECTION
LOWER HEMISPHERE
J09012063

ORIGIN TIME 88 04 01 01H 36M 10.5S +/- 0.38S
LATITUDE 67.493 +/- 0.023 DEG.
LONGITUDE 22.195 +/- 0.046
FOCAL DEPTH 9.0 +/- 2.2 KM

STA	ARR. TIME	RES.	WEIGHT	DIST.	AZIMUTH	
MUG	P 01 36 12.40	0.02	88.0	7.3	241.8	
MUG	S 01 36 13.60	-0.19	9.0	7.3	241.8	
HAK	P 01 36 21.81	-0.07	38.0	69.2	203.7	P UP
KPM	P 01 36 24.84	-0.07	31.2	88.0	159.2	
KPM	S 01 36 35.43	-0.10	2.1	88.0	159.2	
LJV	P 01 36 26.11	0.28	29.5	93.7	180.8	
KLX	P 01 36 36.59	-0.16	16.4	163.4	166.6	
KLX	S 01 36 55.88	-0.53	0.9	163.4	166.6	
VMK	S 01 37 7.59	0.43	0.1	204.3	187.9	

INPUT DATA FOR FAULT PLANE SOLUTION

STN	DIST. KM	AZIMUTH DEGREES		OMEGA(PZ) METER-SEC	OMEGA(SZ) METER-SEC
HAK	69.	204.0	+	0.94E-10	0.22E-09
KPM	88.	159.2		0.15E-09	0.42E-09
LJV	93.	180.9		0.10E-09	0.43E-09
KLX	163.	166.6		0.13E-09	0.68E-09
VMK	204.	187.9		0.76E-10	0.38E-09
MUG	7.	244.8	+	0.00E+00	0.00E+00

DYNAMIC SOURCE PARAMETERS

SIZE MEASURES
SEISMIC MOMENT: 0.110E+12 Nm
LOCAL MAGNITUDE: 1.0

SHEAR WAVE CORNER FREQUENCY RANGE AT CLOSE DISTANCES (130km)
12.6Hz -22.0Hz (15.9Hz)

FAULT RADIUS RANGE 31m - 54m (43m)

STRESS DROP RANGE 0.29MPa - 1.56MPa (0.59MPa)

RANGE OF THE PEAK SLIP AT THE FAULT 0.5mm - 1.6mm (0.8mm)

THE ORIENTATION OF THE RELAXED STRESS

	AZIMUTH	DIP
P-AXIS	146.	40. degrees
T-AXIS	48.	9.

THE HORIZONTAL DEVIATORIC STRESS AS GIVEN BY THE P- AND T-AXES
THE AZIMUTH OF COMPRESSION -38 degrees
THE RELATIVE SIZE 0.78

THE TWO POSSIBLE FAULT PLANES

	STRIKE	DIP	SLIP
PLANE A	103.	70.	37. degrees
PLANE B	179.	124.	204.

THE NORMAL DIRECTIONS OF THE FAULT PLANES

	AZIMUTH	DIP
PLANE A	193.	20. degrees
PLANE B	89.	34.

STATISTICAL INFORMATION

OF 2 FIRST MOTION POLARITY OBSERVATIONS
AT LEAST 2 ARE REQUIRED TO FIT

THE OPTIMUM MECHANISM HAS 0 POLARITY MISFITS

AMPLITUDES FOR P AND S AT 5 STATIONS ARE USED
ONLY MECHANISMS GIVING AN ESTIMATED STANDARD
DEVIATION OF THE AMPLITUDE ERROR FACTOR OF LESS
THAN 1.60 FOR SINGLE P-WAVE OBSERVATIONS ARE
TAKEN AS ACCEPTABLE AND INCLUDED IN THE FIGURES

6.47 % OF ALL MECHANISMS ARE ACCEPTABLE
23.4 % ACCEPTABLE DUE TO FIRST MOTION OBSERVATIONS
27.6 % OF THESE FITTED ALSO THE AMPLITUDES
THE PART OF WELL FITTING PLANES IS 55.2%

THE AMPLITUDE FIT OF THE OPTIMAL MECHANISM
GIVES A MEAN ERROR FACTOR OF 1.16
THIS CORRESPONDS TO A STANDARD DEVIATION FACTOR OF 1.22
FOR SINGLE P-WAVE OBSERVATIONS

THE DOUBLE COUPLE SOLUTION IS SIGNIFICANT
AT 8 % LEVEL
(F-VALUE: F(9, 6) = 3.23)

THE MEASURE OF THE MISFIT TO AN EARTHQUAKE SPECTRUM
P-WAVES 0.25
S-WAVES 0.16

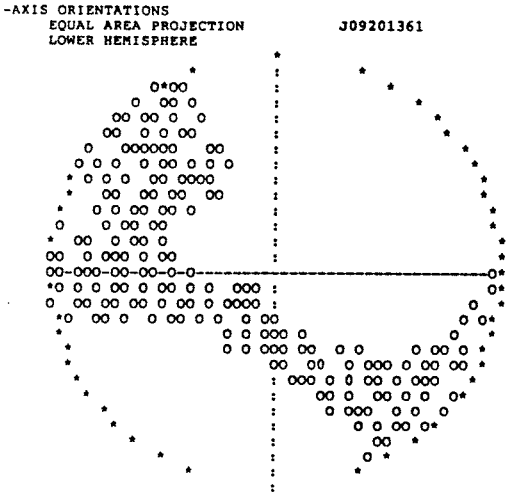
-AXIS ORIENTATIONS
EQUAL AREA PROJECTION
LOWER HEMISPHERE
J09201361

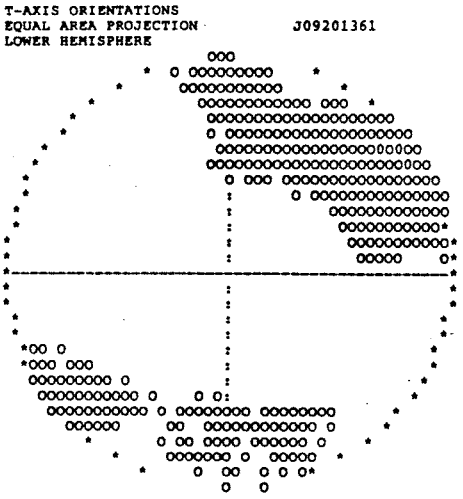
T-AXIS ORIENTATIONS
EQUAL AREA PROJECTION
LOWER HEMISPHERE
J09201361

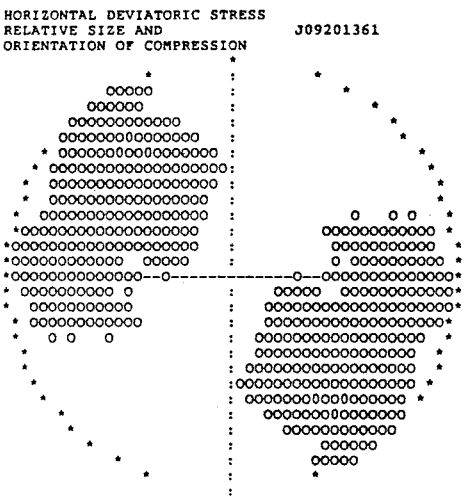
HORIZONTAL DEVIATORIC STRESS
RELATIVE SIZE AND
ORIENTATION OF COMPRESSION
J09201361

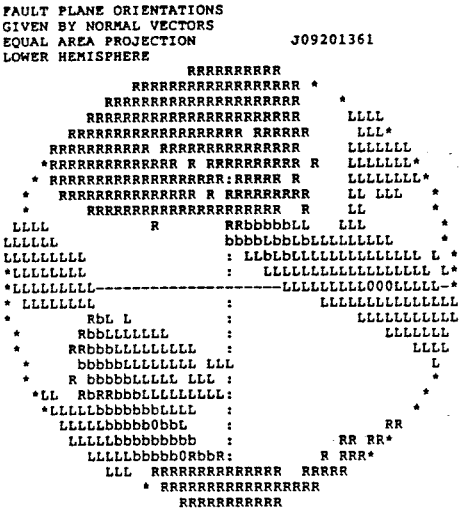
FAULT PLANE ORIENTATIONS
GIVEN BY NORMAL VECTORS
EQUAL AREA PROJECTION
LOWER HEMISPHERE
J09201361

ORIGIN TIME 88 04 04 02H 25M 22.9S +/- 0.73S
LATITUDE 67.779 +/- 0.032 DEG.
LONGITUDE 19.621 +/- 0.097
FOCAL DEPTH 8.2 +/- 4.2 KM

STA	ARR. TIME	RES.	WEIGHT	DIST.	AZIMUTH	
MUG	P 02 25 40.75	-0.02	25.6	108.6	107.7	
MUG	S 02 25 53.93	0.10	1.6	108.6	107.7	
HAK	P 02 25 43.65	0.02	21.9	126.2	138.0	P DOWN
HAK	S 02 25 58.44	-0.35	1.3	126.2	138.0	
LJV	P 02 25 49.79	0.04	16.0	166.6	137.6	
LJV	S 02 26 10.30	0.53	0.9	166.6	137.6	
KPM	P 02 25 51.98	-0.03	6.4	181.7	127.4	
KLX	P 02 26 0.03	-0.04	2.0	242.1	140.5	
VMK	P 02 26 0.88	-0.10	1.9	249.5	158.8	

INPUT DATA FOR FAULT PLANE SOLUTION

STN	DIST. KM	AZIMUTH DEGREES	OMEGA(PZ) METER-SEC	OMEGA(SZ) METER-SEC
MUG	109.	107.9	0.39E-09	0.29E-08
HAK	127.	137.9	- 0.20E-09	0.70E-09
LJV	167.	137.6	0.25E-09	0.12E-08
KPM	182.	127.4	0.36E-09	0.12E-08

DYNAMIC SOURCE PARAMETERS

SIZE MEASURES
SEISMIC MOMENT: 0.491E+12 Nm
LOCAL MAGNITUDE: 1.7

SHEAR WAVE CORNER FREQUENCY RANGE AT CLOSE DISTANCES (130km)
4.8Hz - 8.4Hz (6.4Hz)

FAULT RADIUS RANGE 82m - 143m (107m)

STRESS DROP RANGE 0.07MPa - 0.39MPa (0.17MPa)

RANGE OF THE PEAK SLIP AT THE FAULT 0.3mm - 1.0mm (0.6mm)

THE ORIENTATION OF THE RELAXED STRESS

	AZIMUTH	DIP
P-AXIS	103.	-29. degrees
T-AXIS	27.	24.

THE HORIZONTAL DEVIATORIC STRESS AS GIVEN BY THE P- AND T-AXES
THE AZIMUTH OF COMPRESSION -70 degrees
THE RELATIVE SIZE 0.77

THE TWO POSSIBLE FAULT PLANES

	STRIKE	DIP	SLIP
PLANE A	67.	129.	-4. degrees
PLANE B	154.	87.	141.

THE NORMAL DIRECTIONS OF THE FAULT PLANES

	AZIMUTH	DIP
PLANE A	337.	39. degrees
PLANE B	244.	3.

STATISTICAL INFORMATION

OF 1 FIRST MOTION POLARITY OBSERVATIONS
AT LEAST 1 ARE REQUIRED TO FIT

THE OPTIMUM MECHANISM HAS 0 POLARITY MISFITS

AMPLITUDES FOR P AND S AT 4 STATIONS ARE USED
ONLY MECHANISMS GIVING AN ESTIMATED STANDARD
DEVIATION OF THE AMPLITUDE ERROR FACTOR OF LESS
THAN 1.60 FOR SINGLE P-WAVE OBSERVATIONS ARE
TAKEN AS ACCEPTABLE AND INCLUDED IN THE FIGURES

31.54 % OF ALL MECHANISMS ARE ACCEPTABLE
50.0 % ACCEPTABLE DUE TO FIRST MOTION OBSERVATIONS
62.3 % OF THESE FITTED ALSO THE AMPLITUDES
THE PART OF WELL FITTING PLANES IS 95.6%

THE AMPLITUDE FIT OF THE OPTIMAL MECHANISM
GIVES A MEAN ERROR FACTOR OF 1.14
THIS CORRESPONDS TO A STANDARD DEVIATION FACTOR OF 1.21
FOR SINGLE P-WAVE OBSERVATIONS

THE DOUBLE COUPLE SOLUTION IS SIGNIFICANT
AT 24 % LEVEL
(F-VALUE: F(7, 4) = 2.14)

THE MEASURE OF THE MISFIT TO AN EARTHQUAKE SPECTRUM
P-WAVES 0.24
S-WAVES 0.19

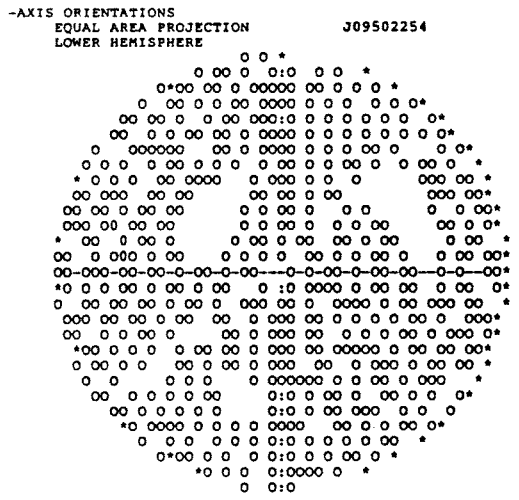
-AXIS ORIENTATIONS
EQUAL AREA PROJECTION
LOWER HEMISPHERE
J09502254

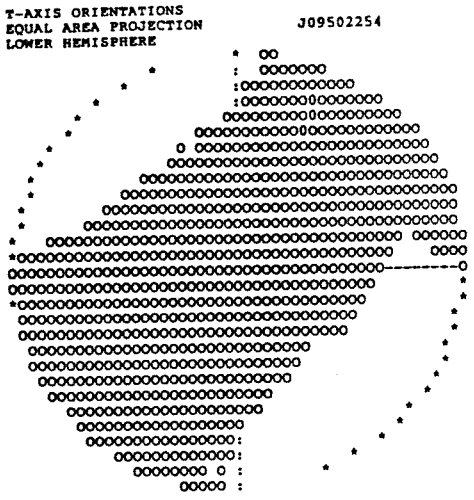
T-AXIS ORIENTATIONS
EQUAL AREA PROJECTION
LOWER HEMISPHERE
J09502254

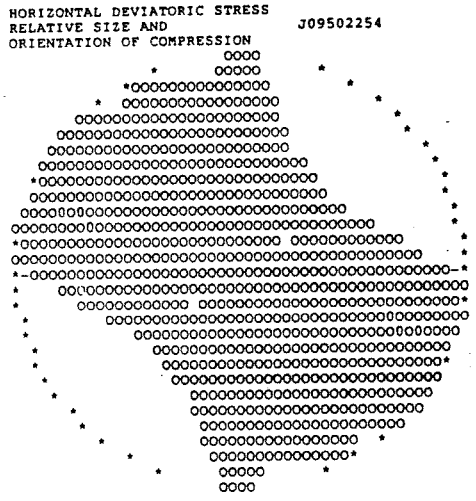
HORIZONTAL DEVIATORIC STRESS
RELATIVE SIZE AND
ORIENTATION OF COMPRESSION
J09502254

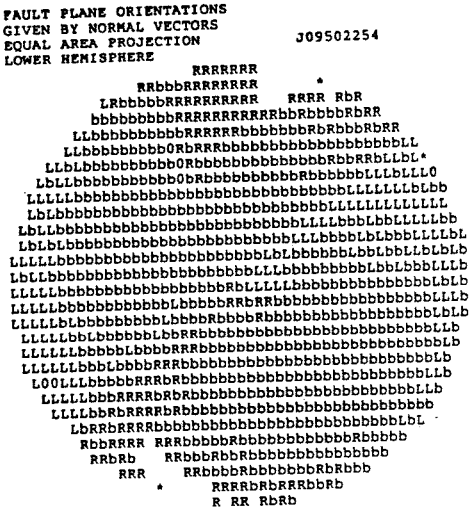
FAULT PLANE ORIENTATIONS
GIVEN BY NORMAL VECTORS
EQUAL AREA PROJECTION
LOWER HEMISPHERE
J09502254

ORIGIN TIME 88 04 04 02H 33M 16.2S +/- 0.18S
LATITUDE 67.662 +/- 0.012 DEG.
LONGITUDE 22.114 +/- 0.034
FOCAL DEPTH 8.6 +/- 2.2 KM

STA	ARR. TIME	RES.	WEIGHT	DIST.	AZIMUTH	
MUG	P 02 33 20.10	-0.02	69.2	22.5	187.6	P DOWN
MUG	S 02 33 23.22	0.19	6.2	22.5	187.6	
KIR	P 02 33 28.50	0.07	35.8	74.6	286.3	
KIR	S 02 33 36.50	-0.95	2.5	74.6	286.3	
HAK	P 02 33 30.36	0.12	31.9	85.7	196.5	
KPM	P 02 33 33.39	-0.27	26.0	106.9	160.9	P DOWN
KPM	S 02 33 46.63	0.11	1.6	106.9	160.9	
LJV	P 02 33 34.59	0.02	24.7	112.5	178.8	P DOWN
LJV	S 02 33 48.54	0.44	1.5	112.5	178.8	
KLX	P 02 33 45.21	-0.12	6.4	182.6	166.8	
KLX	S 02 34 7.17	-0.01	0.4	182.6	166.8	
SO	P 02 33 46.00	0.35	6.3	184.8	96.4	
SO	S 02 34 8.00	0.23	0.3	184.8	96.4	
VMK	P 02 33 50.59	-0.25	2.2	222.5	186.3	
VMK	S 02 34 18.40	1.33	0.1	222.5	186.3	

INPUT DATA FOR FAULT PLANE SOLUTION

STN	DIST. KM	AZIMUTH DEGREES	OMEGA(PZ) METER-SEC	OMEGA(SZ) METER-SEC
MUG	26.	194.6	- 0.19E-08	0.15E-07
HAK	90.	198.2	0.47E-09	0.17E-08
KPM	109.	163.4	- 0.73E-09	0.33E-08
LJV	116.	180.7	- 0.47E-09	0.32E-08
KLX	185.	168.2	0.91E-09	0.53E-08
VMK	226.	187.2	0.39E-09	0.28E-08

DYNAMIC SOURCE PARAMETERS

SIZE MEASURES
SEISMIC MOMENT: 0.101E+13 Nm
LOCAL MAGNITUDE: 2.0

SHEAR WAVE CORNER FREQUENCY RANGE AT CLOSE DISTANCES (130km)
4.7Hz - 9.6Hz (7.0Hz)

FAULT RADIUS RANGE 71m - 146m (98m)

STRESS DROP RANGE 0.14MPa - 1.19MPa (0.46MPa)

RANGE OF THE PEAK SLIP AT THE FAULT 0.7mm - 2.7mm (1.5mm)

THE ORIENTATION OF THE RELAXED STRESS

	AZIMUTH	DIP
P-AXIS	162.	-29. degrees
T-AXIS	64.	-14.

THE HORIZONTAL DEVIATORIC STRESS AS GIVEN BY THE P- AND T-AXES
THE AZIMUTH OF COMPRESSION -22 degrees
THE RELATIVE SIZE 0.84

THE TWO POSSIBLE FAULT PLANES

	STRIKE	DIP	SLIP
PLANE A	115.	100.	-32. degrees
PLANE B	199.	59.	169.

THE NORMAL DIRECTIONS OF THE FAULT PLANES

	AZIMUTH	DIP
PLANE A	25.	10. degrees
PLANE B	289.	31.

STATISTICAL INFORMATION

OF 3 FIRST MOTION POLARITY OBSERVATIONS
AT LEAST 3 ARE REQUIRED TO FIT

THE OPTIMUM MECHANISM HAS 0 POLARITY MISFITS

AMPLITUDES FOR P AND S AT 6 STATIONS ARE USED
ONLY MECHANISMS GIVING AN ESTIMATED STANDARD
DEVIATION OF THE AMPLITUDE ERROR FACTOR OF LESS
THAN 1.60 FOR SINGLE P-WAVE OBSERVATIONS ARE
TAKEN AS ACCEPTABLE AND INCLUDED IN THE FIGURES

8.77 % OF ALL MECHANISMS ARE ACCEPTABLE
32.3 % ACCEPTABLE DUE TO FIRST MOTION OBSERVATIONS
27.2 % OF THESE FITTED ALSO THE AMPLITUDES
THE PART OF WELL FITTING PLANES IS 58.3%

THE AMPLITUDE FIT OF THE OPTIMAL MECHANISM
GIVES A MEAN ERROR FACTOR OF 1.27
THIS CORRESPONDS TO A STANDARD DEVIATION FACTOR OF 1.35
FOR SINGLE P-WAVE OBSERVATIONS

THE DOUBLE COUPLE SOLUTION IS SIGNIFICANT
AT 34 % LEVEL
(F-VALUE: F(11, 8) = 1.35)

THE MEASURE OF THE MISFIT TO AN EARTHQUAKE SPECTRUM
P-WAVES 0.27
S-WAVES 0.22

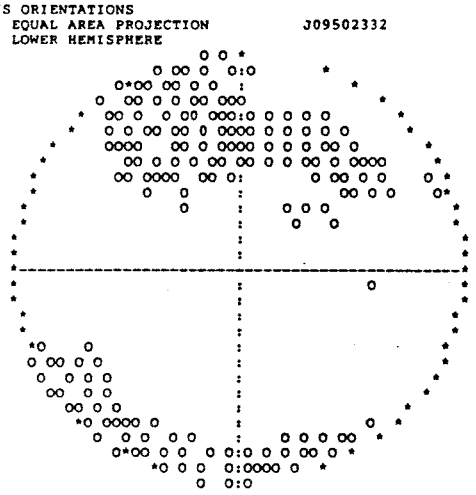
-AXIS ORIENTATIONS
EQUAL AREA PROJECTION
LOWER HEMISPHERE
J09502332

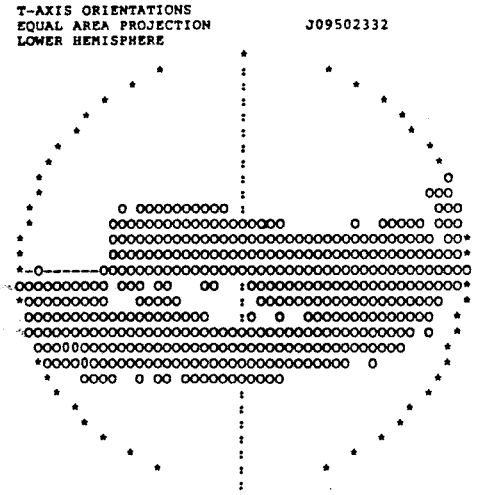
T-AXIS ORIENTATIONS
EQUAL AREA PROJECTION
LOWER HEMISPHERE
J09502332

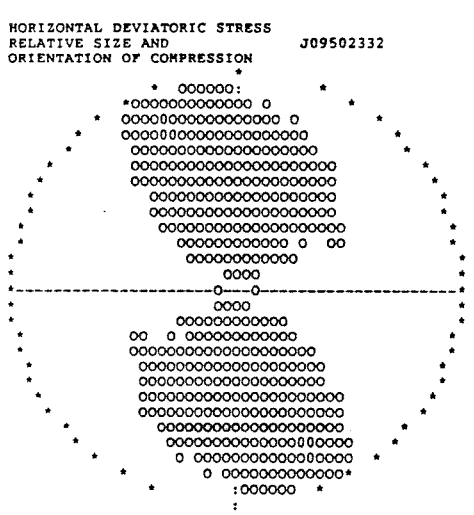
HORIZONTAL DEVIATORIC STRESS
RELATIVE SIZE AND
ORIENTATION OF COMPRESSION
J09502332

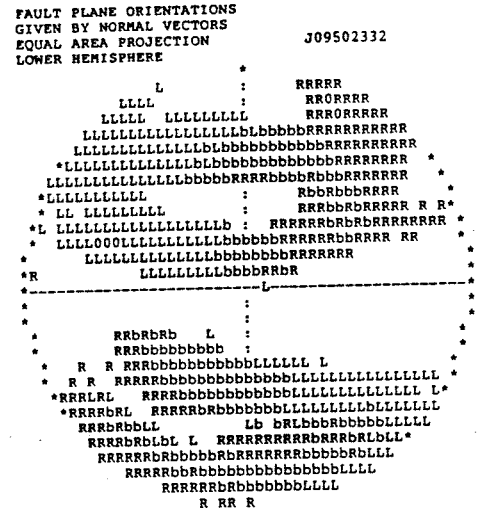
FAULT PLANE ORIENTATIONS
GIVEN BY NORMAL VECTORS
EQUAL AREA PROJECTION
LOWER HEMISPHERE
J09502332

ORIGIN TIME 88 04 04 17H 48M 34.8S +/- 0.08S
LATITUDE 66.387 +/- 0.005 DEG.
LONGITUDE 22.601 +/- 0.025
FOCAL DEPTH 18.5 +/- 1.6 KM

STA	ARR. TIME	RES.	WEIGHT	DIST.	AZIMUTH	
LJV P	17 48 41.33	-0.01	57.4	35.6	327.2	P UP
LJV S	17 48 46.19	0.06	4.7	35.6	327.2	
KLX P	17 48 42.08	0.02	53.6	40.6	151.4	P UP
KLX S	17 48 47.40	0.00	4.3	40.6	151.4	
KPM P	17 48 42.43	-0.02	51.8	43.3	18.0	P UP
KPM S	17 48 48.02	-0.06	4.1	43.3	18.0	
HAK P	17 48 47.44	0.04	35.4	75.7	322.9	
HAK S	17 48 56.71	-0.04	2.4	75.7	322.9	
VMK P	17 48 49.76	0.01	30.1	91.4	210.7	
VMK S	17 49 0.37	-0.52	2.0	91.4	210.7	

INPUT DATA FOR FAULT PLANE SOLUTION

STN	DIST. KM	AZIMUTH DEGREES		OMEGA(PZ) METER-SEC	OMEGA(SZ) METER-SEC
LJV	35.	327.1	+	0.79E-10	0.21E-09
KLX	41.	151.5	+	0.83E-10	0.26E-09
KPM	43.	18.2	+	0.56E-10	0.19E-09
HAK	75.	322.8		0.49E-10	0.31E-09
VMK	92.	210.6		0.13E-10	0.98E-10

DYNAMIC SOURCE PARAMETERS

SIZE MEASURES
SEISMIC MOMENT: 0.377E+11 Nm
LOCAL MAGNITUDE: 0.6

SHEAR WAVE CORNER FREQUENCY RANGE AT CLOSE DISTANCES (130km)
4.7Hz - 7.0Hz (6.0Hz)

FAULT RADIUS RANGE 98m - 146m (115m)

STRESS DROP RANGE 0.01MPa - 0.02MPa (0.01MPa)

RANGE OF THE PEAK SLIP AT THE FAULT 0.0mm - 0.0mm (0.0mm)

THE ORIENTATION OF THE RELAXED STRESS

	AZIMUTH	DIP	
P-AXIS	66.	22.	degrees
T-AXIS	160.	9.	

THE HORIZONTAL DEVIATORIC STRESS AS GIVEN BY THE P- AND T-AXES
THE AZIMUTH OF COMPRESSION 67 degrees
THE RELATIVE SIZE 0.91

THE TWO POSSIBLE FAULT PLANES

	STRIKE	DIP	SLIP	
PLANE A	-69.	81.	157.	degrees
PLANE B	205.	113.	-10.	

THE NORMAL DIRECTIONS OF THE FAULT PLANES

	AZIMUTH	DIP	
PLANE A	21.	9.	degrees
PLANE B	115.	23.	

STATISTICAL INFORMATION

OF 3 FIRST MOTION POLARITY OBSERVATIONS
AT LEAST 3 ARE REQUIRED TO FIT

THE OPTIMUM MECHANISM HAS 0 POLARITY MISFITS

AMPLITUDES FOR P AND S AT 5 STATIONS ARE USED
ONLY MECHANISMS GIVING AN ESTIMATED STANDARD
DEVIATION OF THE AMPLITUDE ERROR FACTOR OF LESS
THAN 1.60 FOR SINGLE P-WAVE OBSERVATIONS ARE
TAKEN AS ACCEPTABLE AND INCLUDED IN THE FIGURES

1.07 % OF ALL MECHANISMS ARE ACCEPTABLE
13.8 % ACCEPTABLE DUE TO FIRST MOTION OBSERVATIONS
7.8 % OF THESE FITTED ALSO THE AMPLITUDES
THE PART OF WELL FITTING PLANES IS 17.2%

THE AMPLITUDE FIT OF THE OPTIMAL MECHANISM
GIVES A MEAN ERROR FACTOR OF 1.24
THIS CORRESPONDS TO A STANDARD DEVIATION FACTOR OF 1.32
FOR SINGLE P-WAVE OBSERVATIONS

THE DOUBLE COUPLE SOLUTION IS SIGNIFICANT
AT 4 % LEVEL
(F-VALUE: F(9, 6) = 4.19)

THE MEASURE OF THE MISFIT TO AN EARTHQUAKE SPECTRUM

P-WAVES	0.22
S-WAVES	0.30

-AXIS ORIENTATIONS
EQUAL AREA PROJECTION J09517484
LOWER HEMISPHERE

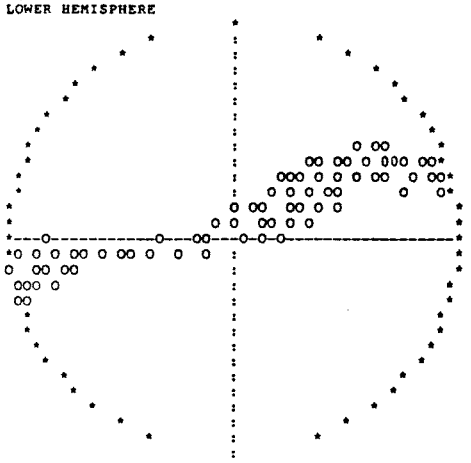

T-AXIS ORIENTATIONS
EQUAL AREA PROJECTION J09517484
LOWER HEMISPHERE

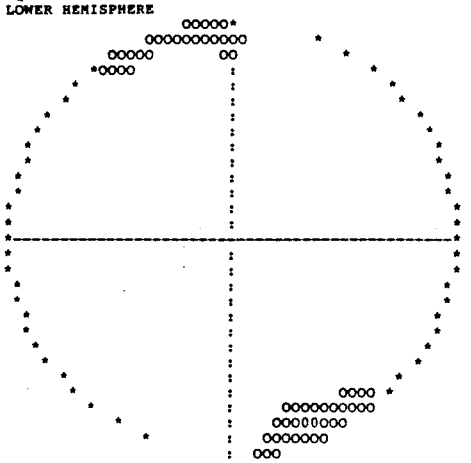

HORIZONTAL DEVIATORIC STRESS
RELATIVE SIZE AND J09517484
ORIENTATION OF COMPRESSION

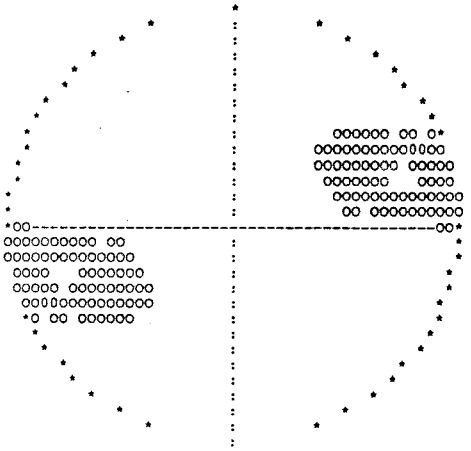

FAULT PLANE ORIENTATIONS
GIVEN BY NORMAL VECTORS
EQUAL AREA PROJECTION J09517484
LOWER HEMISPHERE

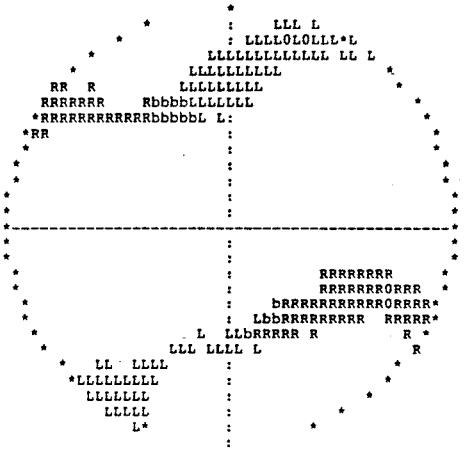

ORIGIN TIME 88 04 07 21H 24M 31.6S +/- 0.58S
LATITUDE 67.974 +/- 0.033 DEG.
LONGITUDE 20.781 +/- 0.092
FOCAL DEPTH 29.1 +/- 2.5 KM

STA	ARR. TIME	RES.	WEIGHT	DIST.	AZIMUTH	
MUG	P 21 24 44.64	-0.04	34.4	78.4	136.3	P DOWN
MUG	S 21 24 54.83	0.34	2.3	78.4	136.3	
HAK	P 21 24 51.16	0.07	22.8	121.9	163.7	
HAK	S 21 25 5.07	-0.67	1.4	121.9	163.7	
LJV	S 21 25 15.13	-0.09	1.0	159.0	157.3	
KPM	P 21 24 57.08	-0.01	16.3	164.0	145.1	
KPM	S 21 25 16.69	0.21	0.9	164.0	145.1	

INPUT DATA FOR FAULT PLANE SOLUTION

STN	DIST. KM	AZIMUTH DEGREES	OMEGA(PZ) METER-SEC	OMEGA(SZ) METER-SEC
MUG	78.	136.0	- 0.17E-09	0.55E-09
HAK	121.	163.7	0.88E-10	0.36E-09
KPM	164.	145.0	0.54E-10	0.70E-09

DYNAMIC SOURCE PARAMETERS

SIZE MEASURES
SEISMIC MOMENT: 0.148E+12 Nm
LOCAL MAGNITUDE: 1.2

SHEAR WAVE CORNER FREQUENCY RANGE AT CLOSE DISTANCES (130km)
 6.8Hz -10.2Hz (8.4Hz)

FAULT RADIUS RANGE 67m - 101m (82m)

STRESS DROP RANGE 0.06MPa - 0.21MPa (0.12MPa)

RANGE OF THE PEAK SLIP AT THE FAULT 0.2mm - 0.4mm (0.2mm)

THE ORIENTATION OF THE RELAXED STRESS

	AZIMUTH	DIP	
P-AXIS	178.	-18.	degrees
T-AXIS	96.	23.	

THE HORIZONTAL DEVIATORIC STRESS AS GIVEN BY THE P- AND T-AXES
THE AZIMUTH OF COMPRESSION 1 degrees
THE RELATIVE SIZE 0.87

THE TWO POSSIBLE FAULT PLANES

	STRIKE	DIP	SLIP	
PLANE A	136.	120.	4.	degrees
PLANE B	228.	93.	150.	

THE NORMAL DIRECTIONS OF THE FAULT PLANES

	AZIMUTH	DIP	
PLANE A	46.	30.	degrees
PLANE B	138.	3.	

STATISTICAL INFORMATION

OF 1 FIRST MOTION POLARITY OBSERVATIONS
AT LEAST 1 ARE REQUIRED TO FIT

THE OPTIMUM MECHANISM HAS 0 POLARITY MISFITS

AMPLITUDES FOR P AND S AT 3 STATIONS ARE USED
ONLY MECHANISMS GIVING AN ESTIMATED STANDARD
DEVIATION OF THE AMPLITUDE ERROR FACTOR OF LESS
THAN 1.60 FOR SINGLE P-WAVE OBSERVATIONS ARE
TAKEN AS ACCEPTABLE AND INCLUDED IN THE FIGURES

13.78 % OF ALL MECHANISMS ARE ACCEPTABLE
50.0 % ACCEPTABLE DUE TO FIRST MOTION OBSERVATIONS
27.3 % OF THESE FITTED ALSO THE AMPLITUDES
THE PART OF WELL FITTING PLANES IS 86.2%

THE AMPLITUDE FIT OF THE OPTIMAL MECHANISM
GIVES A MEAN ERROR FACTOR OF 1.20
THIS CORRESPONDS TO A STANDARD DEVIATION FACTOR OF 1.38
FOR SINGLE P-WAVE OBSERVATIONS

THE DOUBLE COUPLE SOLUTION IS SIGNIFICANT
AT 43 % LEVEL
(F-VALUE: F(5, 2) = 1.67)

THE MEASURE OF THE MISFIT TO AN EARTHQUAKE SPECTRUM
P-WAVES 0.34
S-WAVES 0.24

-AXIS ORIENTATIONS
EQUAL AREA PROJECTION J09821245
LOWER HEMISPHERE

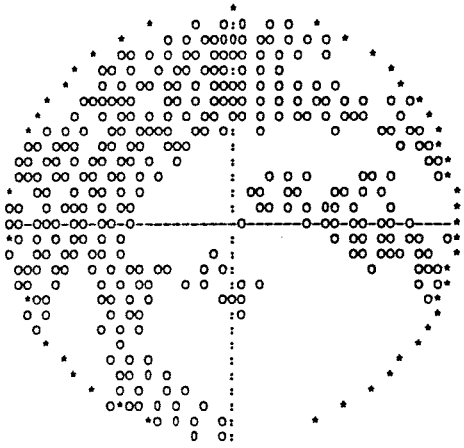

T-AXIS ORIENTATIONS
EQUAL AREA PROJECTION J09821245
LOWER HEMISPHERE

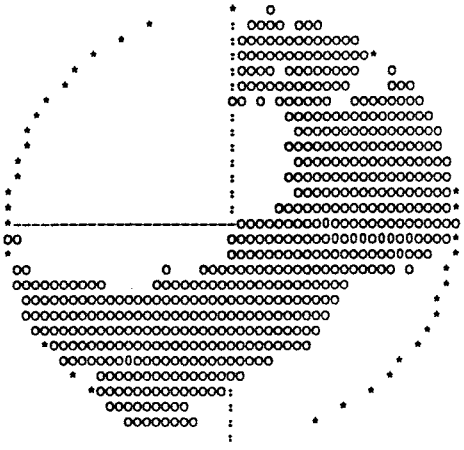

HORIZONTAL DEVIATORIC STRESS
RELATIVE SIZE AND J09821245
ORIENTATION OF COMPRESSION

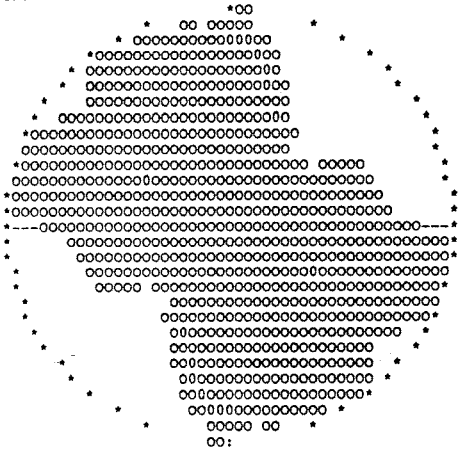

FAULT PLANE ORIENTATIONS
GIVEN BY NORMAL VECTORS
EQUAL AREA PROJECTION J09821245
LOWER HEMISPHERE

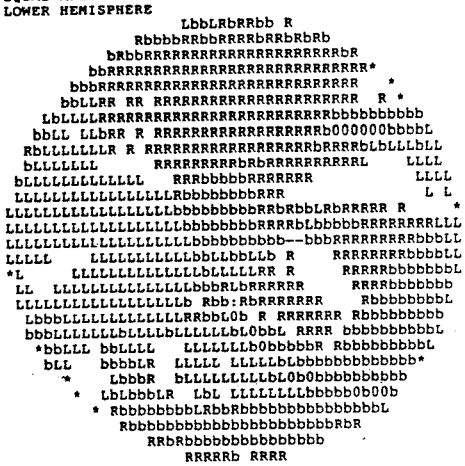

ORIGIN TIME 88 04 08 18H 51M 10.0S +/- 0.45S
LATITUDE 67.539 +/- 0.026 DEG.
LONGITUDE 22.665 +/- 0.051
FOCAL DEPTH 4.3 +/- 4.8 KM

STA	ARR. TIME	RES.	WEIGHT	DIST.	AZIMUTH	
MUG	P 18 51 14.65	0.00	63.7	28.1	252.0	P DOWN
MUG	S 18 51 18.13	0.02	5.5	28.1	252.0	
KPM	P 18 51 24.46	0.00	31.0	88.4	173.2	P UP
KPM	S 18 51 35.20	0.08	2.1	88.4	173.2	
LJV	S 18 51 39.08	-0.21	1.7	104.2	193.1	
KLX	P 18 51 36.83	0.00	16.2	165.4	174.3	

INPUT DATA FOR FAULT PLANE SOLUTION

STN	DIST. KM	AZIMUTH DEGREES		OMEGA(PZ) METER-SEC	OMEGA(SZ) METER-SEC
MUG	28.	252.2	-	0.43E-09	0.35E-09
HAK	84.	215.5		0.53E-10	0.14E-09
KPM	88.	173.3	+	0.69E-10	0.18E-09
LJV	101.	192.7		0.72E-10	0.24E-09
KLX	165.	174.3		0.65E-10	0.12E-09

DYNAMIC SOURCE PARAMETERS

SIZE MEASURES
SEISMIC MOMENT: 0.913E+11 Nm
LOCAL MAGNITUDE: 1.0

SHEAR WAVE CORNER FREQUENCY RANGE AT CLOSE DISTANCES (130km)
9.7Hz -14.2Hz (11.7Hz)

FAULT RADIUS RANGE 48m - 71m (58m)

STRESS DROP RANGE 0.11MPa - 0.35MPa (0.19MPa)

RANGE OF THE PEAK SLIP AT THE FAULT 0.3mm - 0.5mm (0.4mm)

THE ORIENTATION OF THE RELAXED STRESS

	AZIMUTH	DIP	
P-AXIS	61.	5.	degrees
T-AXIS	-27.	-23.	

THE HORIZONTAL DEVIATORIC STRESS AS GIVEN BY THE P- AND T-AXES
THE AZIMUTH OF COMPRESSION 62 degrees
THE RELATIVE SIZE 0.92

THE TWO POSSIBLE FAULT PLANES

	STRIKE	DIP	SLIP	
PLANE A	15.	70.	-13.	degrees
PLANE B	109.	78.	200.	

THE NORMAL DIRECTIONS OF THE FAULT PLANES

	AZIMUTH	DIP	
PLANE A	105.	20.	degrees
PLANE B	199.	12.	

STATISTICAL INFORMATION

OF 2 FIRST MOTION POLARITY OBSERVATIONS
AT LEAST 2 ARE REQUIRED TO FIT

THE OPTIMUM MECHANISM HAS 0 POLARITY MISFITS

AMPLITUDES FOR P AND S AT 5 STATIONS ARE USED
ONLY MECHANISMS GIVING AN ESTIMATED STANDARD
DEVIATION OF THE AMPLITUDE ERROR FACTOR OF LESS
THAN 1.60 FOR SINGLE P-WAVE OBSERVATIONS ARE
TAKEN AS ACCEPTABLE AND INCLUDED IN THE FIGURES

2.37 % OF ALL MECHANISMS ARE ACCEPTABLE
31.0 % ACCEPTABLE DUE TO FIRST MOTION OBSERVATIONS
7.7 % OF THESE FITTED ALSO THE AMPLITUDES
THE PART OF WELL FITTING PLANES IS 26.6%

THE AMPLITUDE FIT OF THE OPTIMAL MECHANISM
GIVES A MEAN ERROR FACTOR OF 1.20
THIS CORRESPONDS TO A STANDARD DEVIATION FACTOR OF 1.26
FOR SINGLE P-WAVE OBSERVATIONS

THE DOUBLE COUPLE SOLUTION IS SIGNIFICANT
AT BETTER THAN 1 % LEVEL
(F-VALUE: F(9, 6) = 9.23)

THE MEASURE OF THE MISFIT TO AN EARTHQUAKE SPECTRUM

P-WAVES	0.38
S-WAVES	0.22

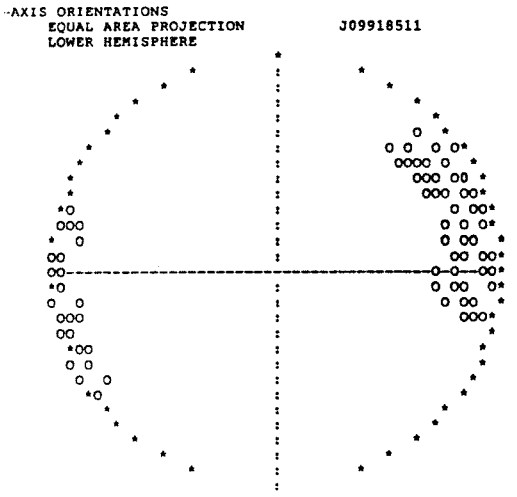
AXIS ORIENTATIONS
EQUAL AREA PROJECTION
LOWER HEMISPHERE
J09918511

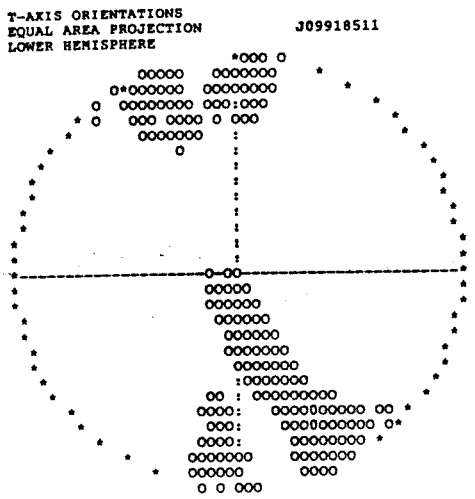
T-AXIS ORIENTATIONS
EQUAL AREA PROJECTION
LOWER HEMISPHERE
J09918511

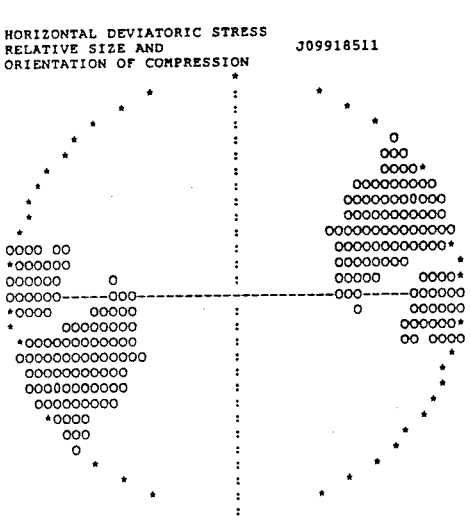
HORIZONTAL DEVIATORIC STRESS
RELATIVE SIZE AND
ORIENTATION OF COMPRESSION
J09918511

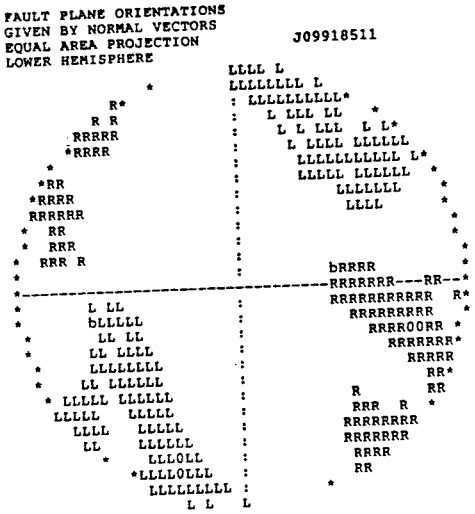
FAULT PLANE ORIENTATIONS
GIVEN BY NORMAL VECTORS
EQUAL AREA PROJECTION
LOWER HEMISPHERE
J09918511

ORIGIN TIME 88 04 10 19H 48M 10.6S +/- 0.24S
LATITUDE 66.175 +/- 0.006 DEG.
LONGITUDE 21.904 +/- 0.023
FOCAL DEPTH 9.6 +/- 14.5 KM

STA	ARR. TIME	RES.	WEIGHT	DIST.	AZIMUTH	
KLX P	19 48 19.34	0.05	46.2	52.4	102.8	P DOWN
KLX S	19 48 25.56	-0.14	3.5	52.4	102.8	
LJV P	19 48 19.70	0.02	44.9	54.8	12.3	
LJV S	19 48 26.56	0.19	3.3	54.8	12.3	
VMK P	19 48 20.13	0.09	43.7	57.1	194.8	
VMK S	19 48 25.90	-1.10	3.2	57.1	194.8	
KPM P	19 48 23.43	-0.10	34.3	78.7	34.2	P UP
KPM S	19 48 32.79	-0.26	2.3	78.7	34.2	

INPUT DATA FOR FAULT PLANE SOLUTION

STN	DIST. KM	AZIMUTH DEGREES		OMEGA(PZ) METER-SEC	OMEGA(SZ) METER-SEC
KLX	53.	103.3	-	0.58E-10	0.95E-10
LJV	54.	12.6		0.46E-10	0.31E-09
VMK	58.	194.5		0.66E-10	0.87E-10
KPM	78.	34.5	+	0.57E-10	0.16E-09

DYNAMIC SOURCE PARAMETERS

SIZE MEASURES
SEISMIC MOMENT: 0.470E+11 Nm
LOCAL MAGNITUDE: 0.7

SHEAR WAVE CORNER FREQUENCY RANGE AT CLOSE DISTANCES (130km)
-0.7Hz - 6.5Hz (4.3Hz)

FAULT RADIUS RANGE 106m --985m (160m)

STRESS DROP RANGE 0.00MPa - 0.02MPa (0.00MPa)

RANGE OF THE PEAK SLIP AT THE FAULT 0.0mm - 0.1mm (0.0mm)

THE ORIENTATION OF THE RELAXED STRESS

	AZIMUTH	DIP
P-AXIS	126.	11. degrees
T-AXIS	212.	-18.

THE HORIZONTAL DEVIATORIC STRESS AS GIVEN BY THE P- AND T-AXES
THE AZIMUTH OF COMPRESSION -55 degrees
THE RELATIVE SIZE 0.93

THE TWO POSSIBLE FAULT PLANES

	STRIKE	DIP	SLIP
PLANE A	-10.	69.	186. degrees
PLANE B	258.	85.	-21.

THE NORMAL DIRECTIONS OF THE FAULT PLANES

	AZIMUTH	DIP
PLANE A	80.	21. degrees
PLANE B	348.	5.

STATISTICAL INFORMATION

OF 2 FIRST MOTION POLARITY OBSERVATIONS
AT LEAST 2 ARE REQUIRED TO FIT

THE OPTIMUM MECHANISM HAS 0 POLARITY MISFITS

AMPLITUDES FOR P AND S AT 4 STATIONS ARE USED
ONLY MECHANISMS GIVING AN ESTIMATED STANDARD
DEVIATION OF THE AMPLITUDE ERROR FACTOR OF LESS
THAN 1.60 FOR SINGLE P-WAVE OBSERVATIONS ARE
TAKEN AS ACCEPTABLE AND INCLUDED IN THE FIGURES

1.51 % OF ALL MECHANISMS ARE ACCEPTABLE
28.6 % ACCEPTABLE DUE TO FIRST MOTION OBSERVATIONS
5.3 % OF THESE FITTED ALSO THE AMPLITUDES
THE PART OF WELL FITTING PLANES IS 21.1%

THE AMPLITUDE FIT OF THE OPTIMAL MECHANISM
GIVES A MEAN ERROR FACTOR OF 1.19
THIS CORRESPONDS TO A STANDARD DEVIATION FACTOR OF 1.28
FOR SINGLE P-WAVE OBSERVATIONS

THE DOUBLE COUPLE SOLUTION IS SIGNIFICANT
AT 4 % LEVEL
(F-VALUE: F(7, 4) = 6.24)

THE MEASURE OF THE MISFIT TO AN EARTHQUAKE SPECTRUM
P-WAVES 0.27
S-WAVES 0.27

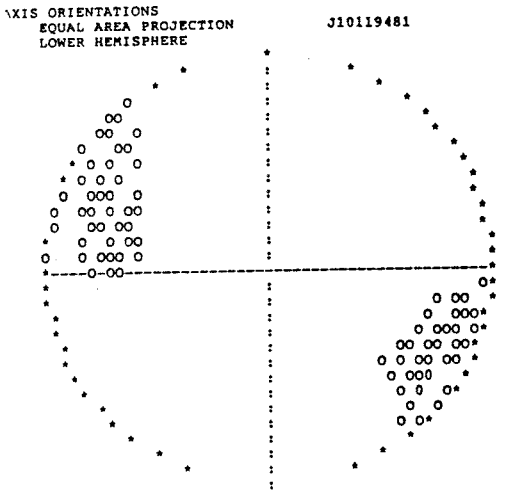
\XIS ORIENTATIONS
EQUAL AREA PROJECTION
LOWER HEMISPHERE
J10119481

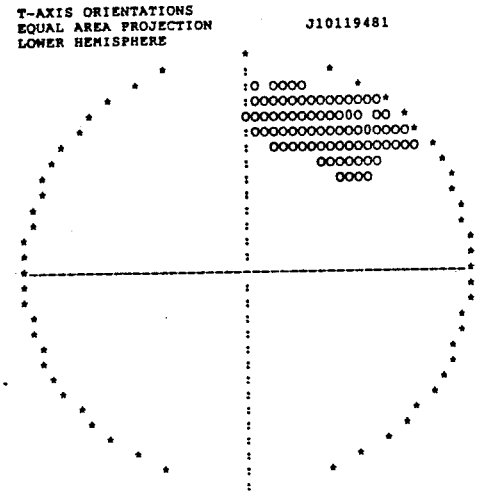
T-AXIS ORIENTATIONS
EQUAL AREA PROJECTION
LOWER HEMISPHERE
J10119481

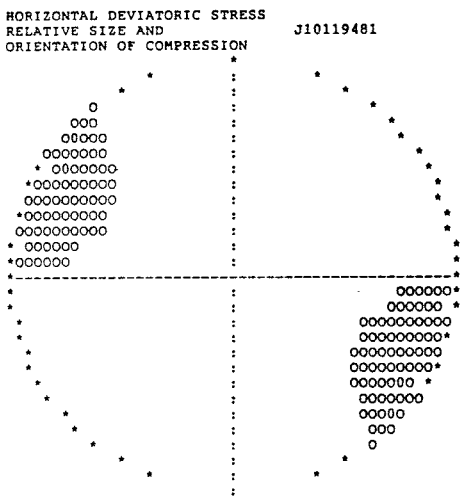
HORIZONTAL DEVIATORIC STRESS
RELATIVE SIZE AND
ORIENTATION OF COMPRESSION
J10119481

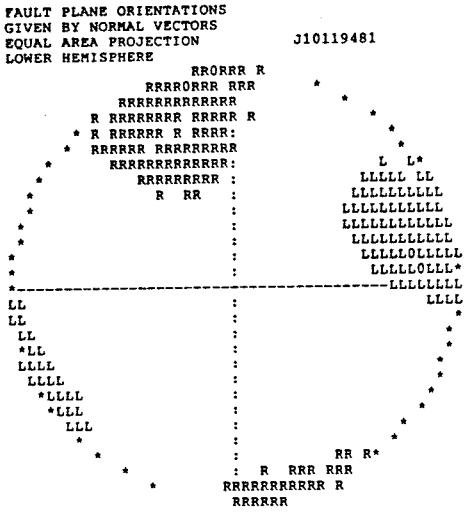
FAULT PLANE ORIENTATIONS
GIVEN BY NORMAL VECTORS
EQUAL AREA PROJECTION
LOWER HEMISPHERE
J10119481

ORIGIN TIME 88 04 16 17H 56M 34.4S +/- 0.33S
LATITUDE 66.312 +/- 0.007 DEG.
LONGITUDE 23.738 +/- 0.060
FOCAL DEPTH 6.2 +/- 4.0 KM

STA	ARR. TIME	RES.	WEIGHT	DIST.	AZIMUTH	
KLX P	17 56 41.34	0.00	52.7	42.0	229.7	P DOWN
KLX S	17 56 46.46	-0.01	4.2	42.0	229.7	
KPM P	17 56 44.52	-0.02	41.3	61.8	323.5	P UP
KPM S	17 56 51.78	-0.25	3.0	61.8	323.5	
LJV S	17 56 57.14	0.04	2.3	79.8	299.3	
HAK P	17 56 53.81	0.08	23.5	118.4	306.3	
HAK S	17 57 8.02	0.05	1.4	118.4	306.3	
VMK S	17 57 8.28	-0.31	1.4	120.6	235.2	
MUG P	17 56 58.52	-0.02	18.4	148.3	330.7	
MUG S	17 57 16.74	0.35	1.1	148.3	330.7	

INPUT DATA FOR FAULT PLANE SOLUTION

STN	DIST. KM	AZIMUTH DEGREES		OMEGA(PZ) METER-SEC	OMEGA(SZ) METER-SEC
KLX	42.	230.1	-	0.89E-10	0.16E-09
KPM	62.	323.6	+	0.10E-09	0.50E-09
HAK	119.	306.4		0.66E-10	0.24E-09
VMK	121.	235.3		0.91E-10	0.21E-09

DYNAMIC SOURCE PARAMETERS

SIZE MEASURES
SEISMIC MOMENT: 0.849E+11 Nm
LOCAL MAGNITUDE: 0.9

SHEAR WAVE CORNER FREQUENCY RANGE AT CLOSE DISTANCES (130km)
5.9Hz -13.6Hz (9.1Hz)

FAULT RADIUS RANGE 50m - 116m (75m)

STRESS DROP RANGE 0.02MPa - 0.28MPa (0.09MPa)

RANGE OF THE PEAK SLIP AT THE FAULT 0.1mm - 0.5mm (0.2mm)

THE ORIENTATION OF THE RELAXED STRESS

	AZIMUTH	DIP
P-AXIS	82.	-18. degrees
T-AXIS	164.	22.

THE HORIZONTAL DEVIATORIC STRESS AS GIVEN BY THE P- AND T-AXES
THE AZIMUTH OF COMPRESSION 78 degrees
THE RELATIVE SIZE 0.87

THE TWO POSSIBLE FAULT PLANES

	STRIKE	DIP	SLIP
PLANE A	-56.	119.	177. degrees
PLANE B	212.	93.	29.

THE NORMAL DIRECTIONS OF THE FAULT PLANES

	AZIMUTH	DIP
PLANE A	214.	29. degrees
PLANE B	122.	3.

STATISTICAL INFORMATION

OF 2 FIRST MOTION POLARITY OBSERVATIONS
AT LEAST 2 ARE REQUIRED TO FIT

THE OPTIMUM MECHANISM HAS 0 POLARITY MISFITS

AMPLITUDES FOR P AND S AT 4 STATIONS ARE USED
ONLY MECHANISMS GIVING AN ESTIMATED STANDARD
DEVIATION OF THE AMPLITUDE ERROR FACTOR OF LESS
THAN 1.60 FOR SINGLE P-WAVE OBSERVATIONS ARE
TAKEN AS ACCEPTABLE AND INCLUDED IN THE FIGURES

3.49 % OF ALL MECHANISMS ARE ACCEPTABLE
32.4 % ACCEPTABLE DUE TO FIRST MOTION OBSERVATIONS
10.8 % OF THESE FITTED ALSO THE AMPLITUDES
THE PART OF WELL FITTING PLANES IS 42.6%

THE AMPLITUDE FIT OF THE OPTIMAL MECHANISM
GIVES A MEAN ERROR FACTOR OF 1.10
THIS CORRESPONDS TO A STANDARD DEVIATION FACTOR OF 1.14
FOR SINGLE P-WAVE OBSERVATIONS

THE DOUBLE COUPLE SOLUTION IS SIGNIFICANT
AT 2 % LEVEL
(F-VALUE: F(7, 4) = 10.03)

THE MEASURE OF THE MISFIT TO AN EARTHQUAKE SPECTRUM

P-WAVES	0.23
S-WAVES	0.25

-AXIS ORIENTATIONS
EQUAL AREA PROJECTION
LOWER HEMISPHERE
J10717563

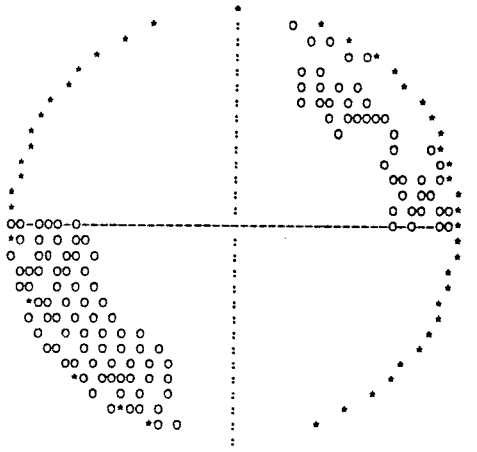

T-AXIS ORIENTATIONS
EQUAL AREA PROJECTION
LOWER HEMISPHERE
J10717563

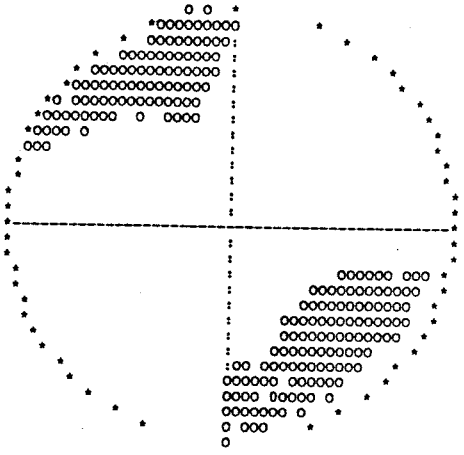

HORIZONTAL DEVIATORIC STRESS
RELATIVE SIZE AND
ORIENTATION OF COMPRESSION
J10717563

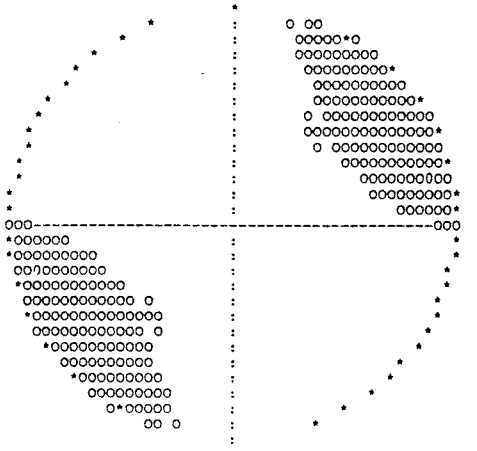

FAULT PLANE ORIENTATIONS
GIVEN BY NORMAL VECTORS
EQUAL AREA PROJECTION
LOWER HEMISPHERE
J10717563

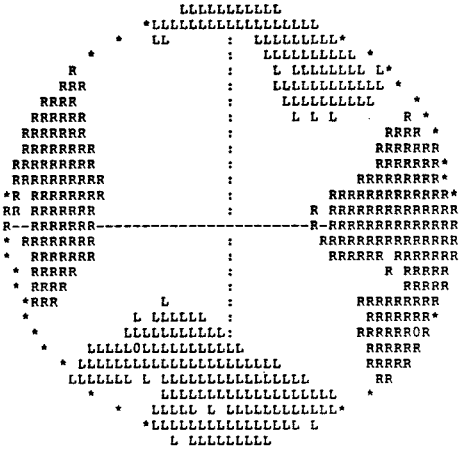

List of SKB reports

Annual Reports

1977–78
TR 121
KBS Technical Reports 1 – 120.
Summaries. Stockholm, May 1979.

1979
TR 79–28
The KBS Annual Report 1979.
KBS Technical Reports 79-01 – 79-27.
Summaries. Stockholm, March 1980.

1980
TR 80–26
The KBS Annual Report 1980.
KBS Technical Reports 80-01 – 80-25.
Summaries. Stockholm, March 1981.

1981
TR 81–17
The KBS Annual Report 1981.
KBS Technical Reports 81-01 – 81-16.
Summaries. Stockholm, April 1982.

1982
TR 82–28
The KBS Annual Report 1982.
KBS Technical Reports 82-01 – 82-27.
Summaries. Stockholm, July 1983.

1983
TR 83–77
The KBS Annual Report 1983.
KBS Technical Reports 83-01 – 83-76
Summaries. Stockholm, June 1984.

1984
TR 85–01
Annual Research and Development Report 1984
Including Summaries of Technical Reports Issued during 1984. (Technical Reports 84-01–84-19)
Stockholm June 1985.

1985
TR 85-20
Annual Research and Development Report 1985
Including Summaries of Technical Reports Issued during 1985. (Technical Reports 85-01-85-19)
Stockholm May 1986.

1986
TR 86-31
SKB Annual Report 1986
Including Summaries of Technical Reports Issued during 1986
Stockholm, May 1987

1987
TR 87-33
SKB Annual Report 1987
Including Summaries of Technical Reports Issued during 1987
Stockholm, May 1988

1988
TR 88-32
SKB Annual Report 1988
Including Summaries of Technical Reports Issued during 1988
Stockholm, May 1989

Technical Reports

1989
TR 89-01
Near-distance seismological monitoring of the Lansjärv neotectonic fault region Part II: 1988
Rutger Wahlström, Sven-Olof Linder, Conny Holmqvist, Hans-Edy Mårtensson
Seismological Department, Uppsala University, Uppsala
January 1989

TR 89-02
Description of background data in SKB database GEOTAB
Ebbe Eriksson, Stefan Sehlstedt
SGAB, Luleå
February 1989

TR 89-03
Characterization of the morphology, basement rock and tectonics in Sweden
Kennert Röshoff
August 1988

TR 89-04
SKB WP-Cave Project
Radionuclide release from the near-field in a WP-Cave repository
Maria Lindgren, Kristina Skagius
Kemakta Consultants Co, Stockholm
April 1989

TR 89-05
SKB WP-Cave Project
Transport of escaping radionuclides from the WP-Cave repository to the biosphere
Luis Moreno, Sue Arve, Ivars Neretnieks
Royal Institute of Technology, Stockholm
April 1989

TR 89-06
SKB WP-Cave Project
Individual radiation doses from nuclides contained in a WP-Cave repository for spent fuel
Sture Nordlinder, Ulla Bergström
Studsvik Nuclear, Studsvik
April 1989

TR 89-07
SKB WP-Cave Project
Some Notes on Technical Issues
Part 1: Temperature distribution in WP-Cave: when shafts are filled with sand/water mixtures
Stefan Björklund, Lennart Josefson
Division of Solid Mechanics, Chalmers University of Technology, Gothenburg, Sweden
Part 2: Gas and water transport from WP-Cave repository Luis Moreno, Ivars Neretnieks
Department of Chemical Engineering, Royal Institute of Technology, Stockholm, Sweden
Part 3: Transport of escaping nuclides from the WP-Cave repository to the biosphere. Influence of the hydraulic cage
Luis Moreno, Ivars Neretnieks
Department of Chemical Engineering, Royal Institute of Technology, Stockholm, Sweden
August 1989

TR 89-08
SKB WP-Cave Project
Thermally incuded convective motion in groundwater in the near field of the WP-Cave after filling and closure
Polydynamics Limited, Zürich
April 1989

TR 89-09
An evaluation of tracer tests performed at Studsvik
Luis Moreno[1], Ivars Neretnieks[1], Ove Landström[2]
[1] The Royal Institute of Technology, Department of Chemical Engineering, Stockholm
[2] Studsvik Nuclear, Nyköping
March 1989

TR 89-10
Copper produced from powder by HIP to encapsulate nuclear fuel elements
Lars B Ekbom, Sven Bogegård
Swedish National Defence Research Establishment
Materials department, Stockholm
February 1989

TR 89-11
Prediction of hydraulic conductivity and conductive fracture frequency by multivariate analysis of data from the Klipperås study site
Jan-Erik Andersson[1], Lennart Lindqvist[2]
[1] Swedish Geological Co, Uppsala
[2] EMX-system AB, Luleå
February 1988

TR 89-12
Hydraulic interference tests and tracer tests within the Brändan area, Finnsjön study site The Fracture Zone Project – Phase 3
Jan-Erik Andersson, Lennart Ekman, Erik Gustafsson, Rune Nordqvist, Sven Tirén
Swedish Geological Co, Division of Engineering Geology
June 1988

TR 89-13
Spent fuel
Dissolution and oxidation
An evaluation of literature data
Bernd Grambow
Hanh-Meitner-Institut, Berlin
March 1989

TR 89-14
The SKB spent fuel corrosion program Status report 1988
Lars O Werme[1], Roy S Forsyth[2]
[1] SKB, Stockholm
[2] Studsvik AB, Nyköping
May 1989

TR 89-15
Comparison between radar data and geophysical, geological and hydrological borehole parameters by multivariate analysis of data
Serje Carlsten, Lennart Lindqvist, Olle Olsson
Swedish Geological Company, Uppsala
March 1989

TR 89-16
Swedish Hard Rock Laboratory – Evaluation of 1988 year pre-investigations and description of the target area, the island of Äspö
Gunnar Gustafsson, Roy Stanfors, Peter Wikberg
June 1989

TR 89-17
Field instrumentation for hydrofracturing stress measurements
Documentation of the 1000 m hydrofracturing unit at Luleå University of Technology
Bjarni Bjarnason, Arne Torikka
August 1989

TR 89-18
Radar investigations at the Saltsjötunnel – predicitions and validation
Olle Olsson[1] and Kai Palmqvist[2]
[1] Abem AB, Uppsala, Sweden
[2] Bergab, Göteborg
June 1989

TR 89-19
Characterization of fracture zone 2, Finnsjön study-site
Editors: K. Ahlbom, J.A.T. Smellie, Swedish Geological Co, Uppsala
Part 1: Overview of the fracture zone project at Finnsjön, Sweden
K. Ahlbom and J.A.T. Smellie. Swedish Geological Company, Uppsala, Sweden.
Part 2: Geological setting and deformation history of a low angle fracture zone at Finnsjön, Sweden
Sven A. Tirén. Swedish Geological Company, Uppsala, Sweden.
Part 3: Hydraulic testing and modelling of a low-angle fracture zone at Finnsjön, Sweden
J-E. Andersson[1], L. Ekman[1], R. Nordqvist[1] and A. Winberg[2]
[1] Swedish Geological Company, Uppsala, Sweden
[2] Swedish Geological Company, Göteborg, Sweden
Part 4: Groundwater flow conditions in a low angle fracture zone at Finnsjön, Sweden
E. Gustafsson and P. Andersson. Swedish Geological Company, Uppsala, Sweden
Part 5: Hydrochemical investigations at Finnsjön, Sweden
J.A.T. Smellie[1] and P. Wikberg[2]
[1] Swedish Geological Company, Uppsala, Sweden
[2] Swedish Nuclear Fuel and Waste Management Company, Stockholm, Sweden
Part 6: Effects of gas-lift pumping on hydraulic borehole conditions at Finnsjön, Sweden
J-E- Andersson, P. Andersson and E. Gustafsson. Swedish Geological Company, Uppsala, Sweden
August 1989

TR 89-20
WP-Cave - Assessment of feasibility, safety and development potential
Swedish Nuclear Fuel and Waste Management Company, Stockholm, Sweden
September 1989

TR 89-21
Rock quality designation of the hydraulic properties in the near field of a final repository for spent nuclear fuel
Hans Carlsson[1], Leif Carlsson[1], Roland Pusch[2]
[1] Swedish Geological Co, SGAB, Gothenburg, Sweden
[2] Clay Technology AB, Lund, Sweden
June 1989

TR 89-22
Diffusion of Am, Pu, U, Np, Cs, I and Tc in compacted sand-bentonite mixture
Department of Nuclear Chemistry, Chalmers University of Technology, Gothenburg, Sweden
August 1989

TR 89-23
Deep ground water microbiology in Swedish granitic rock and it's relevance for radionuclide migration from a Swedish high level nuclear waste repository
Karsten Pedersen
University of Göteborg, Department of Marine microbiology, Gothenburg, Sweden
March 1989

TR 89-24
Some notes on diffusion of radionuclides through compacted clays
Trygve E Eriksen
Royal Institute of Technology, Department of Nuclear Chemistry, Stockholm, Sweden
May 1989

TR 89-25
Radionuclide sorption on crushed and intact granitic rock
Volume and surface effects
Trygve E Eriksen, Birgitta Locklund
Royal Institute of Technology, Department of Nuclear Chemistry, Stockholm, Sweden
May 1989

TR 89-26
Performance and safety analysis of WP-Cave concept
Kristina Skagius[1], Christer Svemar[2]
[1] Kemakta Konsult AB
[2] Swedish Nuclear Fuel and Waste Management Co
August 1989

TR-89-27

Post-excavation analysis of a revised hydraulic model of the Room 209 fracture, URL, Manitoba, Canada
A part of the joint AECL/SKB characterization of the 240 m level at the URL, Manitoba, Canada

Anders Winberg[1], Tin Chan[2], Peter Griffiths[2], Blair Nakka[2]
[1] Swedish Geological Co, Gothenburg, Sweden
[2] Computations & Analysis Section, Applied Geoscience Branch, Atomic Energy of Canada Limited, Pinawa, Manitoba, Canada

October 1989